

Handbook T-IX

Engineering Science and Technology

LEDESMA-ALBERT, Aida *Coordinator*

ECORFAN®

Coordinator

LEDESMA-ALBERT, Aida. PhD

Editor in Chief

VARGAS-DELGADO, Oscar. PhD

Executive Director

RAMOS-ESCAMILLA, María. PhD

Editorial Director

PERALTA-CASTRO, Enrique. MSc

Web Designer

ESCAMILLA-BOUCHAN, Imelda. PhD

Web Diagrammer

LUNA-SOTO, Vladimir. PhD

Editorial Assistant

TREJO-RAMOS, Iván. BsC

Translator

DÍAZ-OCAMPO, Javier. BsC

Philologist

RAMOS-ARANCIBIA, Alejandra. BsC

ISBN: 978-607-8695-60-7

ECORFAN Publishing Label: 607-8695

HESTH Control Number: 2021-09

HESTH Classification (2021): 301121-1001

©ECORFAN-México, S.C.

No part of this writing protected by the Federal Copyright Law may be reproduced, transmitted or used in any form or by any means, graphic, electronic or mechanical, including, but not limited to, the following: Quotations in radio or electronic journalistic data compilation articles and bibliographic commentaries. For the purposes of articles 13, 162,163 fraction I, 164 fraction I, 168, 169,209 fraction III and other relative articles of the Federal Copyright Law. Infringements: Being compelled to prosecute under Mexican copyright law. The use of general descriptive names, registered names, trademarks, or trade names in this publication does not imply, even in the absence of a specific statement, that such names are exempt from the relevant protection in laws and regulations of Mexico and therefore free for general use by the international scientific community. HCE is part of ECORFAN Media (www.ecorfan.org)

Handbooks

Definition of Handbooks

Scientific Objectives

To support the International Scientific Community in its written production of Science, Technology and Innovation in the CONACYT and PRODEP research areas.

ECORFAN-Mexico, S.C. is a Scientific and Technological Company in contribution to the formation of Human Resources focused on the continuity in the critical analysis of International Research and is attached to the RENIECYT of CONACYT with number 1702902, its commitment is to disseminate research and contributions of the International Scientific Community, academic institutions, agencies and entities of the public and private sectors and contribute to the linkage of researchers who perform scientific activities, technological developments and training of specialized human resources with governments, businesses and social organizations.

To encourage the interlocution of the International Scientific Community with other study centres in Mexico and abroad and to promote a wide incorporation of academics, specialists and researchers to the serial publication in Science Niches of Autonomous Universities - State Public Universities - Federal IES - Polytechnic Universities - Technological Universities - Federal Technological Institutes - Teacher Training Colleges - Decentralised Technological Institutes - Intercultural Universities - S&T Councils - CONACYT Research Centres.

Scope, Coverage and Audience

Handbooks is a product edited by ECORFAN-Mexico S.C. in its Holding with repository in Mexico, it is a refereed and indexed scientific publication. It admits a wide range of contents that are evaluated by academic peers by the double-blind method, on topics related to the theory and practice of the CONACYT and PRODEP research areas respectively with diverse approaches and perspectives, which contribute to the dissemination of the development of Science, Technology and Innovation that allow arguments related to decision-making and influence the formulation of international policies in the field of science. The editorial horizon of ECORFAN-Mexico® extends beyond academia and integrates other segments of research and analysis outside that field, as long as they meet the requirements of argumentative and scientific rigour, in addition to addressing issues of general and current interest of the International Scientific Society.

Editorial Board

AYALA - GARCÍA, Ivo Neftalí. PhD
University of Southampton

CARBAJAL - DE LA TORRE, Georgina. PhD
Université des Sciences et Technologies de Lille

CASTILLO - LÓPEZ, Oscar. PhD
Academia de Ciencias de Polonia

CERCADO - QUEZADA, Bibiana. PhD
Intitut National Polytechnique Toulouse

DECTOR - ESPINOZA, Andrés. PhD
Centro de Microelectrónica de Barcelona

FERNANDEZ - ZAYAS, José Luis. PhD
University of Bristol

HERNANDEZ - ESCOBEDO, Quetzalcoatl Cruz. PhD
Universidad Central del Ecuador

HERRERA - DIAZ, Israel Enrique. PhD
Center of Research in Mathematics

MAYORGA - ORTIZ, Pedro. PhD
Institut National Polytechnique de Grenoble

NAZARIO - BAUTISTA, Elivar. PhD
Centro de Investigacion en óptica y nanofisica

Arbitration Committee

ARREDONDO - SOTO, Karina Cecilia. PhD
Instituto Tecnológico de Ciudad Juárez

ARROYO - FIGUEROA, Gabriela. PhD
Universidad de Guadalajara

BAEZA - SERRATO, Roberto. PhD
Universidad de Guanajuato

BARRON, Juan. PhD
Universidad Tecnológica de Jalisco

BAUTISTA - SANTOS, Horacio. PhD
Universidad Popular Autónoma del Estado de Puebla

CASTAÑÓN - PUGA, Manuel. PhD
Universidad Autónoma de Baja California

CASTILLO - TOPETE, Víctor Hugo. PhD
Centro de Investigación Científica y de Educación Superior de Ensenada

CORTEZ - GONZÁLEZ, Joaquín. PhD
Centro de Investigación y Estudios Avanzados

CRUZ - BARRAGÁN, Aidee. PhD
Universidad de la Sierra Sur

GONZÁLEZ - LÓPEZ, Samuel. PhD
Instituto Nacional de Astrofísica, Óptica y Electrónica

Assignment of Rights

By submitting a Scientific Work to ECORFAN Handbooks, the author undertakes not to submit it simultaneously to other scientific publications for consideration. To do so, the author must complete the Originality Form for his or her Scientific Work.

The authors sign the Authorisation Form for their Scientific Work to be disseminated by the means that ECORFAN-Mexico, S.C. in its Holding Mexico considers pertinent for the dissemination and diffusion of their Scientific Work, ceding their Scientific Work Rights.

Declaration of Authorship

Indicate the name of 1 Author and a maximum of 3 Co-authors in the participation of the Scientific Work and indicate in full the Institutional Affiliation indicating the Unit.

Identify the name of 1 author and a maximum of 3 co-authors with the CVU number -PNPC or SNI-CONACYT- indicating the level of researcher and their Google Scholar profile to verify their citation level and H index.

Identify the Name of 1 Author and 3 Co-authors maximum in the Science and Technology Profiles widely accepted by the International Scientific Community ORC ID - Researcher ID Thomson - arXiv Author ID - PubMed Author ID - Open ID respectively.

Indicate the contact for correspondence to the Author (Mail and Telephone) and indicate the Contributing Researcher as the first Author of the Scientific Work.

Plagiarism Detection

All Scientific Works will be tested by the PLAGSCAN plagiarism software. If a Positive plagiarism level is detected, the Scientific Work will not be sent to arbitration and the receipt of the Scientific Work will be rescinded, notifying the responsible Authors, claiming that academic plagiarism is typified as a crime in the Penal Code.

Refereeing Process

All Scientific Works will be evaluated by academic peers using the Double-Blind method. Approved refereeing is a requirement for the Editorial Board to make a final decision which will be final in all cases. MARVID® is a spin-off brand of ECORFAN® specialised in providing expert reviewers all of them with PhD degree and distinction of International Researchers in the respective Councils of Science and Technology and the counterpart of CONACYT for the chapters of America-Europe-Asia-Africa and Oceania. The identification of authorship should only appear on a first page, which can be removed, in order to ensure that the refereeing process is anonymous and covers the following stages: Identification of ECORFAN Handbooks with their author occupancy rate - Identification of Authors and Co-authors - PLAGSCAN Plagiarism Detection - Review of Authorisation and Originality Forms - Assignment to the Editorial Board - Assignment of the pair of Expert Referees - Notification of Opinion - Statement of Observations to the Author - Modified Scientific Work Package for Editing - Publication.

ECORFAN Engineering Science and Technology

Volume IX

The Handbook will offer volumes of selected contributions from researchers who contribute to the scientific dissemination activity of the Tecnológico de Estudios Superiores de Jocotitlán in their areas of research in Engineering and Technology Sciences. In addition to having a total evaluation, in the hands of the directors of the Tecnológico de Estudios Superiores de Jocotitlán, the quality and timeliness of its chapters, each individual contribution was refereed to international standards (RESEARCH GATE, MENDELEY, GOOGLE SCHOLAR and REDIB), the Handbook thus proposes to the academic community, recent reports on new developments in the most interesting and promising areas of research in the Engineering and Technology Sciences.

For future volumes:

<http://www.ecorfan.org/handbooks/>

LEDESMA-ALBERT, Aida. PhD

Coordinator

Engineering Science and Technology T-IX

Handbooks

Tecnológico de Estudios Superiores de Jocotitlán – Mexico.

October, 2021

DOI: 10.35429/H.2021.9.1.1.128

Content	Page
<p>1 Description and control of solar cell protection material for quality assurance of a photovoltaic panel SALAZAR-PERALTA, Araceli, PICHARDO-SALAZAR, José Alfredo, PICHARDO-SALAZAR, Ulises and SORIANO-VARGAS Orlando <i>Tecnológico de Estudios Superiores de Jocotitlán</i> <i>Centro de Bachillerato Tecnológico Industrial y de Servicios No. 161</i> <i>Centro de Estudios Tecnológicos Industrial y de Servicios No. 23</i></p>	1-23
<p>2 Four dimensions for the commercialization of technologies in public institutions of higher education (IHE) VARGAS-G., Jaqueline, RODRÍGUEZ-H., Gloria P. and GONZÁLEZ-PASTRANA, Juvelia <i>Tecnológico de Estudios Superiores de Jocotitlán</i></p>	24-32
<p>3 Students of public higher education institutions and their economic impact during COVID-19, case study, 2020 AYALA-RÍOS, Irma Amelia, GONZÁLEZ-CRUZ, Saúl and LÓPEZ-SÁNCHEZ, Iván</p>	33-50
<p>4 Construction element from debris and demolition waste as a post-disaster strategy OGURI, Leticia & ESCOBAR, Marlem Guadalupe <i>Tecnológico de Estudios Superiores de Jocotitlán</i></p>	51-69
<p>5 Structural characterisation of copper oxide by X-ray diffraction LÓPEZ, Roberto, NAMIGTLE, Jesús and MASTACHE, Jorge <i>Tecnológico de Estudios Superiores de Jocotitlán</i></p>	70-96
<p>6 Redesign of a fatigue machine guide plate based on topology optimization SOTO-MENDOZA, Gilberto, MARTÍNEZ-GARCÍA, José, EDMUNDO- MASTACHE, Jorge and HERNÁNDEZ-GÓMEZ, Luis Héctor <i>Tecnológico de Estudios Superiores de Jocotitlán</i> <i>Instituto Politécnico Nacional</i></p>	97-113
<p>7 Noise level evaluation in the resin figures manufacturing process GARCÍA-SANCHEZ, Viviano, MALDONADO-ONOFRE, Daniel, MIER- QUIROGA, Luis Antonio and COUTIÑO-MORENO, Elvis <i>Instituto Tecnológico de Toluca</i> <i>Tecnológico de Estudios Superiores de Jocotitlán</i></p>	114-128

Chapter 1 Description and control of solar cell protection material for quality assurance of a photovoltaic panel

Capítulo 1 Descripción y control del material de protección de las celdas solares para el aseguramiento de calidad de un panel fotovoltaico

SALAZAR-PERALTA, Araceli†*, PICHARDO-SALAZAR, José Alfredo, PICHARDO-SALAZAR, Ulises and SORIANO-VARGAS, Orlando

1,4 *Tecnológico de Estudios Superiores de Jocotitlán, Carretera Toluca Atlacomulco km 44.8, Ejido de San Juan y San Agustín, Jocotitlán, Mexico.*

2 *Centro de Bachillerato Tecnológico Industrial y de Servicios No. 161, Exhacienda la Laguna S/N Barrio de Jesús 2nd Section, San Pablo Autopan, Toluca. State of Mexico.*

3 *Centro de Estudios Tecnológicos Industrial y de Servicios no. 23. Avenida, Del Parque s/n, 52000 Lerma de Villada, Mexico.*

ID 1st Author: *Araceli, Salazar-Peralta* / **ORC ID:** 0000-0001-5861-3748, **Researcher ID Thomson:** U-2933-2018, **CVU CONACYT ID:** 300357

ID 1st Co-author: *José Alfredo, Pichardo-Salazar* / **ORC ID:** 0000-0002-8939-9921

ID 2nd Co-author: *Ulises, Pichardo-Salazar* / **ORC ID:** 0000-0002-3758-2038

ID 3rd Co-author: *Orlando, Soriano-Vargas*

DOI: 10.35429/H.2021.9.1.1.23

A. Salazar, J. Pichardo, U. Pichardo and O. Soriano

* araceli.salazar@tesjo.edu.mx

A. Ledesma (Coord.). Engineering Science and Technology. Handbooks-©ECORFAN-México, Estado de México, 2021.

Abstract

Global warming and climate change coincide in their main causes, the massive emission of greenhouse gases, which retain heat in the atmosphere and on the earth's surface through the so-called greenhouse effect. The generation of electricity by means of fossil fuels is an important emitter of greenhouse gases (CO₂, CH₄, N₂O), and halogenated compounds containing F, Cl, and Br. With the purpose of contributing to the construction of viable solutions to the current energy situation of the country and in the foundation of a sustainable future, the use of solar energy for the generation of electricity by means of solar panels represents an option. The purpose of this study is to describe and control the solar cell protection material Ethylene-Vinyl-Acetate (EVA), as a contribution to the Quality Assurance of solar panels, since the function of this material is essential for the protection of solar cells, which are a vital part of the solar panel. The tests performed were: Gel content, adhesion test, and durability tests. The results obtained were within specification according to IEC 61215. From this work it is concluded that it is important to continue testing the whole process and components of the solar panels in order to guarantee the useful life of the finished product, as well as to contribute to sustainable development.

Control, Ethylene vinyl acetate, Solar cells, Solar panel

Resumen

El calentamiento global y el cambio climático coinciden en la principal de sus causas, la emisión masiva de gases efecto invernadero, los cuales retienen el calor dentro de la atmósfera y sobre la superficie terrestre a través del denominado efecto invernadero. La generación de electricidad por medio de combustibles fósiles es un importante emisor de gases efecto invernadero (CO₂, CH₄, N₂O), y compuestos halogenados que contienen F, Cl, y Br. Con el propósito de contribuir en la construcción de salidas viables a la situación energética actual del país y en la cimentación de un futuro sostenible, el uso de la energía solar para la generación de energía eléctrica por medio de los paneles solares, representa una opción. Este estudio tiene como finalidad describir y controlar el material de protección de las celdas solares Etilen-Vinil-Acetato (EVA), como contribución al Aseguramiento de Calidad de los Paneles solares, ya que la función de dicho material es primordial para la protección de las celdas solares, las cuales son parte vital del panel solar. Los ensayos realizados fueron: Contenido en gel, Prueba de adherencia, y Ensayos de durabilidad. Los resultados obtenidos estuvieron dentro de especificación conforme a la Norma IEC 61215. De este trabajo se concluye que es importante seguir realizando ensayos en todo el proceso y componentes de los paneles solares para poder garantizar la vida útil del producto terminado, así como contribuir al desarrollo sustentable.

Control, Etilen vinil acetato, Celdas solares, Panel solar

1.1 Introduction

Global warming is a current problem, which consists of an increase in the earth's temperature, reflected in the oceans and the atmosphere, caused mainly by the emission of greenhouse gases emitted by human activity.

Global warming and climate change coincide in their main causes, the massive emission of different greenhouse gases or gases that retain heat in the atmosphere and on the earth's surface through the so-called greenhouse effect.

The greenhouse effect is a natural process by which the heat from the Sun is retained in the Earth's atmosphere thanks to the layer of greenhouse gases found in it. These gases in normal quantities maintain the temperature of the planet at approximately 33°C above what it would be if they did not exist, so the planet would be too cold for life to develop on it. Moreover, the greenhouse effect is now becoming so intense due to our emissions that it is beginning to have serious repercussions on the environment. Currently, developing countries depend primarily on crude oil to meet their energy needs, and for more than two-thirds of these, dependence is vital as it covers about 70% of needs.

In order to reduce environmental pollution and provide solutions to such problems, in 1993 Mexico joined the international effort to mitigate global climate change by acceding to the United Nations Framework Convention on Climate Change and ratifying the Kyoto Protocol in 2000. Mexico also supported the Latin American and Caribbean Initiative for Sustainable Development at the World Summit on Sustainable Development in Johannesburg, South Africa, in which the goal of implementing the use of at least 10% renewable, non-polluting energy of the total energy percentage by the year 2010, according to data from the Ministry of Energy.

Renewable energy

Renewable energies are those that are produced continuously. All renewable energy sources (except tidal and geothermal) ultimately come from the sun. Its energy causes the differences in atmospheric pressure that give rise to winds, a source of wind energy. It also causes the evaporation of water which then precipitates to form rivers, a source of hydropower. Plants and algae use the sun for photosynthesis, the source of all organic matter (or biomass) on Earth. Finally, the sun is used directly as solar energy, both thermal and photovoltaic. These sources are inexhaustible on a human scale, although in the case of biomass, this is the case as long as natural cycles are respected.

Geothermal energy. The Earth's heat is harnessed to obtain hot water, steam or electricity from groundwater. New technologies even make it possible to exploit hot rock deposits. This energy is used in areas with high geothermal activity, such as Iceland.

Biomass energy. Organic plant or animal materials are burned or chemically processed to produce fuels (such as biodiesel), heat and electricity. It has been the most widely used energy by humans and in many poor regions of the world it is still the main source of energy.

Hydropower. River water has been used for centuries to power machinery, for example, to grind corn. Today, this energy is mainly used to generate electricity. Hydroelectric technology is one of the most developed, cost-effective and reliable.

Ocean energy. The swaying of water from tides or waves, ocean currents, even the temperature difference between the water at the sea surface and the deep sea, could also be used to generate energy. At present, however, there is no commercially viable system of this type.

Wind energy. Wind has for centuries been captured by sails and blades for transportation and mechanical work. Modern wind turbines allow electricity to be obtained cleanly and efficiently. These machines can dump large amounts of energy into the grid or meet small demands.

Despite efforts to grow and modernize the electricity sector, electricity still does not reach nearly millions of people in rural areas. The growing demand for electricity in Mexico, along with the constant emission of pollutants into the atmosphere from the burning of fossil fuels, has also increased interest in the exploitation of alternative sources of renewable energy, which can help solve the demand for electricity without the problems of pollution.

One such alternative source is solar energy. In this Chapter, relevant topics on the description and control of the protection material of a Solar Panel are addressed, which are structured in seven sections named as follows:

Section 1.2 Background of solar energy.

Section 1.3 Structure of a solar panel

Section 1.4 Solar Cell Operation

Section 1.5 General information about the protective material of the solar cell (EVA)

Section 1.6 Function of the solar cell's protective material (EVA)

Section 1.7 Characteristics of the protective material (EVA).

Section 1.8 Tests for the control and quality assurance of the protective material (EVA) in the solar panel.

One such alternative source is solar energy. In this Chapter, relevant topics on the description and control of the protection material of a Solar Panel are addressed, which are structured in 7 sections named as follows:

1.2 Background on solar energy

Photovoltaic solar energy directly transforms sunlight into electricity using a technology based on the photovoltaic effect.

In general, solar energy can be described as energy that is received from sunlight and converted into electrical energy for human use. It is more economical and feasible, since the sun is within everyone's reach, on the other hand, solar panels are elements built with the main purpose of converting solar energy into electrical energy. They are constructed from an element called silicon, which participates in the process of creating electrical energy from sunlight. Solar energy can have a direct or indirect impact. A solar panel on cloudy days, contrary to popular belief, can produce energy perfectly well.

The photovoltaic effect was first discovered in 1839 by the French physicist Alexander-Edmond Becquerel. His studies were fundamental to the development of the use of photovoltaics.

1.2.1 Photovoltaic effect

The photovoltaic effect; converts the light energy carried by photons of light into electrical energy capable of driving electrons fired from the semiconductor material through an external circuit.

Sunlight is made up of photons or energetic particles. These energetic particles are of different energies, corresponding to the different wavelengths of the solar spectrum.

When photons hit a photovoltaic cell, they can be reflected or absorbed, or they can pass through it. It is the absorbed photons that transfer their energy to the electrons in the atoms of the cells.

To produce a useful electric current, the released electrons must be extracted from the material before they recombine with the "holes". One way to achieve this is to introduce chemical elements into the semiconductor material that help produce excess electrons and holes. These elements that significantly alter the intrinsic properties of semiconductors are called dopants and the process of their incorporation into the semiconductor is called doping.

The semiconductor material does not store electrical energy at any time, the only thing it does is to generate it, or rather, transform radiant energy only when it affects it. Not all photons behave in the same way when producing electricity by photovoltaic effect, some frequencies are more suitable than others to produce this effect depending on the types of semiconductor materials used.

Spectral response is a measure of the efficiency with which a photovoltaic device converts light energy into electrical energy for a given frequency of incident light.

For example, In a monocrystalline silicon cell, such conversion efficiency is only significant for wavelengths between 350 and 1100 nanometers, with a maximum around 800 nanometers, while for amorphous silicon the range is from 350 to 800 nanometers, with a maximum around 520 nanometers. (Obaya J, 2002).

1.2.2 Solar panels

A single cell is not capable of providing a voltage that can be used in practice, only generating a voltage of a few tenths of a volt (usually around half a volt for silicon cells) and a maximum power of one or two watts. To obtain adequate voltages and power, a number of cells must be connected in series to produce voltages of 6, 12 or 24 volts, which are accepted in most applications. This set of interconnected cells, assembled and protected against external agents, is called solar panel or photovoltaic module.

The cell connection process is automatic and is carried out by means of special welds that join the front face of one cell to the back face of the adjacent one. Between 30 and 40 cells, depending on their characteristics, are needed to produce a nominal 12 volt panel.

1.2.3 Principle of operation

Theoretical principles of operation. Some of the photons, which come from solar radiation, strike the first surface of the panel, penetrate it and are absorbed by semiconductor materials, such as silicon or gallium arsenide. The electrons, atomic sub-particles that form part of the exterior of the atoms, and which are housed in orbitals of quantized energy, are hit by the photons (they interact) freeing themselves from the atoms to which they were originally confined. This allows them to subsequently circulate through the material and produce electricity. The complementary positive charges that are created on the atoms that lose electrons (similar to positive charge bubbles) are called holes and flow in the opposite direction of the electrons in the solar panel.

It should be noted that, just as the flow of electrons corresponds to real charges, i.e., charges that are associated with real mass displacement, the voids are actually charges that can be considered virtual since they do not involve real mass displacement. (Fernandez, M. 2010).

1.2.4 Types of commercial photovoltaic panels

The different types of panels can be classified according to different criteria:

- According to the type of cells they contain. Thus, we speak of monocrystalline, polycrystalline and amorphous panels.
- According to the type of material the cells are made of: silicon panels, gallium arsenide, cadmium telluride, silicon film, etc.
- Considering the power it is capable of producing. There are mini-panels with as little as 1 W or 2 W of power, such as those used to keep a car battery charged, and we can also find large panels with power ratings of up to 300 W. The most common power ratings that can be found in the market are: 5W, 10W, 20W, 35W, 40W, 60W, 75W, 100W and 175W.
- Depending on the voltage or voltage, the maximum potential difference that a panel can provide is V_{oc} (Open Circuit Voltage), although the effective working voltage is always lower, depending on the number of cells, we are talking about 6 panels of 12 V or 24 V. The most used are those of 12 V, coinciding with the voltage of the most used accumulators.
- Depending on whether they take advantage of radiation on one side or on both sides. The bifacial panels, developed by the Spanish A. Luque, are also capable of capturing the reflected radiation (albedo) from the back of the panel, installing them on a white surface, being able to obtain an increase in useful power of about 20%. (Fernandez, M. 2010).

1.2.5 Ethylene vinyl acetate (EVA) material

The EVA is adhered to the cells, but it is usually reinforced as the rear base of the module for greater safety with the material called TPT (Tedlar-PET-Tedlar), which consists of a three-layer sandwich laminate formed by a layer of polyester film between two layers of PVF. (Marcillo Proaño, W. and Moreno Garrido, F. 2008).

1.2.6 Types of cells

Monocrystalline cells: are formed by sections of a single silicon (Si) crystal.

Polycrystalline cells: when they are formed by small crystallized particles.

Amorphous cells: when the silicon has not crystallized.

The efficiency of the cells is higher the larger the crystals are, but they also increase in weight, thickness and cost. The efficiency of monocrystalline cells can reach 20% while that of amorphous cells cannot reach 10%, although their cost and weight are much lower.

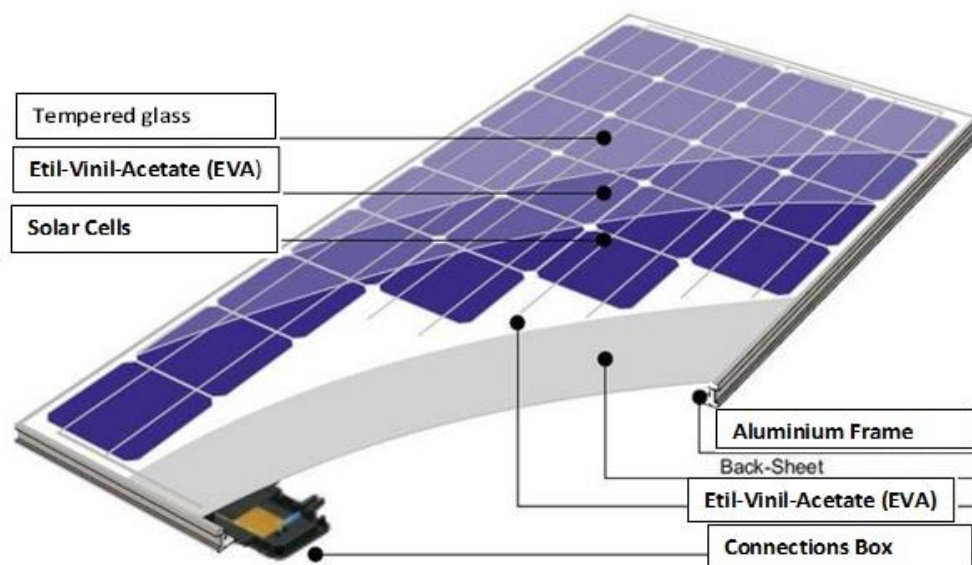
1.2.7 High-performance polycrystalline solar panels (photovoltaic)

To provide the solar cells with maximum protection under the most adverse environmental operating conditions, they are encapsulated between a tempered glass cover and an ethylene vinyl acetate (EVA) cover with polyvinyl fluoride and a backing sheet. The laminate is mounted on an anodized aluminum frame to provide structural strength and ease of installation.

1.3 Structure of a solar panel

The structure of a crystalline cell solar module generally consists of the following parts: an aluminum frame, structured glass, interconnected solar cells, EVA protection material, the back sheet, the frame and the junction box. Fig. 1.1. There is also the option of manufacturing another type of module. In this case, a second glass plate is laminated in place of the back sheet.

Figure 1.1 Parts of a solar panel



Source: Own elaboration

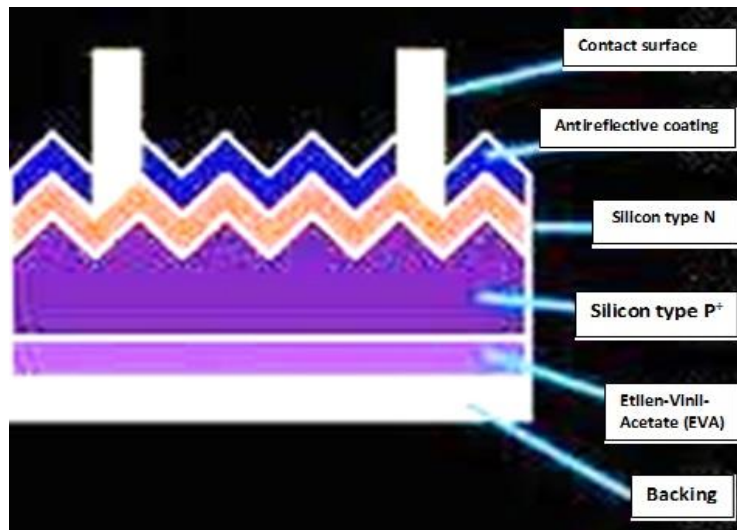
1.3.1. Structured glass

Soda, lime and silica tempered glass with a thickness between 3 and 4 mm, with low iron content. It has very good solar radiation transmission and provides protection against atmospheric agents and impacts. The outer surface of the glass is anti-reflective and is treated to prevent the retention of dust and dirt. The inner surface is generally roughened, which allows good adhesion with the cell encapsulating material Ethylene-Vinyl-Acetate (EVA), as well as facilitating the penetration of solar radiation.

1.3.2 Solar cell

Solar cells are direct conversion devices that directly transform the sun's energy into electrical power (DC) without any intermediate processes. Since power $P=IV$, then it is necessary to understand how current I and voltage V are generated in the cell. In turn, I is the result of charges moving in a given direction. The charges are already in the material, but in semiconductors they are in a bound state. Under the action of light, the charges become free, capable of forming a current. The charges are directed in a certain direction to form a current thanks to the action of the electric field created in the cell. Fig. 1.2.

Figure 1.2 Layers of a solar cell: (1) Contact surface, (2). Anti-reflective coating, (3). N- type silicon, (4). Silicon type P+, EVA (5), Backing (6)



Source: Own elaboration

The physical structure, or atomic arrangement, of semiconductors can be divided into three groups: single crystal, polycrystalline and amorphous. The single crystal structure is characterized by a periodic arrangement of atoms obtaining a three-dimensional geometric shape of a parallelepiped. Such is the case of silicon which shares each of its four valence electrons in a covalent bond with each neighboring silicon atom, the solid, therefore, consists of a basic unit of 5 silicon atoms, the original atom plus the four atoms with which it shares its valence electrons.

1.3.2.1 Components of the cell

1.3.2.1.1 Silicon plate doped with phosphorus and boron to obtain a positive and a negative side

1.3.2.1.2 Anti-reflective layer in the form of cones or pyramids that capture the sun's rays more easily

1.3.2.1.3 Grids or fingers. These are responsible for collecting the charges produced in the solar cell

1.3.2.1.4 Bussbar

The Bussbar is the main collector, it passes in the negative and positive part of the cell, where the ribbon is joined to form chains of cells Fig. 1.3.

Figure 1.3 Cell strings



Source of reference: Own elaboration

1.3.2.1.5 EVA

Two layers of Ethyl-Vinyl-Acetate (EVA) are used between the cell matrix. This copolymer is in direct contact with the cells in such a way that it protects the connections between them and provides resistance against vibrations and impacts. In addition, it allows the transmission of solar radiation and is not degraded by ultraviolet radiation.

1.3.2.1.6 Back-Sheet (Tedlar)

This material is regularly used as a three-layer laminate. The outer layer is polyvinyl fluoride (PVF, commercially called TED-LAR). This, together with the front cover, protects the module from moisture and other atmospheric agents, but does not electrically insulate it; a second layer of polyester (Polyethylene Terephthalate) is used for this purpose. Another layer of TEDLAR is used for the internal part. This plastic composite sheet is opaque in nature, usually white in color to reflect the sunlight that the cells do not store onto the roughened back side of the front cover, which reflects the light back into the cells.

The modules are produced by first connecting the individual cells to form strings. Fig. 1.3. These are then reconnected to each other and then laminated by means of equipment called a laminator with all components placed on top of each other except the frame. The purpose of the lamination process is to fix the EVA to protect the cells from external factors and the environment for as long as possible.

1.3.3 Solar panel applications

- Microwave and radio repeater stations.
- Electrification of villages in remote areas.
- Medical posts in rural areas.
- Power for cottages.
- Emergency communication systems.
- Environmental and water quality data monitoring systems.
- Lighthouses, buoys and maritime navigation beacons.
- Water pumping for irrigation systems, drinking water in rural areas and livestock watering troughs.
- Beacons for aeronautical control and signals.
- Cathodic protection systems.
- Desalination systems.
- Signals in railway networks.
- Recreational vehicles.
- Recreational vehicles and boats.
- Railway signalling.

Solar panels are undoubtedly one of the best modern inventions, as well as being probably the invention that contributes the most to the ecology. Solar panels are modules that use the energy that comes from solar radiation, and there are several types, such as those for domestic use that produce hot water or photovoltaic solar panels that produce electricity. Photovoltaic solar panels are composed of cells that convert light into electricity. These cells take advantage of the photovoltaic effect, whereby light energy produces positive and negative charges on two nearby semiconductors of different types, thereby producing an electric field with the capacity to generate current. Photovoltaic solar panels can also be used in solar vehicles. The standardized parameter to classify their power is called peak power, and corresponds to the maximum power that the module can deliver under standardized conditions, which are:

Radiation of 1000 W/m², Cell temperature of 25 °C (not ambient temperature). (Fernandez, M. 2010).

1.4 Solar Cell operation

1.4.1 Structure

Photovoltaic cells are made of semiconductors. Semiconductors are elements that have a very small electrical conductivity, but superior to that of an insulator. The most commonly used are those made of silicon. When the sun's rays strike the cells, the P - N junction of its semiconductors together with its conductive metal helps to produce energy. In this junction, the P-N junction are positive and negative charges that help to produce electric current, due to a potential difference that is created when the cell is illuminated.

1.4.2 Operation of a solar cell

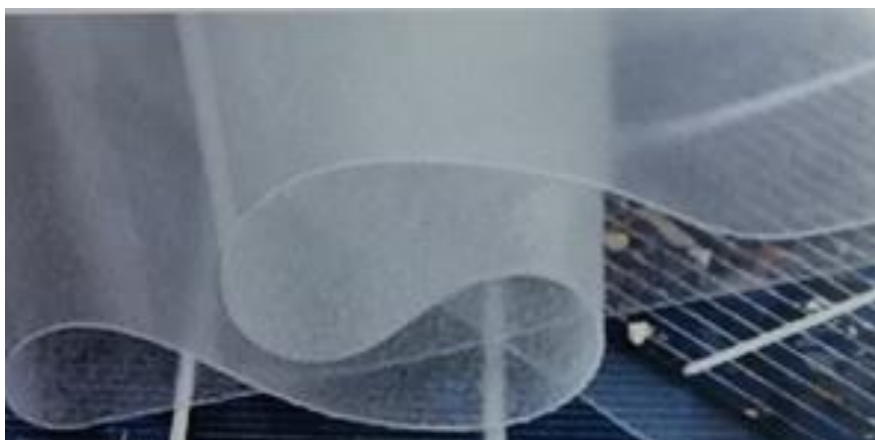
A solar cell is generally composed of silicon, a semiconductor material, which becomes electrically conductive when power is supplied. For this reason, solar cells are predominantly made of silicon, as this material is more than sufficient and has been the most technologically researched to date. There are crystalline solar cells and thin-film solar cells. Crystalline solar cells are divided into polycrystalline and monocrystalline.

The difference between the two types of cells lies in the cell structure. Monocrystalline solar cells consist of a single crystal, while polycrystalline solar cells consist of many small individual crystallites. Monocrystalline solar cells have a higher degree of efficiency, but are more expensive due to the much more complex production. After cutting each of the so-called wafers made from a block of silicon, they are purely and exclusively positively or negatively doped with the addition of foreign atoms, which makes them conductive. The stronger the doping, the more charge carriers are available and the higher the current flow. If two differently doped layers are trapped together, a PN junction is created which creates an electric field.

1.5 Overview of the EVA solar cell protection material

The coating material is one of the most important components of a solar module today and must meet many requirements. Fig. 1.4.

Figure 1.4 Roll of Ethylene-Vinyl-Acetate (EVA) Material



Source: Own elaboration

It is mainly used for bonding and encapsulating solar cells and is intended to protect them against the effects of long-term weathering. The encapsulated protective material used must have the best possible properties against water vapor and oxygen; otherwise, the metal contacts and interconnections may degrade, and the solar module will become unusable. The protective material may also show colour changes (yellowing), due to excessive absorption of oxygen or water vapor and thus cause a loss of transmission.

A high degree of transmission is very important for the material used, since the transmission of the material is directly related to the generation of electricity. The higher the transmission of a material, the lighter the cell can absorb and convert it into electricity. In addition, a good protective material must have a relatively high thermal resistance, as well as good thermal conductivity, since modules can heat up to 90 degrees in direct sunlight. The material must be able to withstand that temperature; the better the thermal conductivity of the encapsulation material, the better the heat can be dissipated. The encapsulation material also ensures greater stability of the module and serves as protection in case of glass breakage. The material used as solar cell protection must, among other things, have a high level of stability against UV radiation, since short-wave radiation can yellow the material and reduce transmission Fig. 1.5, Due to the different materials incorporated with different coefficients of thermal expansion, the protection material must compensate for the stresses occurring so that no cell breakage or damage to the module occurs. All the properties listed here must be fulfilled with a good material in order to produce durable and efficient modules, it should be mentioned that ethylene vinyl acetate is a thermoplastic material.

Figure 1.5 Yellowish EVA material due to degradation



Source: Own elaboration

1.5.1 Introduction to plastics

Plastics are materials consisting of organic or semi-organic macromolecular polymers. They are characterized by an extraordinary range of physical and chemical properties and have therefore become established in almost all areas. In order to use a polymer substance as a material, the polymer must be prepared with additives such as processing aids, stabilizers, pigments and fillers. As a result, mechanical strength, thermal stability or chemical resistance can be individually adapted as required. Plastics are manufactured in a wide variety of types and can now be processed with high precision. In addition, plastics have the advantage over metal, wood and other materials that they can be produced with less energy. Many different plastics technology processes can be used in the preparation and post-processing of plastics, which makes processing simpler and more economical in many respects. In addition, many processes are run simultaneously during material forming, which enables high throughput in production and thus makes the products very economical. Due to the low specific weight of plastics, they are also very suitable as packaging and transport material. In addition, there are very good recycling options for plastics, especially thermoplastics. Due to the many possible uses and the relatively low prices, plastics have established themselves as the highest performing products at affordable prices. Manufacturing costs are essentially determined by material costs. Therefore, an appropriate choice of materials and material-saving construction is economical.

The use of ecologically sensitive plastic is particularly important. In addition to all the advantages, there are some disadvantages that cause problems and risks. Non-renewable raw materials, such as oil or natural gas, are used in the production and processing of plastics, which are harmful to the environment. Since many plastic products today are disposable items, poisonous gases and toxins arise in the case of multiple combustion, especially due to plastics.

Supply of plastics. Plastics consist of many monomers bonded together to form a polymer.

1.5.2 Classification of plastics

Plastics can be classified into certain classes of plastics according to the structure and binding mechanism of the macromolecules. A distinction is made between the following macromolecular types straight chain molecules

Branched-chain molecules

Weakly cross-linked chain molecules

Strongly cross-linked chain molecules

Based on these types of molecules and the resulting binding mechanism, plastics can be divided into the following categories:

1.5.2.1 Thermoplastics

Thermoplastics, also called plastomers, are plastics whose macromolecules form linear or branched molecular chains. These are connected to each other by weak physical binding forces. The more branches the molecules in the chain have, the closer they can be placed next to each other and therefore have greater binding forces. This process of placing them very close to each other and thus having greater binding forces is called crystallization.

However, due to the long molecular compounds, it is not possible to achieve a complete crystalline structure with plastics, which is why we also speak of semi-crystalline thermoplastics. Due to the partially crystalline area of thermoplastics, they are never completely transparent when not colored. This is due to the different scattering of light at the crystal edges.

1.5.2.2 Elastomers

Elastomers are dimensionally stable, but elastically deformable plastics. The glass transition point is below room temperature. Examples of elastomers are: Tires, rubber or gaskets. Elastomer macromolecules have weak cross-linking, which makes them particularly elastic and flexible.

1.5.2.3 Duroplastics or thermosets

Thermosets, which are also known as thermosets, like elastomers, are crosslinked plastics. However, compared to elastomers, thermosets have significantly more crosslinking points and are therefore much harder and tougher. They are very hard and brittle at room temperature and, like elastomers, cannot melt or dissolve.

Cross-linked plastics retain their rigidity even at higher temperatures, which is why they are also called temperature-resistant. At a certain temperature (decomposition temperature), thermosets and elastomers decompose.

1.5.3 Polymerization

In polymerization, a chain reaction takes place, in which unbundled molecules (monomers) are knotted into macromolecules and then form a polymer. A polymerization can only take place if the monomers contain double bonds.

For all types of polymerization, the reaction principle is identical and can be divided into the following sections: Initial reaction. Growth reaction, chain transfer, termination reaction. A distinction is made between the types of polymerization taking into account the reactive particles and can be divided into the following categories: radical polymerization, ionic polymerization, polymerization with transition metal compounds (catalysis).

The most widely used and proven material in the production of photovoltaic modules to date is Ethylene-Vinyl-Acetate (EVA), which is a thermoplastic material.

1.5.4 Properties of thermoplastic polymers

A defining characteristic of thermoplastic polymers is that they can be heated from the solid state to the viscous liquid state and, upon cooling, return to the solid state; furthermore, this cooling cycle can be applied many times without degrading the polymer. The reason for such behavior is that thermoplastic polymers consist of linear (branched) macromolecules that do not crosslink when heated. In contrast, thermosets and elastomers undergo a chemical change when heated, which causes their molecules to cross-link permanently. In fact, thermoplastics deteriorate chemically with repeated heating and cooling. In plastics molding, a distinction is made between new or virgin material and plastics that have been previously molded and have undergone thermal cycling (*e.g.* scrap and defective parts). For some applications only virgin material is accepted. Thermoplastic polymers also degrade progressively when subjected to temperatures below the conversion temperature from the crystalline state to an amorphous state (T_m), this long-term effect is called thermal aging and involves slow chemical deterioration. Some of the thermoplastic polymers are more susceptible to thermal aging than others, and for the same material, the rate of deterioration is temperature dependent.

1.5.5 Thermoplastic Ethylene-Vinyl-Acetate (EVA)

This thermoplastic is known as EVA, a compound based on a copolymer of ethylene with vinyl acetate; this copolymer has elastic properties, which are enhanced by the action of peroxides. The incorporation of the vinyl acetate monomer produces a reduction in the crystallinity of the material, so the properties of ethyl vinyl acetate (EVA) depend largely on the molecular weight and the vinyl acetate content.

The main property of EVA is shock absorption; its main component is latex. Latex is a resin obtained from more than one hundred species of shrubs or oil, which becomes sticky with heat and easily breaks down with cold, so after being initially treated in plates, ethyl acid, vinyl and acetate must be added to obtain EVA (Marcillo Proaño, W. and Moreno Garrido, F. 2008).

1.5.6 EVA composition

The vinyl acetate content in the copolymer varies from 5% to 50%, although for optimal applications the vinyl acetate content should be in the range of 5% to 20%; with 30% to 50% vinyl acetate, it has elastomeric properties.

1.5.6.1 Vinyl acetate content in EVA

The properties of EVA are highly dependent on the molecular weight and vinyl acetate content. Increased vinyl acetate helps to:

- Decrease the crystallinity of EVA.
- The density of EVA increases.
- EVA becomes clear.
- EVA becomes more flexible at low temperatures.
- EVA becomes more impact resistant.
- If the vinyl acetate content is higher than 50%, EVA is amorphous and transparent.
- The higher the percentage of vinyl acetate (VA), the material will exhibit greater expansion with heat.

1.5.6.2 Properties of EVA

- Excellent optical properties;
- High flexibility at low temperatures;
- Good puncture and impact resistance;
- High elasticity and easy processing;
- Good bending strength;
- Low shrinkage temperature;
- Excellent noise insulation;
- Good vibration absorption properties;
- Good resistance to ultraviolet light;
- High mechanical strength in relation to its density;
- Excessive plasticity (when stretched they do not recover). (Marcillo Proaño, W. and Moreno Garrido, F. 2008).

1.6 Role of EVA as a protection material in Photovoltaic Modules

EVA completely covers the cells, preventing the entry of micro or nano quantities of air, as well as the presence of water (humidity) in the cell.

It serves as an electrical insulator, a material that protects the cells (cells) from exposure to the environment and chemical materials, resistant to vibration and also to mechanical shock, the panel is subjected to climatic changes and temperature that can vary from below zero degrees. above 50 ° C, in addition to the degrading effects of ultraviolet radiation, it is stable at high temperatures (180 ° C for short periods of time). (Marcillo Proaño, W. and Moreno Garrido, F. 2008).

1.7 Characteristics of EVA protection material

Ethylene vinyl acetate is a thermoplastic polymer, it is recyclable, incinerable, easy to handle, moldable and non-toxic, it is manufactured in sheets of various thicknesses and sizes, easy to glue, simple to cut, can be painted, washed and has minimal or no water absorption capacity, is resistant to degradation by sunlight, resists chemical attacks and absorption of solvents, in addition to offering its degree of solar energy transmittance, it is quite useful to cover the cells or cells, characteristics for which it is used in photovoltaic modules or solar panels. (Obaya J, 2002).

Ethylene vinyl acetate (EVA) is a copolymer of ethylene and vinyl acetate with relatively strong branches and low crystalline proportions. In the production of vinyl acetate, ethene, oxygen and acetic acid are reacted in a gas-phase process in the presence of a palladium catalyst added to the vinyl acetate. This catalytic addition method, also used by Wachter Very, is a widespread process in the chemical industry.

The vinyl acetate content in EVA copolymers can influence the properties for certain applications. The following properties decrease with increasing VAC content: stiffness, toughness, dimensional stability in heat, electrical insulation values, chemical resistance, electrostatic charge. On the other hand, the following properties increase with increasing VAC content: impact resistance, light transmission and gloss, stress cracking and weathering resistance.

The vinyl acetate content for solar module films suitable for EVA should be in the range of 28-33%. The Etimex brand films used by Scheuten Solar have certain properties that are particularly suitable for applications in the solar sector and have been established over the years. The films have a melting range between 60 and 110°C and can be processed very well under vacuum. At temperatures above 110°C, the molecules cross-link to form a transparent, elastic and heat-resistant layer that protects the modules from the effects of weathering for a long time.

However, working with EVA requires great care. For example, crosslinking does not start at a certain temperature, but rather over a wide temperature range. This means that an exact process time must be determined for each lamination process at a given temperature. Because sensitive webs occur again and again below or above the bonds, they have a negative effect on the properties of the module. therefore, an extraction is carried out to determine the gel content at regular intervals, which provides information on the crosslinking or degree of branching of the material. A good network should be in the range of 80-95% gel content. The short shelf life of films in air is also an issue. After about 4 hours in air, the films become unusable because important additives diffuse out and the necessary adhesion to the glass and subsequent film can no longer be guaranteed. Ethylene vinyl acetate can only be melted once and cannot be processed further after crosslinking, which offers poor repair options in the production of solar modules. Several embedding materials, especially from the field of thermoplastic elastomers, have been able to solve these problems and can be used as an alternative material in addition to EVA. Polymers are still rarely or not at all used in solar module production, so there is very little experience in h The EVA position is bonded to the cells, but it is also often used as a post-module base for added security with the material called TPT (Tedlar-PET-Tedlar) which consists of a three-layer sandwich laminate made of a layer of polyester film between two layers of PVF. (Marcillo Proaño, W. and Moreno Garrido, F. 2008).

1.8 Tests for the Control and Quality Assurance of the Protective Material (EVA) in Solar Panels

Methodology

1.8.1 Gel content

This gel content test is intended to determine the amount of vinyl acetate present in the Ethylene-Vinyl-Acetate, which is directly related to the resistance of the material. This test tests the resistance of the encapsulation layer material of the module, ensuring that the current conduction pathways of the cells are hermetically isolated from the elements.

In this test the content was determined in five different points of the module to obtain an average of the gel content of the whole material, for this purpose the following activities were carried out:

- 1.8.1.1 A temperature of 105 ° C was set in the Memmert Stove.
- 1.8.1.2 5 Glass flasks with their respective lids and 5 Whatman Brand # 51 filter papers were placed in the oven for 2 hours.
- 1.8.1.3 After 2 hours, the flasks, lids and filter papers were removed from the oven.
- 1.8.1.4 The filter papers were placed in the desiccator.
- 1.8.1.5 The flasks with their respective lids were placed in a clean place for later use.
- 1.8.1.6 5 Samples of 10x10 cm were cut out of the laminated EVA.
- 1.8.1.7 1.00 gram of EVA (W1) was weighed from each sample.
- 1.8.1.8 100 ml of toluene was prepared for each sample (by dissolving 0.0865 grams of BHT in 100 ml of toluene).
- 1.8.1.9 Each EVA sample was placed in a bottle with 100 ml of the prepared toluene solution, and the bottles were capped.

1.8.1.10 The flasks were placed in the oven at $60\text{ }^{\circ}\text{C} (\pm 5)$ for 24 hours.

1.8.1.11 The flasks were removed from the oven and their respective lids were removed and allowed to stand for 1 hour.

1.8.1.12 Each filter paper was weighed and the weight was recorded as (W2).

1.8.1.13. In the fume hood area, a glass funnel was placed over a 1000 ml Erlenmeyer flask and filter paper was placed over the funnel and the samples were filtered.

1.8.1.14. It was put to a temperature of $105\text{ }^{\circ}\text{C}$ in the oven and the samples were placed with the filter paper and allowed to dry to constant weight.

1.8.1.15. Each filter paper was weighed with the sample residue and the weight (W3) was recorded.

1.8.1.16 The percentage of gel content was calculated with the following formula:

$$\% \text{ gel content} = \frac{w3 - w2}{w1} \times 100 \quad (1)$$

1.8.2 Adhesion test

The adhesion test measures the adhesion between individual materials and is given in N / cm. The adhesion should be at least 25 N / cm in all tests and should be distributed as evenly as possible throughout the laminate. The adhesion of the protective material must have on the one hand, a good adhesion to the glass and, on the other hand, a good reflection and weather resistance.

This test was carried out using equipment (dynamometer), which separates the bus tape from the silicon cell vertically and records the force versus distance across the bar when the cable (tape) is pulled from the bottom upwards. of the cell. Fig.1.6. It is used to measure how hard the solder penetrated the cell and defects such as under soldering or over solder penetration can be detected.

Figure 1.6 Dynamometer for adhesion test



Source: Own elaboration

1.8.3 Durability tests

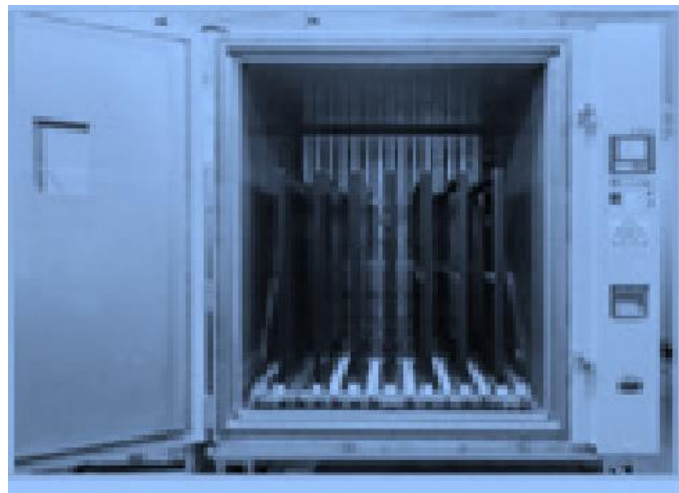
1.8.3.1 General

Solar panels must be tested with durability tests, which are intended to provide information on the useful life of the panel when it is in operation, since it will be exposed to the elements, sudden climatic changes (temperature, humidity, salt spray, dew, etc.), and environmental agents of the place where it is installed.

IEC and JIS standards stipulate that the modules must be tested for inclusion in an environment with a temperature of 85°C and a humidity of 85, they also require that the modules must be tested through 10 cycles of temperature fluctuations between -40°C and 85°C (where a cycle lasts 24 hours or less and the humidity is 85% and the temperature is 85°C).

The hot and humid climate is difficult not only for people, but also for solar modules. Prolonged exposure to high temperature and high humidity can accelerate the degradation of materials used in solar modules and can result in insulation failure or reduced electrical output [Kahtris R. (2011)]. In this test, solar modules are placed inside a heat and humidity test chamber. Figure 1.7. The electrical output of the modules and the harmful effects on them are carefully controlled. A dew condensation and freeze dew test is also performed in recognition of the fact that geographic areas susceptible to high temperatures and high humidity contents are also often prone to dew and frost condensation induced by temperature changes. Between day and night. In this test, dew and frost condensation is generated inside the test chamber, and the electrical output and any effects on the materials are monitored.

Figure 1.7 Thermal shock test chamber



Source: Own elaboration

1.8.3.2 Testing regulations

Photovoltaic panels must comply with a series of guarantees, regulations and be certified. This ensures that the modules are able to withstand the different environmental conditions to which they are exposed during their lifetime (IEC61730, IEC 61215, IEC 61646 or IEC61701).

Perform durability tests according to the specifications of IEC 61215, IEC 61646. The climatic tests to be performed are:

UV preconditioning with a bandwidth of 280 to 385 nm; with a maximum irradiation intensity of 250W / m²; at a module temperature of +60 to ± 5 ° C; and total UV irradiation of 15kWh / m² and a minimum of 5kWh / m² in the bandwidth between 280 and 320nm. This test is intended to precondition the module with ultraviolet light, prior to thermal cycling.

1.8.4 Thermal shock test

50 or 200 thermal cycles from -40°C to $+85^{\circ}\text{C}$.

Purpose

The purpose of this test is to determine the ability of the module to resist thermal imbalance, fatigue and other stresses caused by repeated temperature changes.

Apparatus:

- A climatic chamber with automatic temperature control, means to circulate air within, and means to minimize condensation on the module during the test, capable of thermally cycling one or more modules.
- Equipment for mounting or supporting the module(s) in the chamber to allow free circulation of the surrounding air. The thermal conduction of the support or stand should be low, so that, for practical purposes, the module(s) is thermally insulated.
- Equipment to measure and record the temperature of the module(s) with an accuracy of $\pm 1^{\circ}\text{C}$. Temperature sensors should be placed on the front or rear surface of the module near the center. If more than one module is tested at the same time, it will be sufficient to monitor the temperature of a representative sample.
- Equipment to apply a current equal to the maximum power current of the module(s) under test.
- Equipment to control the current flow through each module during the test.

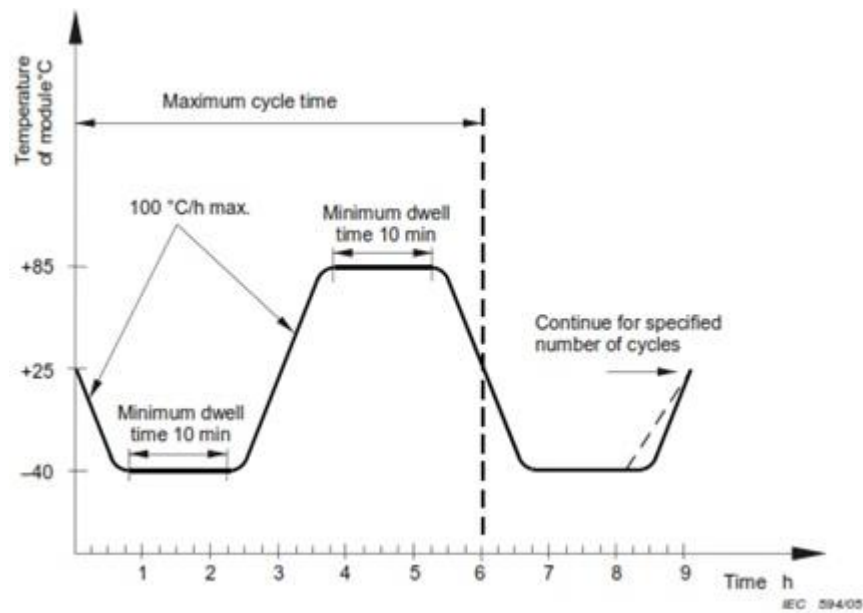
Process:

- Install the module(s) at room temperature in the chamber Fig. 7.7.
- Connect the temperature monitoring equipment to the temperature sensors. Connect each module to the appropriate power supply by connecting the positive terminal of the module to the positive terminal of the power supply and the second terminal accordingly.

During the 200 thermal cycle test, set the current flow to the maximum measured power of the current STC within $\pm 2\%$. The current flow shall be maintained only when the module temperature is above 25°C . No current flow is required during the thermal cycle 50 test.

- Close the chamber and cycle the module(s) between module temperatures of $-40^{\circ}\text{C} \pm 2^{\circ}\text{C}$ and $85^{\circ}\text{C} \pm 2^{\circ}\text{C}$, according to the profile in Figure 1.8. The rate of temperature change between the high and low ends shall not exceed $100^{\circ}\text{C}/\text{h}$ and the module temperature shall remain stable at each end for a period of at least 10 minutes. The cycle time shall not exceed 6 hours unless the module is hot, a capability requiring a longer cycle.
- During the test, record the module temperature and monitor the current flow through the modules.

Figure 1.8 Temperature Profile for Thermal Shock Testing



NOTE: In a module with parallel circuits, an open circuit in one branch will cause a discontinuity in the voltage, but will not cause it to go to zero

Source of reference: IEC 61215

Final measurements.

After a minimum recovery time of 1 h, measure the panel power.

Requirements.

The requirements are as follows:

- No interruption of current flow during the test.
- No evidence of visual defects as defined in clause 7.
- Maximum output power degradation shall not exceed 5% of the value measured before the test.
- The insulation resistance shall meet the same requirements as for the initial measurements.

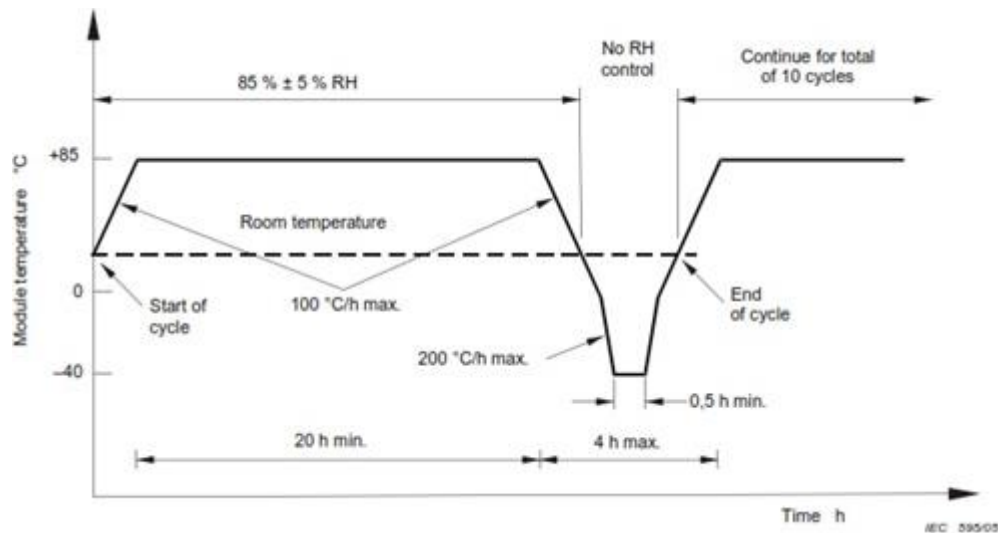
1.8.5 Freezing Test Humidity: 10 cycles from -40°C to +85°C with 85% relative humidity.

Objective

The purpose of this test is to determine the ability of the module to withstand the effects of high temperatures and humidity followed by freezing temperatures. It should be mentioned that this is not a thermal shock test.

Apparatus

- A climatic chamber with automatic temperature and humidity control, capable of subjecting one or more modules to the freezing cycle specified in Figure 1.9.

Figure 1.9 Humidity-freezing cycle

Reference source: IEC 61215

- Equipment for mounting or supporting the module(s) in the chamber, in order to allow free circulation of the surrounding air. The thermal conduction of the support or stand should be low, so that, for practical purposes, the module(s) is (are) thermally insulated.
- Equipment for measuring and recording the module temperature to an accuracy of $\pm 1^\circ\text{C}$. (It is sufficient to monitor the temperature of a representative sample, if more than one module is being tested).
- Equipment for monitoring, throughout the test, the continuity of the internal circuit of each module.

Process

- Place a suitable temperature sensor on the front or rear surface of the modules.
- Install the module(s) at room temperature in the climatic chamber.
- Connect the temperature monitoring equipment to the temperature sensors.
- After closing the chamber, run the module(s) 10 complete cycles according to the profile in Figure 1.9. The maximum and minimum temperature shall be $\pm 2^\circ\text{C}$, specified levels and relative humidity shall be maintained within $\pm 5\%$ of the specified value at all temperatures above ambient temperature.
- During the test, record the module temperature.

Final measurements:

After a recovery time of between 2 h y 4 h, repeat the power and insulation resistance measurement test.

Requirements

The requirements are as follows:

- No evidence of visual defects as defined in clause 7.
- The degradation of the maximum output power shall not exceed 5% of the value measured before the test.
- The insulation resistance shall meet the same requirements as for the initial measurements.

1.8.6 Damp Heat Test: 1000h at + 85 ° C and 85% relative humidity

Thermal and climatic chambers have been developed for large specimens. The test chambers are available in 5 standard sizes (8, 12, 16, 21 and 28 m²). The unit consists of a fan, a cooling unit, humidification and heating equipment, an on/off system and a control system.

This test is intended to determine the module's ability to withstand the effects of long-term moisture penetration.

Process

The test was conducted in accordance with IEC 60068-2-78 with the following provisions:

a) Preconditioning.

- The modules are introduced into the chamber without preconditioning.

b) Test conditions:

- Test temperature: 85 ° C ± 2 ° C.
- Relative humidity: 85% ± 5%.
- Test duration: 1000 h.

1.9 Results

The importance of verifying and controlling the protection material in solar panels is of vital importance to ensure their useful life. As we all know, Quality Assurance is a system that focuses on products, from their design to the moment they are shipped to the customer and concentrates its efforts on defining processes and activities that allow to obtain products according to specifications.

The average results obtained for gel content (Section 1.8.1) were 82.5 to 87.5%, which indicates that the material will behave correctly during its useful life, ensuring that the modules will not degrade before 25 years. See Table 1.1.

Table 1.1 EVA gel content results

No. of Panel	Gel content in %	Gel content in %	Mean	Laminating temperature (°C)	Laminating time (Minutes)
1	85, 90, 91, 83, 82		86.2	145	16
2	79, 80, 90, 92, 91		86.5	146	16
3	80, 82, 79, 82, 90		82.5	146	15.30
4	90, 84, 85, 87, 91		87.5	147	16
5	78, 82, 84, 86, 85		83	146	15.30

Source of consultation: Own elaboration

Regarding the adhesion test (Section 2.2), the results obtained are within specification, higher than the minimum established value (25N / cm). Table 1.2, which ensures a good and permanent connection.

Table 1.2 Adhesion test results. After lamination at 150 °C

Sample	Values in 4 areas of the sample in N/cm	Average values in N/cm
1	40, 50, 50, 55	48.8
2	56, 55, 45, 55	52.8
3	56, 55, 50, 56	54.3
4	45, 47, 50, 53	48.8
5	46, 48, 50, 51	48.8

Source: Own elaboration

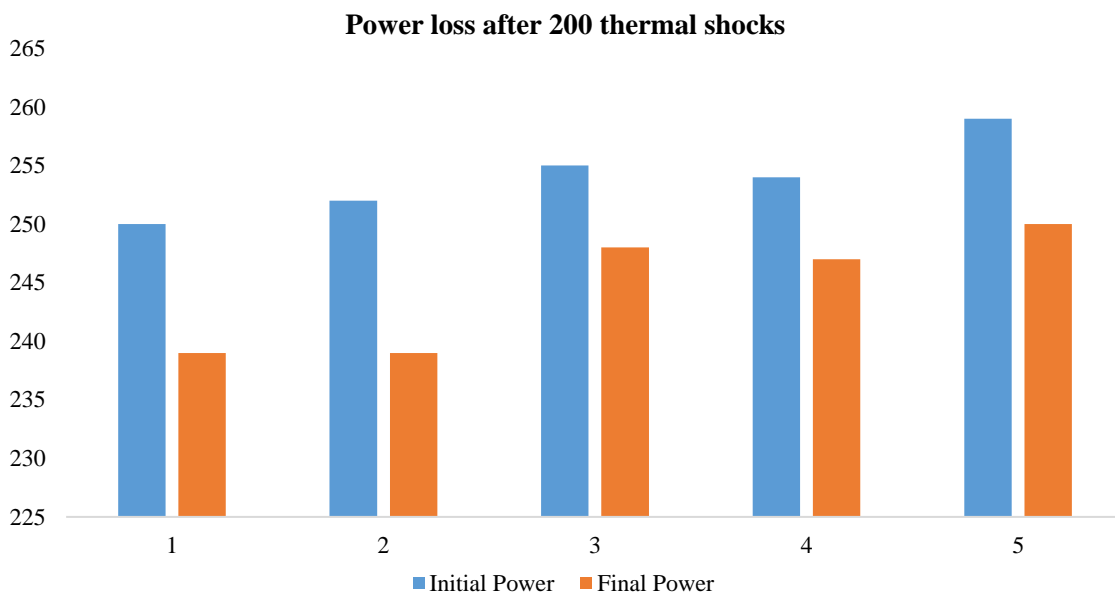
In the ultraviolet (UV) preconditioning test (Section 1.8.4), the EVA did not show any color change. Regarding the 200 thermal cycling tests (Section 1.8.5), it was found that after the test, the power change in 80% of the solar panels is within specification, only one of them showed power slightly above 5%, which is good, and indicates that the EVA served its purpose well, since no discoloration was observed in the material after the test. Table 1.3.

Table 1.3 Power output of solar panels after exposure to 200 thermal shocks

Initial power in Watt	Power after 200 thermal shocks in Watt	Power loss in %. Specification: 5% maximum
250	239	4.4
252	239	5.1
255	248	2.7
254	247	2.8
259	250	3.5

Source: Own elaboration

Graphic 1.1 Power of solar panels after being subjected to 200 thermal shocks



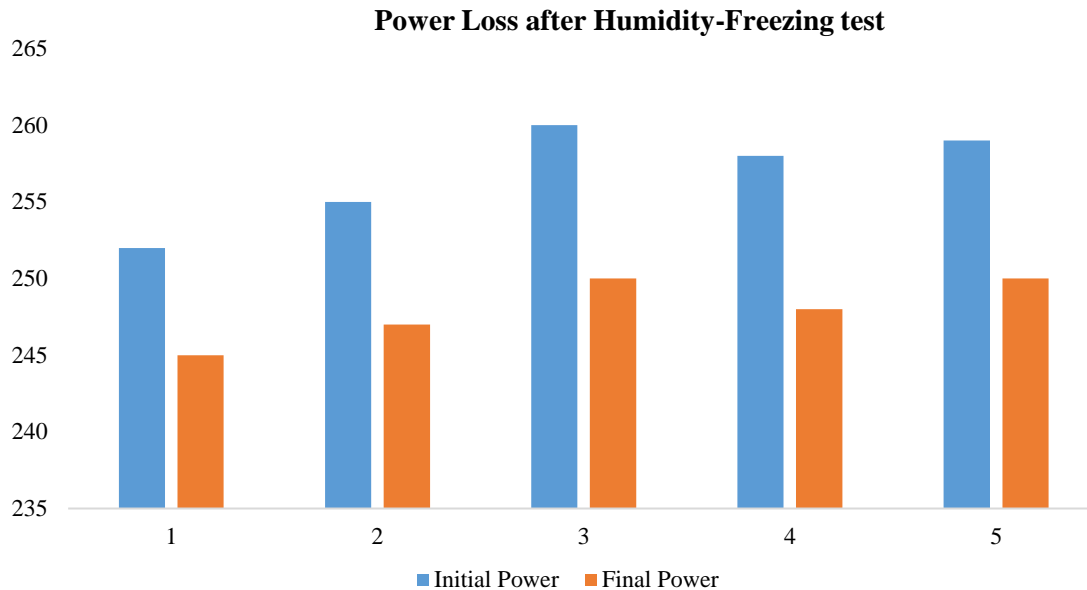
Source: Own elaboration

Regarding the freezing humidity test, discussed in section 1.8.5 the solar panels held up, as the power change was 2.8 to 3.9% after the test. Table 1.4, which indicates the good performance of the EVA protection material, as it also showed no colour change.

Table 1.4 Power of solar panels before and after the freezing humidity test

Initial power	Power after 200 thermal cycles	% Power loss Specification 5% maximum
252	245	2.8
255	247	3.1
260	250	3.8
258	248	3.9
259	250	3.5

Source: Own elaboration

Graphic 1.2 Power results after the Humidity-Freezing test

Source: Own elaboration

After the heat-humidity test. Section 1.8.6, no defects were found in the modules, as well as no color change in the EVA protective material.

1.10 Acknowledgements

- To the Centro de Cooperación Academia Industria (CCAI), for its support in the preparation of this chapter.
- To all the collaborators for their dedication and commitment to the realization of this chapter.

1.11 Conclusions

In this chapter, topics of interest for the quality assurance of the encapsulating material of solar panels were addressed, which gives us an idea of the importance of using Metrology in any section of the process for its control. The measurement allows us to know if the characteristics that we want to control in any process are within or out of specification according to the established standards, so that helps us to take preventive actions and continuous improvement in the processes.

With the gel content test, it was found that the lamination process was correct since the gel content values were found to be 82.5% to 87.5% above the specified 80%.

In the adhesion test it was possible to corroborate that the force necessary to peel off the material was within the specification of 50 N / cm to 56N / cm, values above the minimum established in the Standard 40N / cm.

The UV preconditioning test allowed us to confirm that after the test the EVA did not show any colour change, indicating that it did not degrade.

In relation to the durability tests of the solar panels, this study gives us the guideline to ensure the correct operation of the solar panels for at least 25 years, since the measurement of the power loss at the end of the tests allows us to ensure it.

According to the results of the thermal cycles, the number of thermal cycles determines the useful life of a solar panel, the 200 thermal cycles correspond to 25 years of power generation from a solar panel in optimal conditions, if up to this cycle the panel does not decrease by 5% in terms of power loss, so it is assured that it has a longer life than those that degrade before meeting the recommended number of cycles.

In addition, the material after testing showed no significant visible damage (fractures, cracks, bent or deformed surfaces, as well as ground faults).

1.12 References

A. Gabor, M. Ralli, S. Montminy, L. Alegria, C. Bordonaro, J. Woods, L. Felton, “Soldering induced damage to thin Si solar cells and detection of cracked cells in modules”. Proceedings of the 21st EUPVSEC, Dresden, Germany, 2006, pp. 2042–2047.

Halm, V. Mihailitchi, G. Galbiati, L. Koduvelikulathu, R. Roescu, C. Comparotto, R. Kopecek, K. Peter, J. Libal, “The Zebra cell concept - large area n-type interdigitated back contact solar cells and one-cell modules fabricated using standard industrial processing equipment”, Proceedings of the 27th EUPVSEC, Frankfurt am Main, Germany, 2012, pp. 567-570.

Schneider, M. Pander, T. Korvenkangas, S. Aulehla, R. Harney, T. Hort-tana, “Cell to Module Loss Reduction and Module Reliability Enhancements by Solder Ribbon Optimization”, Proceedings of the 29th EUPVSEC, Amsterdam, Netherlands, 2014, pp. 165-170.

Barrera, P. (2009). “Simulación y caracterización de celdas solares multijuntura y de silicio cristalino para aplicaciones espaciales”. (Tesis de Doctorado). Universidad Nacional de General San Martín Comisión Nacional de Energía Atómica Instituto de Tecnología. República Argentina.

C. Ferrara, “Philip Why do PV Modules Fail?, in: Proceedings of the International Conference on Materials for Advanced Technologies, Singapore”, Energy Procedia 15, 2011, 379–387.

Cengel, Y., y Hernán, P. J. (2004). “Transferencia de calor”. México: McGraw-Hill.

Duran, J. C., Bruno, C. J., y Bolzi, C. G. (2002). “Convenio de cooperación CONAE-CNEA: Desarrollo, fabricación y ensayo de paneles solares para misiones satelitales argentinas.” Profesional Independiente, 20(1), 0329-5184.

Kunze, S. Kajari-Schröder, X. Breitenmoser, B. Bjørneklett, “Quantifying the risk of power loss in PV modules due to micro cracks” Solar Energy Materials and Solar Cells 95, 2011, pp. 1131-1137.

M. Sander, S. Dietrich, M. Pander, M. Ebert, M. Karraß, R. Lippmann, M. Broddack and D. Wald, “Influence of manufacturing processes and subsequent weathering on the occurrence of cell cracks in PV modules” Proceedings of the 28th EUPVSEC, Paris, France, 2013, pp. 3275-3279.

IEC 61215 Cualificación del diseño y homologación Año: 2005. Edición: 2. Silicio Cristalino

P. Hacke, K. Terwilliger, S. Glick, D. Turdell, N. Bosco, S. Johnston, S. Kurtz, “Test-to-Failure of Crystalline Silicon Modules”, in: Proceedings of 35th IEEE Photovoltaic Specialists Conference, Hawaii, 2010, pp. 248–250.

R. Kahtri, S. Agarwal, I. Saha, S.K. Singh, B. Kumar, “Study on Long Term Reliability of Photovoltaic Modules and Analysis of Power Degradation Using Accelerated Aging Tests and Electroluminescence Technique”, in: Proceedings of the 1st International Conference on Silicon Photovoltaics, Freiburg, Energy Procedia 8, 2011, 396–401.

S. Kajari-Schroder, I. Kunze, U. Eitner, M. K. “ontges, Spatial and orientational” distribution of cracks in crystalline photovoltaic modules generated by mechanical load tests, Solar Energy Materials and Solar Cells 95 (2011) 3054–3059.303.

Chapter 2 Four dimensions for the commercialization of technologies in public institutions of higher education (IHE)

Capítulo 2 Cuatro dimensiones para la comercialización de tecnologías en instituciones públicas de educación superior (IES)

VARGAS-G., Jaqueline†*, RODRÍGUEZ-H., Gloria P. and GONZÁLEZ-PASTRANA, Juvelia

Tecnológico de Estudios Superiores de Jocotitlán, Business Management Engineering, Mexico.

ID 1st Author: *Jaqueline, Vargas-G.* / **ORC ID:** 0000-0003-4672-7259

ID 1st Co-author: *Gloria P., Rodríguez-H.* / **CVU CONACYT ID:** 1157260

ID 2nd Co-author: *Juvelina, González-Pastrana* / **CVU CONACYT ID:** 1157228

DOI: 10.35429/H.2021.9.1.24.32

J. Vargas, G. Rodríguez and J. González

* jaqueline.vargas@tesjo.edu.mx

A. Ledesma (Coord.). Engineering Science and Technology. Handbooks-©ECORFAN-México, Estado de México, 2021.

Abstract

An essential element in the scientific and technological development has been the institutions of higher education (IHE), their role in economic development has been transcendental. The IHE's contribute to innovation in the development of applied research aimed at generating useful technologies for society, in incorporating new technologies and in the direct or indirect application of technological innovations. The aspects worked by IHE are research, the generation of knowledge and technology, however, the challenge that currently arises for the IHE's refers to the approach and management of their structures and actions and the preparation of their resources in the sense to place the technologies generated at the disposal of the market and society. In this context, the objective of this work was the application of a radar framework of critical success factors (RFCSF) for the commercialization of technologies in public universities, to a Technological Institute of Higher Studies in Mexico. The RFCSF allows monitoring four dimensions (Strategy and management, Culture and Structure, Market and Technologies and finally Individual Competencies) and sixteen indicators associated with these dimensions, in order to provide a diagnosis and improvements in the technology commercialization process.

Technological transfer, Technological commercialization, Public Institutions of Higher Education

Resumen

Un elemento esencial en el desarrollo científico y tecnológico han sido las instituciones de educación superior (IHE), su papel en el desarrollo económico ha sido trascendental. Las IES contribuyen a la innovación en el desarrollo de la investigación aplicada orientada a generar tecnologías útiles para la sociedad, en la incorporación de nuevas tecnologías y en la aplicación directa o indirecta de las innovaciones tecnológicas. Los aspectos trabajados por las IHE son la investigación, la generación de conocimiento y la tecnología, sin embargo, el reto que se plantea actualmente para las IHE se refiere al planteamiento y gestión de sus estructuras y acciones y a la preparación de sus recursos en el sentido de poner las tecnologías generadas a disposición del mercado y de la sociedad. En este contexto, el objetivo de este trabajo fue la aplicación de un marco de radar de factores críticos de éxito (RFCSF) para la comercialización de tecnologías en universidades públicas, a un Instituto Tecnológico de Estudios Superiores de México. El RFCSF permite monitorear cuatro dimensiones (Estrategia y gestión, Cultura y estructura, Mercado y tecnologías y finalmente Competencias individuales) y dieciséis indicadores asociados a estas dimensiones, con el fin de proporcionar un diagnóstico y mejoras en el proceso de comercialización de tecnología.

Transferencia tecnológica, Comercialización tecnológica, Instituciones Públicas de Educación Superior

2.1 Introduction

The commercialisation (transfer, licensing and assignment) of technology has nowadays been consolidated as an important activity between universities, Higher Education Institutions (HEIs), companies and governments. This activity constitutes the main point in the construction of a knowledge-based economy, so that this economy is the tool that generates value and wealth. However, to achieve a knowledge-based economy, it is necessary that the knowledge generated in universities and HEIs is made available to businesses and society (Padilla, 2010; Kirchberger; Pohl, 2016; Sira, 2016; Miller; Mcadam; Mcadam, 2016).

The commercialisation of technologies depends on the effects of organisational and individual variables ranging from specialised institutes to the business sector (Santiago, 2006). It is a multidimensional, complex, multidisciplinary and inter-organisational process. For its monitoring and analysis it is necessary to take into account a large number of dimensions and factors (Sira, 2016). Therefore, it is necessary to use indicators that can provide elements for universities to plan and direct management, research and development processes for the commercialisation of technologies.

Over the last few years, a large number of studies have been carried out in order to identify actors and factors involved in the commercialisation of technologies generated in universities. These studies mainly involve Technology Innovation Nuclei in Universities - NITs or Technology Transfer Offices - TTOs; intellectual property, patents, university-firm relations and innovation management (Sorensen; Chambers, 2008; Hoye; Pries, 2009; Swamidas; Vulasa, 2009; Azevedo; Mazzoni; Silveira, 2013; Gómez; Daim; Robledo, 2013; Días; Porto, 2014; Vega-Jurado et al. 2017).

Moreover, it has been perceived that institutions have difficulties in carrying out a self-diagnosis to identify opportunities related to the production and commercialisation of technology. Therefore, it is necessary to know the reality of the factors that involve the commercialisation of technologies in universities and higher education institutions.

The first part of this paper presents the background and context of technology commercialisation in universities, section 2 considers the theoretical definitions that underpin this work, section 3 describes the methodology and research design, section 4 presents and discusses the data collected from one HEI based on the study and analysis of factors associated with the radar framework, the last section presents the conclusions.

2.2 Theoretical reference

In Latin America, where the production of knowledge is mainly carried out by public universities, it is necessary to investigate and propose significant changes in order to support innovation processes. Changes that consider substantial changes in the curriculum, academic structure, educational training, accompanied by fundamental transformations in administration, management and organisation of activities related to the invention, dissemination and commercialisation of knowledge and technologies (Didriksson, 2004; De Benedicto, 2011; Pastrana et al. 2020; Alonso et al. 2020).

With the advent of the Bayh Dole Act in the United States in 1980, the range of government-funded research expanded. The impact of this had a decisive influence on the impetus for the negotiation of research results and on the importance given to applied research by universities. Therefore, a new definition of the university's mission was necessary, the so-called "third mission" understood in a broad sense as the effective transfer of knowledge and technologies from the university to organisations and society (Rodríguez; Casani, 2011; De Benedicto, 2011).

At the same time, there is a general interest in what concerns the scientific field to establish a common element which is the generation and transmission of knowledge to contribute to local and regional development, for the empowerment of individuals in an environment of constant change (Calderón-Martínez, 2017).

In this way, the third mission can be formalised through three axes: a) the first axis, which explains corporate acceptance: where the university as a generator of technology in the R+D+i (Research, Development and Innovation) system, acts as an agent and at the same time as a space that dynamises innovation processes. That is to say, the generation of innovation that society needs, and which encompasses activities that universities carry out with different social agents with which they have a relationship and to which they transfer knowledge; b) Second axis, where the university, through the implementation of knowledge transfer processes, acts as an entrepreneurial agent. That is, an entrepreneurial university based on the process of commercialisation of university research results; and c) Third axis, of social cooperation, related to the extension function acting in the sustainable development and growth of the social community where the university is integrated, facilitating greater dissemination in R&D&I processes in the knowledge society and economy (Campos, 2007; Calderón-Martínez, 2017; Fernandes; O' Sullivan 2021).

As can be seen, the second axis points to the conception of the third mission with the entrepreneurial activity of the university, i.e. as a basic institution for the transfer of knowledge. The entrepreneurial university proposed by Etzkowitz et al. 2000; Etzkowitz, 2004, has as one of its objectives the development, commercialisation of technologies and support for the entrepreneurial culture. The entrepreneurial university is consolidated in new policies and culture for an adequate management of transfer instruments such as patents, licences or the creation of technology-based and social enterprises.

It should be noted that, in order to achieve an industrial, commercial and social goal, technology, from a general perspective, includes the knowledge, methods and materials used and generated. It commonly combines results with techniques in order to make science work in practice, therefore, it may also conceive processes as know-how and unique business practices (Anokhin, 2011).

2.3 Methodology

The present work is classified in the context of applied and descriptive research, with a qualitative approach associated with empirical research based on the Radar Framework of Critical Success Factors (González et. al 2018) (see Table 2.1 and Fig. 2.1), whose referential framework, endorsed by specialists, assesses four dimensions and sixteen variables that are used in the present work, which was tested in public universities in southeastern Brazil, so now it is intended to apply it to a TES in Mexico.

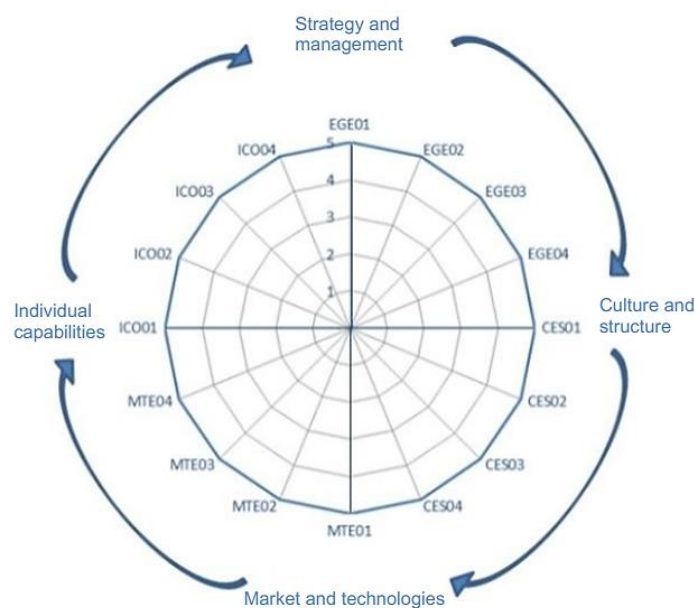
Table 3.1 shows four dimensions considered by specialists to identify the critical success factors for the commercialisation of technologies in public universities, each dimension contains four variables that serve as identifiers to assess each dimension. The radar graph (see Fig. 2.1) shows in a more visual way the values of each dimension and variable.

Table 2.1 Critical Success Factors (CSF) Framework for Commercialisation

Dimensions	Acronyms	Factors	Variables
Strategy and management	EGE	Public and governmental policies Strategic planning Top management Intellectual property	<i>EGE01</i> <i>EGE02</i> <i>EGE03</i> <i>EGE04</i>
Culture and structure	CES	Organisational Culture Entrepreneurial training Structure for technology development (Technological support) Structure and promotion of entrepreneurship	<i>CES01</i> <i>CES02</i> <i>CES03</i> <i>CES04</i>
Market and technologies	MTE	Market orientation University-business link Quality and applicability of technologies Dissemination of new technologies	<i>MTE01</i> <i>MTE02</i> <i>MTE03</i> <i>MTE04</i>
Individual skills	ICO	Reputation and quality of scientific output Know-how for innovation Entrepreneurial profile of researchers Problem-solving competence	<i>ICO01</i> <i>ICO02</i> <i>ICO03</i> <i>ICO04</i>

Source: González et al., 2018

Figure 2.1 FCE radar for commercialization of technologies in public universities, (radar graph)



Source: González, 2018

In this work we sought to apply the Radar Framework (González et. al 2018) in a Tecnológico de Estudios Superiores (TES) in the State of Mexico, where we used a questionnaire sent by email to staff related to the processes of entrepreneurship, intellectual property and commercialisation of technologies in universities.

The questionnaire was elaborated and applied considering the dimensions and factors related to the Framework. For each factor, two or more questions were created, with associated answers on a 5-point likert scale (1- strongly disagree to 5 - strongly agree).

15 people were contacted (Table 2.2), 2 administrative employees and 13 teachers of the TES case study from which 9 responses were obtained (2 administrative employees and 7 teachers).

Table 2.2 TES, contacted and number of responses obtained

Institution	Number of people contacted	Number of responses
TES	15	9

Source: Own elaboration

The data obtained were classified and represented in radar map graphs to allow for better interpretation and analysis of the information collected. This in order to provide an adequate view of the characteristics of the critical success factors that impact technology commercialisation. The results will be described below.

2.4 Results and discussion

In this section, the characteristics of the TES in the case study are presented. Additionally, a radar map is generated identifying the critical factors for the commercialisation of technologies based on the data collected.

2.4.1 Description of the TES

The TES that is the subject of this research is located in the North of the State of Mexico.

It has 12 degrees programmes (Electromechanical Engineering, Industrial Engineering, Computer Systems, Mechatronics Engineering, Business Management Engineering, Logistics Engineering, Chemical Engineering, Materials Engineering, Animation and Visual Effects Engineering, Tourism, Architecture and Public Accountant) and a master's programme in Industrial Engineering.

This TES is part of a programme for the strengthening of the academia-industry relationship based on the creation of linkage centres called: Centros de Cooperación Academia Industria (CCAI), which since 2014 have been implemented in four higher education institutions in the State of Mexico. The programme aims to promote the development of competences associated with the strategic areas identified in the State Development Plan and the Innovation Agenda, strengthening the infrastructure of the CCAIs in technological lines of cross-cutting application that are closely related to the productive sector.

The CCAIs are born from the link established by the Mexican Agency for International Development Cooperation (AMIXID) and South Korea through the Korean Development Institute (KDI) with the project "Improving Innovation Capacities for the Sustainable Development of the Mexican Economy" and with the advice of the Korea Polytechnic University (KPU) in the framework of the Knowledge Sharing Program (KSP), with the aim of improving the competitiveness and productivity of companies, mainly MSMEs in the State of Mexico, through basic and applied research projects, technology transfer and training of highly specialised human resources in technological areas.

It has been considered that this TES, for this study due to its characteristics, whose structure dedicated to linking and technology transfer is concentrated in a four-storey building, where it houses areas of: training in robotics, physical characterisation of materials, plastics and metal mechanics, work areas for companies, a training and meeting room, a reverse engineering laboratory, and spaces for stays of researchers and students. During the development and growth that has taken place in the almost seven years since its creation, it has made collaboration agreements with various companies with a tendency towards projects related to materials characterisation, additive manufacturing, polymers and process and product optimisation.

2.4.2 Radar Chart - Critical Success Factors for Commercialising Technologies

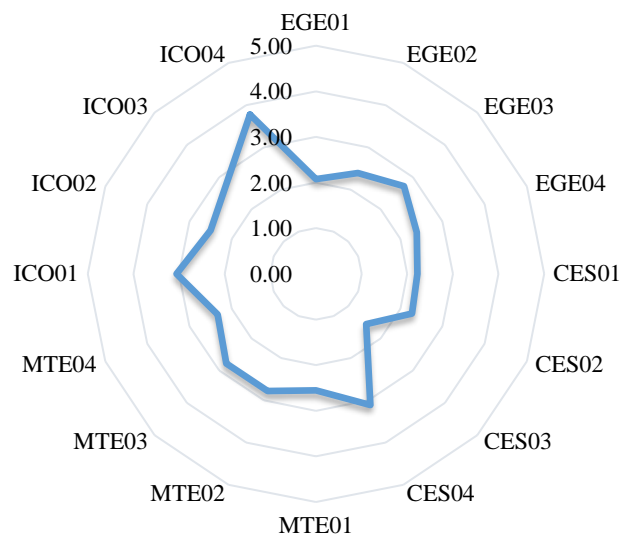
The values represented in table 2.2 were collected on the basis of the questionnaire applied in the TES and were used to generate the radar graph representation (Table 2.3). In column three the average corresponds to each of the factors and column four shows the average for each dimension.

Table 2.3 Values and averages for dimensions and factors according to the responses collected from the questionnaires

Dimension	Factor	Average	Average size
Strategy and management	EGE01	2.07	2.39
	EGE02	2.39	
	EGE03	2.72	
	EGE04	2.39	
Culture and structure	CES01	2.22	2.29
	CES02	2.28	
	CES03	1.56	
	CES04	3.11	
Market and technologies	MTE01	2.56	2.61
	MTE02	2.78	
	MTE03	2.78	
	MTE04	2.33	
Individual skills	ICO01	3.06	3.02
	ICO02	2.50	
	ICO03	2.78	
	ICO04	3.78	

Source: Own elaboration

Figure 2.2 shows the radar graph originating from table 2.3 This radar graph of the TES shows the visual representation of the results of the perception of the critical factors for the commercialisation of technologies. The ideal state would be when the perception of the variables shows a value close to 5 (Strongly Agree), because it would reflect that these variables meet the requirements for technology commercialisation. In this case we linked four dimensions and each dimension contains four variables that indicate the ideal performance of the organisation to perform technology commercialisation. The trend showing the respondents' perception of the variables corresponding to each of the dimensions indicates that only three variables were rated as "agree": CES04 Structure and encouragement of entrepreneurship (Dimension Culture and Structure), the variable ICO01 Reputation and quality of scientific output, and the variable ICO04 Problem-solving competence (Dimension Individual Competences). The perception of the variable CES03 Structure for technology development corresponding to the Culture and Structure Dimension is that there is insufficient support for technological development.

Figure 2.2 Radar chart of the TES

Source: Own elaboration

2.5 Data analysis and discussion

Analysing the overall average of dimensions, the dimension "Culture and Structure" has the lowest score, while the dimension "Individual Competences" has the highest score. The Culture and Structure dimension includes the set of ideas, values, behaviours and concepts shared by the members of the institution, in addition to considering the relevance of teaching entrepreneurship, as well as the mechanisms and instruments to provide support for the development of entrepreneurship. The result obtained here indicates that it is necessary to strengthen strategies to manage technological support services and generate awareness to develop a solid structure that serves as a basis for the development of technologies that meet the needs of the environment to help generate value and innovations.

The Individual Competences dimension involves the coordination and motivation of people to develop and implement techniques and knowledge that can be applied to solve real problems in the environment. In this institution, the factor with the highest score is problem-solving competence, which may refer to the fact that technologies are developed with a focus on problem solving.

In general, it is necessary to generate strategies to strengthen each of the four dimensions and their respective variables.

2.6 Conclusions

The main objective of the work presented here was the application of a Framework radar of critical success factors for the commercialisation of technologies in public universities, which was initially applied in Brazilian public universities.

The scientific motivation originated from the intention to apply the model (framework-radar) in a higher education institution in order to contribute to the improvement of technology commercialisation and innovation processes and thus achieve greater efficiency and effectiveness in the context of such institutions.

The data analysis allowed to show the perception of the respondents on the four dimensions and the sixteen variables of the model with the scores given to each of them, the radar map provides a graphical view of the collected answers, showing a picture in which it is possible to follow up processes that can help to improve and adapt procedures that support decision making.

Through the data resulting from the application of the model, the institution can focus on specific aspects to improve and develop capacities to commercialise technologies.

A limitation of this study is the relatively small number of responses collected. Therefore, it is intended to carry out more applications of the model to institutions of this type, such as the other three institutions that are part of the programme for strengthening the academy-industry relationship in the State of Mexico. As a suggestion for future research, it is proposed to carry out comparative analyses between public and private institutions.

2.7 References

Azevedo, A. M., Mazzoni, M. O., & Silveira, M. A. (2013). Academic research in technology innovation management and related thematic areas in Brazil. *Journal of Technology Management & Innovation*, Volume 8, 271-284.

Alonso Betancourt, L. A., Moya Joniaux, C. A., Vera Crespo, M. D., Corral Joniaux, J. A., & Jimmy, J. (2020). Vínculo universidad–empresa: vía para la formación profesional del estudiante. *Vínculo*, 41(13).
Anokhin, S. W. (2011). A conceptual framework for misfit technology commercialization. *Technological Forecasting and Social Change*, 78(6) , 1060-1071.

Calderón-Martínez, M. G. (2017). Tercera misión de la universidad. Una revisión de la literatura sobre emprendimiento académico. *Latindex*, ISSN: 2448-5101 Año 3 Número 1 , 364-373

Campos, E. B. (2007). La Tercera Misión de la Universidad: El reto de la Transferencia del conocimiento. *Revista madri+ d*, (41), 2.

Dias, A.A.; Porto,G.S. (2014). Como a USP transfere tecnologia? *Organizações & Sociedade*, 489-507.
Didriksson, A. (2004). La universidad desde su futuro. *Pro-Posições*. v. 15 , 63-73.

De Benedicto. (2011). Apropriação da inovação em agrotecnologias:estudo multicaso em Universidades Brasileiras. **Tese** (Doutorado em Inovação)UFLA.

Etzkowitz, H., Webster, A., Gebhardt, C., & Terra, B. R. C. (2000). The future of the university and the university of the future: evolution of ivory tower to entrepreneurial paradigm. *Research policy*, 29(2), 313-330.

Etzkowitz, H. (2004). The evolution of entrepreneurial university. *International Technology and Globalization* , p.64-77.

Fernandes, G., & O’Sullivan, D. (2021). Benefits management in university-industry collaboration programs. *International Journal of Project Management*, 39(1), 71-84.

Gomez, F., T. Daim y J. Robledo,(2014) Characterization of the Relationship Between Firms and Universities and Innovation Performance: The Case of Colombian Firms, *Journal of Technology Management & Innovation*, 9, 70-83

González, J. V., Zambalde, A. L., Grützmann, A., & Furtado, T. B. (2018, September). Critical Success Factors (CSF) to Commercializing Technologies in Universities: The Radar Framework. In *International Conference on Electronic Government and the Information Systems Perspective* (pp. 123-135). Springer, Cham.

Hoye, K., & Pries, F. (2009). ‘Repeat commercializers’, the ‘habitual entrepreneurs’ of university-industry technology transfer. . *Technovation*, v. 29, 682-689.

Kirchberger, M. A. (2016). Technology Commercialization: a literature review of success factors and antecedents across different contexts. *Technology Transfer* , 1077-1112.

Miller, K., McAdam, R., Moffett, S., Alexander, A., & Puthusserry, P. (2016). Knowledge transfer in university quadruple helix ecosystems: an absorptive capacity perspective. *R&d Management*, 46(2), 383-399.

- Padilla, D. À. (2010). Factores determinantes de la transferencia tecnológica en el ámbito Universitario. La perspectiva del investigador. *Dialnet.Economía Industrial* , 91-106.
- Pastrana Corral, S. A., Matos Columbié, Z. D. L. C., & Caro Sapiens, M. E. (2020). La vinculación universidad-empresa en el proceso pedagógico de servicio social para el desarrollo social sostenible de la comunidad.
- Rodríguez P. J.; Casani Fernández de N. F. (2007). La Transferencia de tecnología en España Diagnóstico y perspectivas. *Dialnet.Economía Industrial*, 15-22
- Sádaba, I. (2008). Propiedad intelectual: ¿ bienes públicos o mercancías privadas? Madrid: Catarata
- Santiago, C. V. & de Arellano, A. R. (2006). Análisis de los factores que influyen en el éxito de la transferencia tecnológica desde los institutos tecnológicos a las Pymes: los casos de España y Brasil. *Journal of Technology Management & Innovation*, 1(4), 57-70.
- Sira, S. (2016). Letter to the editor: Factors affecting the university technology transfer processes to promote effective and efficient interaction with external sectors. *Revista Ingeniería UC*, Vol. 23, No. 2, , 223 - 236.
- Sorensen, J. A., & Chambers, D. A. (2008). Evaluating academic technology transfer performance by how well access to knowledge is facilitated – defining an access metric. *The Journal of Technology Transfer*, v. 33(5), 534-547
- Swamidass, P. M.; Vulasa, V. (2009). Why university inventions rarely produce income? Bottlenecks in university technology transfer. *The Journal of Technology Transfer*, v. 34 , 343-363.
- Vega-Jurado, J., Kask, S., & Manjarrés-Henriquez, L. (2017). University industry links and product innovation: cooperate or contract? . *Journal of Technology Management & Innovation*, Volume 12, Issue 3, 1-8

Chapter 3 Students of public higher education institutions and their economic impact during COVID-19, case study, 2020

Capítulo 3 Los alumnos de instituciones públicas de educación superior y su impacto económico durante el COVID-19, caso de estudio, 2020

AYALA-RÍOS, Irma Amelia†, GONZÁLEZ-CRUZ, Saúl and LÓPEZ-SÁNCHEZ, Iván

ID 1st Author: *Irma Amelia, Ayala-Ríos* / **ORC ID:** 0000-0002-2303-089X, **CVU CONACYT ID:** 599469

ID 1st Co-author: *Saúl, González-Cruz* / **ORC ID:** 0000-0002-7014-8137, **CVU CONACYT ID:** 1168654

ID 2nd Co-author: *Iván, López-Sánchez* / **ORC ID:** 0000-0001-5221-5722, **CVU CONACYT ID:** 599471

DOI: 10.35429/H.2021.9.1.33.50

I. Ayala, S. González and I. López

A. Ledesma (Coord.). Engineering Science and Technology. Handbooks-©ECORFAN-México, Estado de México, 2021.

Abstract

The economic impact on students caused by COVID-19 seriously affected the economy of families, as well as the teaching-learning process. Unfortunately, educational institutions from preschool to higher education, which is the subject of our analysis, were forced to close their facilities. The objective of this research is to determine the economic impact generated in higher education students as a consequence of COVID-19. Supported by a case study and with the help of an electronic survey, we intend to identify elements that will help us to know the degree of economic impact on higher education students. In order to achieve the research objective, we will work under the model of a case study that will allow us to clearly and objectively identify those factors that had a significant impact on the economy of students at the higher education level. The type of research included in the study is conclusive - descriptive. The research approach is qualitative, since a survey is used to review the information under study.

COVID-19, Impact, Economics, Impact, Students

Resumen

El impacto económico en los alumnos causado por el COVID-19 afectó seriamente la economía de las familias; así como el proceso de enseñanza-aprendizaje, lamentablemente las instituciones de educación desde el nivel preescolar hasta el superior que es nuestro tema de análisis; se vieron en la necesidad de cerrar sus instalaciones. El objetivo de la presente investigación es conocer el impacto de tipo económico que se generó en los estudiantes de educación superior como consecuencia del COVID-19. Apoyados en un caso de estudio y con la ayuda de una encuesta electrónica se pretende identificar elementos que nos ayuden a conocer el grado de afectación económica en los estudiantes de educación superior. Para lograr dar cumplimiento al objetivo planteado en la investigación, se trabajará bajo el modelo de un caso de estudio que permitirá de manera clara y objetiva identificar aquellos factores que impactaron de forma significativa en la economía de alumnos a nivel superior. El tipo de investigación que comprende el estudio es concluyente – descriptiva. El enfoque de la investigación es cualitativo, debido a que se utiliza una encuesta para la revisión de la información objeto de estudio.

COVID-19, Impacto, Economía, Afectación, Estudiantes

3.1 Introduction

The COVID-19 pandemic poses a challenge to the global socio-economic system. The measures of "social distancing" that have been taken in the world and in the different countries of the Latin American region to mitigate the speed of COVID-19 contagion have generated a strong economic contraction which, among the most notable consequences, has us immersed in a context of forced digitalisation between the different productive sectors.

And in the case of education, the academic sector has been directly affected and forced into a context of forced digitalisation among the different productive sectors.

There are a number of doubts and unknowns to be answered, "how long schools may remain closed, how student learning will be affected, and to what extent this will affect the poorest and most vulnerable populations are difficult questions to answer" ¹; as we can see, as this source also publishes, at the level of our university students it is important to consider that not everything has been said.

The social consequences generated by the COVID-19 outbreak are diverse; however, one of them, and the most marked at local, state, national and global levels, is economic. In the educational sphere, there were various academic aspects such as the limited student-teacher interrelationship, and together with this, the new techniques and changes in the teaching-learning process, adding to this, perceived by both parties, an extra burden of activities due to the use of technology, which to a certain extent generated academic stress.

The projections were not at all encouraging as the International Monetary Fund predicted: "Economic crisis: According to International Monetary Fund (IMF) forecasts, the world economy will shrink by 3% in 2020, much more than during the global financial crisis of 2008-95. This crisis will have serious consequences for both governments and families, and will hit both the demand and supply side of education: ∞ School dropouts will increase and many of these students will drop out of school for good. The highest dropout rate will be concentrated among vulnerable groups. When schools reopened after nearly an academic year of closure due to the Ebola crisis in Sierra Leone, girls were 16 percentage points less likely to go to school.

The higher dropout rate is likely to be accompanied by an increase in child labour and child and adolescent marriages. ∞ The impact on learning will be even greater due to economic pressures on households. Even for students who do not drop out of school, their households may pay less for school inputs (such as books or tutoring) until the economy recovers. In addition, many parents may switch their children from private to public schools, overburdening public systems and reducing their quality. ∞ On the supply side, the economic impact will hit schools and teachers. Fiscal pressures will lead to a fall in educational investment, reducing the resources available to teachers. In addition, the quality of education will suffer (whether while online education is provided or when classes resume), as the health crisis will affect some teachers directly and others will suffer financial pressures due to salary cuts or delays in payments. The lack of student assessments during closures means that teachers will be blind to learning at the same time as they try to support their students from a distance. Finally, "school supply may contract as lack of revenue forces public schools to close".²

Unfortunately, the reality in higher education has exceeded projections, as a large number of university students were forced to seek employment opportunities and leave their academic training in the background, because the economy of each family became very vulnerable to such a public health condition.

3.2 Development

Since the COVID-19 pandemic was declared by the World Health Organisation (WHO) in March 2020, plans to control the effects of this virus on the entire population have been implemented in all countries of the world. Governments decreed the limitation of people's mobility in the social and work environment. Then, this situation also affected universities, which established virtual teaching-learning processes. This challenge was faced by higher education institutions, highlighting the structural deficits and limitations of e-services in the progress of the academic path. The face-to-face institutions urgently migrated to remote teaching, alluding to the willingness of teachers who turned their home spaces into improvised classrooms, while they delved into educational technologies.

On the other hand, we have the students who, surprised by the confinement they had never experienced before, had to face and adapt to the virtual modality. It is too early to estimate the educational consequences that this situation may have on them, pointing out the worsening of inequalities in the case of students whose families do not have economic or cultural capital, as defined by various international organisations (World Bank, 2020; Organisation for Economic Co-operation and Development [OECD], 2020; Organisation of Ibero-American States [OEI], 2020; UNESCO, 2020; United Nations Children's Fund [UNICEF], 2020).

Those most affected by this pandemic are students who are furthest removed from the digital culture. While this crisis is leaving us with many doubts about the future of schooling, it is imperative to assess the quality of remote learning and the personal and academic difficulties these students have faced.

Whatever the results, it is necessary to analyse the quality of remote learning received by students in order to diagnose evidence-based scenarios for the short and medium term.

According to the press release Number 185/21 published on 23 March 2021, in its social communication, INEGI presents results of the survey for the measurement of the impact of COVID-19 on education (ECOVID-ED) 2020, it suggests:

Measuring the impact of the COVID-19 pandemic in different fields is a new challenge faced by countries around the world. Specifically, the field of education has been particularly affected, given the recommendations of social distancing. In order to provide interesting and up-to-date information, the National Institute of Statistics and Geography (INEGI) presents the results of the Survey for the Measurement of the COVID-19 Impact on Education (ECOVID-ED) 2020. ECOVID-ED 2020 provides information on the impact of the temporary cancellation of face-to-face classes in the country's educational institutions on the educational experience of children, adolescents and young people aged 3 to 29, both in the past school year 2019-2020, the current school year 2019-2020, and the current school year 2021-2021. The data collection was carried out through telephone interviews, under the sampling framework derived from the National Numbering Plan of the Federal Telecommunications Institute (IFT) for both mobile and fixed telephones; given its probabilistic selection, it allows to expand its results to the country's population (94% of the telephone-using population).

3.2.1 Characteristics of the distance learning class

By level of schooling, 55.7% of the population in higher education used a laptop as a tool to receive classes, while 70.2% of primary school students used a smartphone. In 28.6 per cent of households with an enrolled population aged 3 to 29, additional expenditure was made to purchase smartphones, in 26.4 per cent to contract fixed internet service and in 20.9 per cent to purchase furniture such as chairs, tables, desks or to adapt space for study. 56.4% of households think that the benefit of distance learning is that it does not put the students' health at risk, followed by the advantages of family life (22.3%) and saving money on various expenses such as fares and school materials (19.4%).

In terms of the main disadvantages, 58.3 per cent said that they do not learn or learn only in person, followed by the lack of monitoring of students' learning 27.1 per cent and the lack of technical capacity or pedagogical ability of parents or tutors to transmit knowledge 23.9 per cent. For all age groups, more than half of the students are very willing to attend face-to-face classes once the government allows it; the 13-18 age group is the most willing with 64.1%, followed by the 6-12 age group with 60.7%.

According to research by the IDB and Universia Banco Santander, the following challenges have been identified among the most outstanding ones:

3.2.2 Inequity in the expeditious construction of a technology infrastructure

In the case of universities where there was already some experience in digitisation processes, a satisfactory response to the situation could be given, while in universities where there was no preliminary experience in tele-education, great difficulties have been identified in responding immediately to the creation of an effective technological platform, compromising some educational systems and the training of thousands of students. As a consequence, depending on the response capacity of each university, an imbalance in the implementation of resources and the deployment of competences has been evidenced.

3.2.3 The lack of assessment or accreditation tools for student knowledge in an e-learning context

Virtual assessment differs from face-to-face assessment, so there is a need to develop other methodologies that respond to the context. Considering that training and experience in virtual teaching are scarce, there has been a deficiency in the regulations and legality that cover assessment methods.

3.2.3 Few teachers trained for tele-education and the importance of accreditation

As in the case of accreditation of student knowledge, the pedagogical dynamics of virtual education varies from face-to-face education, showing how in some cases students have been overloaded due to the teacher's lack of knowledge of the management of virtual pedagogy. Considering the novelty of the digital context, teachers are challenged to incorporate new educational mechanisms, making accreditation a standardised solution.

3.2.4 The digital divide and limited access to technologies

Many students in the region have difficulty accessing computers or do not have connectivity at their disposal, resulting in an increased dropout rate. Mexico has long had many problems with internet connectivity, and with the pandemic this exacerbated and highlighted the shortcomings of this service. For 20 years the internet service in our country has not evolved according to the current needs of academic institutions; in conjunction with the above, economic conditions, such as income, education and digital skills have been considered as some of the main causes of the current digital divide in Mexico and then in the Tecnológico de Estudios Superiores de Jocotitlán..

3.2.5 The psychological effect of confinement impacts on students' ability to learn

Many students live in environments that are not conducive to adapting to virtual formats, considering their home conditions, network availability and access to the required technologies.

3.2.6 Research paralysis in the context of the pandemic

As a consequence of the social distancing protocols imposed, the research capacity of universities has been compromised. Clinical teachings and laboratories require face-to-face attendance, so there is a challenge in how to make them sustainable.

3.2.7 The risk of university financial sustainability

Late payment of tuition fees and the dropout of some students has put their financial health at risk.

3.2.8 The risk to the economic health of universities

In the case of public universities, the economic recovery of countries in the Latin American region implies the generation of significant adjustments in university budgets, creating a financial and economic dilemma that includes additional adjustments in the financing of socio-economic scholarships (which is considered a tool that reduces the incidence of student dropout).

The advantages identified in the process

3.2.9 The university's educational model influences its responsiveness

Universities that had begun a transition to digitization before the pandemic and had a technological infrastructure in place already had some experience in developing a digital culture, with students and faculty more adapted to mechanisms such as digitized procedures and face-to-face courses delivered in a hybrid format and with online curricular content.

3.2.10 Financial investment in resources for educational continuity and bridging the digital divide

Some universities have made efforts to facilitate access to virtual classes, especially in rural areas or areas with less connectivity, generating an extension of resources and mitigating cases of abandonment. Among the activities identified to reduce the digital divide, surveys have been carried out among the student and teaching population to help identify technological equipment needs. Among the resources made available are tablets and laptops, Zoom and Webex licences for the virtualisation of courses, SIMS cards or modems to improve the educational experience, data for free downloads and food vouchers as an extension of the benefit that some students received at the university.

3.2.11 Continuous pedagogical training processes for teachers

Through webinars and tutorials, ongoing efforts have been made to help teachers adapt to tele-education. It has highlighted the importance of the value of collaboration and solidarity of more skilled colleagues with those who are in the process of learning the mechanics of virtual pedagogy.

3.2.12 The facilitation of remote working by university administrative staff

3.2.12.1 The institutional strength of universities

If there is a strong relationship between deans, professors and the university government, and if there are shared ideals and no power struggles, it is possible to mobilise the university from a face-to-face to a virtual form in a short period of time.

Today's higher education students are facing great challenges, ranging from family, psychological, social, work-related and, above all, economic challenges.

The pandemic situation caused by COVID-19 has generated that higher education students tend to suspend or even worse, forget their studies in order to look for a job opportunity that will allow them to help themselves and their families with the minimum household expenses such as food and basic services.

Nowadays, higher education students suffer from a crisis of concentration for their studies, derived from each and every one of the needs they face, which are diverse and of different magnitude; from no longer having family support due to the death of one of the members of their family who supported the household and education expenses, which in most cases are their parents, or, without reaching the extreme of absence, the loss of the source of employment, which resulted in not having the necessary resources to be able to continue with their studies.

A very marked vulnerability in higher education students that has resulted from the pandemic we are still experiencing is the increase in their economic difficulties and conditions, since unfortunately their level of income has been impacted in such a way that what in a certain way was their resource to maintain their studies has nowadays become secondary for many of them, due to the fact that the local and national economy has suffered devastating damage, thus generating a crisis of lack of opportunities to find employment.

It is worth noting that there are several conditions that have curbed the expectations of students; that not even the government itself has been able to offer a plan or scheme to rescue all those university students from the situation in which they find themselves, just at the national level have stopped many projects, programs and economic resources where unfortunately students at this level do not figure either.

The institutions of higher education are a fundamental and important part of this whole crisis process, because unfortunately their student population, as well as society in general, has had a very drastic impact on the economy, first and foremost on each of the students, and jointly on the members of their families.

In order to give an overview of the magnitude of this impact on higher education students, we can say that, first of all, many of them have had to stop their studies in a radical and untimely manner, as they have had to look for work opportunities to support their family economy, a situation that has not been so easy for them either; This is due to the fact that the workplaces that before the arrival of the pandemic regularly hired personnel during the different seasons of the year, to this day these same companies continue to cut personnel due to the precarious economic situation at the local, state, national and international level, a not at all favourable condition; because in addition to abandoning their studies, job opportunities are very limited; to the extent that many of them have hired themselves out to work as construction assistants or in small establishments to be able to obtain an income that at least allows them to cover their basic needs.

The outlook is not at all encouraging for the student sector that is the subject of this research, as time goes by and we see that a good number of our students are already preparing for professional internships, social services and of course professional residencies; however, employers are still very closed to opening their doors to these future generations about to graduate, each one of the governments has a very big task and unfortunately we observe that they do not seem to be interested in the future of our new generations, every day the social problems continue to grow, the most marked for the students being the lack of job opportunities.

The economy for higher education students has not been selective; that is to say that it is not only the fact of covering basic needs such as food; but as time goes by and the insecure health condition does not improve; regardless of government statistics, students who make the effort to maintain their studies are already thinking about whether or not to re-enroll for the next semesters, or what is more critical; parents at this time are in a great dilemma to consider whether or not to enroll their children in the next semester; They are already thinking about whether or not to re-enroll for the next semesters, or what is more critical, parents are currently in a great dilemma to consider whether to enroll their children at a higher level or momentarily wait to see what will happen with the pandemic condition.

The wear and tear that higher education students are still suffering seems to have no end in sight, because in addition to all the material aspects, the days of teaching and hours in front of a computer have not brought good news in terms of academic achievement and performance; of course this could certainly be a great subject for study and analysis, but the opportunity to address it goes hand in hand with all the impact that the current public health situation has brought.

It is very true that researchers have analyzed the great differences that exist in our country in comparison with other countries in terms of technology, since unfortunately many of our students have to borrow or rent computer equipment to be able to receive their classes, while others struggle to pay for a basic internet service to at least receive advice that will allow them to continue with their academic training. "Marion Lloyd presents very specific information for the case of Mexico, in the context of Latin America. In both cases, Mexico fares quite badly. In 2016, the country ranked 87th in the world and 8th in Latin America in access to ICTs, behind Uruguay, Argentina, Chile, Costa Rica, Brazil, Colombia and Venezuela, in that order, according to indicators from the International Telecommunications Union (ITU), based in Switzerland.

There is also a large digital divide within the country: only 45 per cent of Mexicans have a computer and 53 per cent have access to the internet at home, according to the 2018 National Survey on the Availability and Use of Information Technologies in Households (ENDUTIH). As expected, such access is not evenly distributed, with 73 percent of the population in urban areas having access to the internet, compared to 40 percent in rural areas. Even more worrying, only 4 percent of rural residents have internet at home). "3

The crisis that we are experiencing worldwide in all areas, but especially in education, which is the subject of this article, has triggered a restructuring and rethinking of the provision of educational services and supply at all levels, as the intensive use of all kinds of technological platforms and media have come to occupy a central place in each of the institutions and homes to ensure and guarantee the continuity of learning.

Unfortunately, the foundations of this technological environment applied to education have not yet been laid; that is to say, a whole range of platforms have been implemented in an unexpected and unplanned manner in order to get ahead in the last three school cycles, where teachers and students have had to learn together in each of the subjects taught.

It is important to highlight that in this case, the central theme of our study is the economic impact that our higher education students have had to face in a titanic way; First of all, the fact of not having technological resources has not been easy for them, a situation that has generated a great gap of technological inequality among our students in public higher education institutions. Digital tools became essential to continue with academic activities during the coronavirus pandemic; however, this situation highlighted the lack of training of teachers and students in the use of these tools, as well as the inequality of access to technological resources in the population, in such a way that nobody was prepared for such a sudden and drastic change in education; To the extent of changing and innovating the entire methodology of the teaching-learning process and bringing it together with digital platforms; a situation that after almost a year and a half of this public health condition has not achieved a total mastery of them, and what is more regrettable and worrying; the level or degree of academic achievement of each of our students.

On the other hand, and this has been mentioned in many of the studies, the role of parents in the basic levels has been of great help and support for their children, as they have had to assume the role of guides, advisors and tutors for them in order to accredit the corresponding school cycle.

The face of the higher level is very different, as students have had to make decisive decisions to convince themselves whether or not to continue with their professional studies, as the central point of our topic is the protagonist in their decisions "the economy"; both personal and family.

It is very important to emphasise that we should not confine ourselves to an environment in which the precarious economic conditions of our students only began as a consequence of the pandemic; the reality is that this was emphasised even more by this public health condition, because before the arrival of COVID-19 the world was already facing a learning crisis; Many of them were not enrolled in any level of education and what is more regrettable is that it was no longer a priority to continue studying, because the economy of each of the economic zones of our country already brings a great background where the primary activity is primarily to ensure a source of work that allows the family to support themselves and their families.

Unfortunately, many of the students at the public higher education level have been immersed in the loss of first-line family members and what is more regrettable; their parents have lost their source of employment, a condition that has forced them to seek family sustenance and leave their academic training on another plane. School dropout rates have increased considerably and many of our students have left school for good, with no possibility of returning to continue their education. The highest dropout rate has been found among vulnerable groups.

It is likely that the higher dropout rate is accompanied by an increase in informal work, which in many cases has also led to a high rate of vandalism as a consequence of the lack of employment.

The negative impact on the teaching-learning process will continue to increase due to economic pressures within households. Even in the case of students who do not drop out of school, their households will be able to pay less for each of the requirements and inputs demanded by the institutions; until the economy shows a better and safer trend; on the other hand our public institutions are presenting a very worrying condition; as many parents who could afford a private or private institution are now in search of a private institution; Today they are looking for a public educational alternative; a situation that puts public schools in check with an overload, because although they intend to have more educational enrolment, their conditions and facilities do not allow them to receive all those young people who wish to continue their higher education.

On the academic side, the economic impact is hitting schools and teachers. Tax conditions will lead to a drop in educational investments, which will reduce the resources available to teachers.

In addition, the quality of education is suffering, as the health crisis has affected teachers directly and others will suffer economic pressures due to salary cuts or delays in payments. The failure to properly assess students during closures means that teachers will be blind to learning while trying to support their students in the officially sanctioned "online" mode.

The issue of the digital divide, the socio-economic situation of students and their families is a factor that is increasingly aggravated, students who are in a difficult economic situation have more complications of having poor or no access to information technologies and equipment, because of the cost of a laptop or Internet connection or because in the areas or regions or neighbourhoods there is low connectivity or signal.

For example, in populations far from the municipal capitals, they have limited electricity services and even less internet service; for which this condition complicates the student's work, as he/she must travel several kilometres to have good connectivity that at least allows him/her to carry out the elaboration of academic activities and products.

Under these conditions and many others, the economic deterioration of the student is being added to, as it has had such an impact that it is already very difficult to convince them to resume their academic activities; unfortunately they tell us that their economic conditions at the moment are not the best to think about continuing their studies, as they have decided to support their parents or relatives to have at least the minimum necessary to support their family.

The students are going through an economic, psychological, social and family wear and tear that affects them considerably, it is important to consider that within the institutions they implement strengthening and support programmes; analysing the financial conditions of the institution, so that our students do not feel forgotten and do not think that they are just one more number within the entire student community.

3.3 Theoretical framework

The COVID-19 pandemic poses a challenge to the global socio-economic system. The measures of "social distancing" that have been taken in the world and in the different countries of the Latin American region to mitigate the speed of COVID-19 contagion have generated a strong economic contraction which, among the most notable consequences, has us immersed in a context of forced digitalisation between the different productive sectors.

And in the case of education, the academic sector has been directly affected and forced into a context of forced digitalisation among the different productive sectors.

Since their foundation, universities, like any other social institution, have had to face devastating epidemics that have impacted their daily functioning. And they have survived and continued with their mission even with their doors closed. In 1665, Cambridge University closed because of an epidemic of the Black Death that struck England.

Today, temporary closures of higher education institutions (HEIs) due to the COVID-19 pandemic are no longer newsworthy because most countries have already ceased to operate in person.

Considering the information and estimates from UNSCO IESALC, (2020) indicate that the temporary closure affects approximately 23.4 million higher education students (ISCED 5, 6, 7 and 8) and 1.4 million teachers in Latin America and the Caribbean; this represents approximately more than 98% of the higher education student and teacher population in the region.

DE (Distance Education) is complex in nature and scope, involving a wide range of non-traditional forms. DE is complex in nature and scope, involving a wide range of non-traditional forms of teaching and learning.

Broadly speaking, it is teaching that takes place away from the place of learning, requires the use of technologies (Moore and Kearsley, 2012), allows for flexible time management and gives greater autonomy to learners (Vlachopoulos and Makri, 2019).

There is already evidence that the closure of schools caused by COVID-19 has increased inequality of opportunity, particularly in families with low socio-cultural and economic capital (Cabrera, 2020; Cabrera, Pérez and Santana, 2020).

Students have also been forced to adapt to an educational model whose contents were designed for face-to-face learning and which required them to manage their time better and, therefore, to be more disciplined and organised. In fact, authors such as Giesbers et al. (2013) and Moallen (2015) have shown that students prefer blended learning models that combine synchronous and asynchronous learning.

The World Bank has undertaken research into the possible effects of the pandemic on higher education, some of the data analysed up to May 2020 is described below.

The COVID-19 pandemic is having profound impacts on education. With school closures at all levels in almost every part of the world, the damage will now be even more severe as the health emergency translates into a deep global recession. This report describes the multidimensional impact on education systems and outlines actions that countries can take in response.

Even before the COVID-19 pandemic, the world was facing a learning crisis. Most countries were far from achieving the 48% sustainable development goal. That goal commits the world to ensuring "inclusive and equitable quality education and promoting lifelong learning opportunities" for all by 2030, but so far even universal quality schooling at the primary level, let alone at the secondary, tertiary or lifelong learning level, has proved unattainable in many countries. The learning poverty rate has shown that before the pandemic, 53% of 10-year-olds cannot read or understand simple text in low- and middle-income countries. And this crisis does not affect the most vulnerable equally: the most vulnerable have poor access to schooling, high dropout rates and access to low quality education. Without aggressive policy action, the impacts on education and the economy will exacerbate the learning crisis.

Children and youth who are forced to drop out of school may not return, while those who do may have lost valuable time and find that their schools have been affected by budget cuts and economic damage to communities. Many students have lost the most important meal they received each day. And with poorer households hard hit by the ensuing economic crisis, the opportunity gaps between rich and poor will become even wider. Beyond these short-term impacts on access to education and learning, countries will ultimately be affected by significant long-term losses in terms of education and human capital. However, there is much that can be done to reduce these short-term impacts and ultimately turn the response to the crisis into long-term improvements to education. This report describes the main impacts affecting the education sector as a result of the pandemic and presents the policy response - policies that can mitigate the damage to students and communities in the short term; boost education revival, with an emphasis on closing education and access gaps that may have widened; and support 'building back better' education systems as they regain their equilibrium, accelerating their path of improvement and moving away from the learning crisis.

3.4 Background

Prior to coronavirus The American Bar Association defines distance education, also known as online learning and technology-mediated instruction, as any course in which students are separated from each other or from face-to-face faculty for more than one-third of the instruction and involves the use of technology to support regular, substantive interactions among students and among faculty members. Currently, many faculties in different fields are required to deliver undergraduate and graduate courses through distance education, even though they may have little or no training in how to conduct technology-mediated instruction online.

On the other hand, it is worth remembering that online education is conceptualised as electronically supported learning, which relies on the Internet for teacher/student interaction and the distribution of class materials. From this simple definition emerges an almost infinite number of ways of teaching and learning outside traditional classrooms and away from university campuses. With online education, students can participate in a virtual classroom from anywhere with Internet access and electricity. It can include audio, video, text, animations, virtual training environments and chats with teachers. It is a rich learning environment, with much more flexibility than a traditional classroom. When used to its full potential, it has been shown that online education can be more effective than pure face-to-face instruction. It has the potential to be engaging, fun and tailored to fit almost anyone's schedule, as long as it is managed correctly.

The basic types of online education programmes:

- 100% online education: Fully online degrees are earned from the comfort of your home without mandatory visits to your university or college campus.
- Hybrid education: Hybrid education allows students to take a combination of online and on-campus courses. Prior to the coronavirus pandemic, the global education technology sector, which includes online learning, was growing at approximately 15.4% per year, with big-name companies such as Google and Microsoft investing heavily in the industry, according to data reported by Kenneth Research. The United States is the largest market, with rapid growth also occurring in India, China and South Korea, according to a report by ICEF Monitor, a market research study focused on international education. Factors such as convenience, geography and the need to work while studying are driving most of the growth in online learning, especially in the higher education sector.

The global education sector has been a late adopter of digital technologies and only around 3% of all education spending worldwide was spent on digital initiatives. The growth of online teaching and learning had been held back by concerns about cost; lack of reliable access to digital devices and high-speed internet connections, especially among poorer families or countries; and widespread attitudes that online learning was inferior to traditional learning methods. Surprisingly, this pandemic has now forced everyone to experiment and improvise with digital learning.

3.5 Literature review

Supported by various sources, we can say that in most cases there are references from different health organisations and opinions in electronic sources, which allow us to be the main ones to strengthen the present study.

3.6 Methodology

In order to fulfil the objectives, set out in the research, an extensive bibliographical review of different primary and secondary sources has been carried out. In this sense, the methodological aspects are listed below with a general character that will allow the design and execution of the instrument for the collection of relevant information for the study, which will be applied and used to fulfil the objective.

As mentioned above, the methodological aspects of the study are presented below:

Type of research

Concluding – Descriptive

Approach:

The research approach is quantitative, the latter due to the fact that a quantitative approach instrument is used for the review of the information provided by students belonging to public higher education institutions on the economic impact during COVID 19, case in the Tecnológico de Estudios Superiores de Jocotitlán of the year 2020, the object of study.

Description of the research:

This study contemplates the application of an instrument that allows the elaboration of the diagnosis of the situation of students belonging to public higher education institutions on the economic impact during COVID 19, case the Tecnológico de Estudios Superiores de Jocotitlán of the year 2020.

Population and sample

Population:

The population under study are the students belonging to public higher education institutions, for the period 2021, on the economic impact during COVID 19; the Tecnológico de Estudios Superiores de Jocotitlán, is a public institution of higher education, offers 12 careers, divided into 9 engineering, among which we find Engineering in Computer Systems, Business Management, Mechatronics, Electromechanical, Industrial, Logistics, Chemistry, Materials and Digital Animation; and 3 Bachelor's Degrees; Public Accountant, Architecture and Tourism with specialisation in Gastronomy; for the analysis of this case, the population considered are 247 students, belonging to the Bachelor's Degree in Public Accountant.

Sample:

For the sample design of the present research, items will be selected in such a way that each unit has a chance of being selected. Therefore, the students to be subjected to this research will be selected using simple random selection techniques, i.e. selection applied through random number generators with the use of calculation software (Excel).

Sample

For finite populations where $N= 247$ students of the Bachelor of Public Accountancy.

The technically calculated sample is as follows:

$$n = \frac{Z^2(p*q)}{e^2 + \frac{Z^2(p*q)}{N}} \quad (1)$$

Statistical formula for calculating finite population samples.

Where:

n = sample size= 150.33

Z = desired level of confidence=1.96 95% confidence

p = proportion of the population with the desired characteristic (success)= 0.05

q = proportion of the population without the desired characteristic (failure)=0.05

e = level of error willing to make = 0.05 error of 5% error

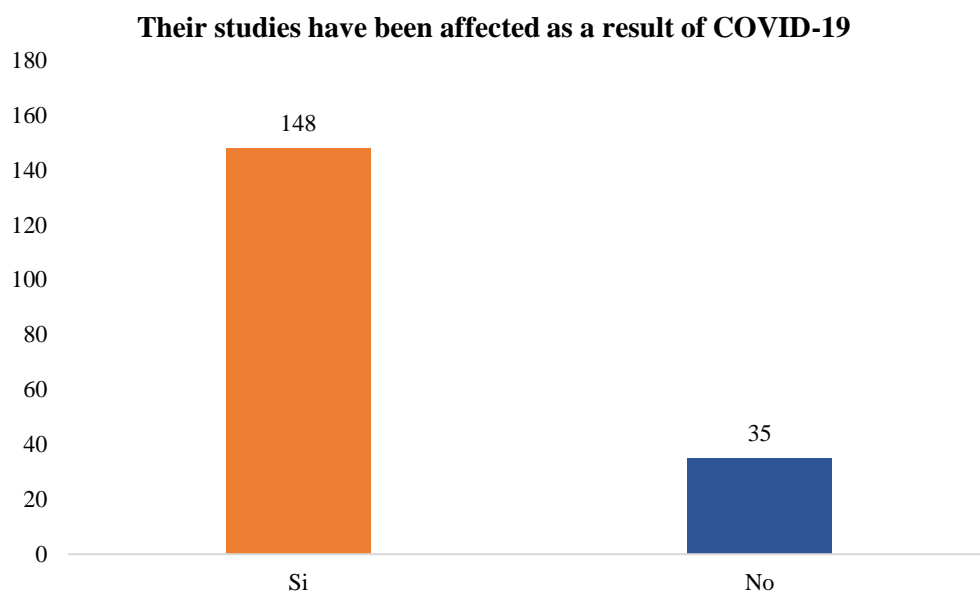
N = population size =247

Therefore, for a population of 247 students, 95% confidence level and 5% margin of error, a sample of 151 students, subject to study, is obtained. In this case there will be 183 students.

3.7 Results

According to the results obtained from the survey applied to students of public higher education institutions on the economic impact during COVID 19, in the case of the Tecnológico de Estudios Superiores de Jocotitlán, it was concluded that 80.87% of the students who answered the survey have been affected to a great extent, to the extent of making a radical change in different aspects of their daily lives.

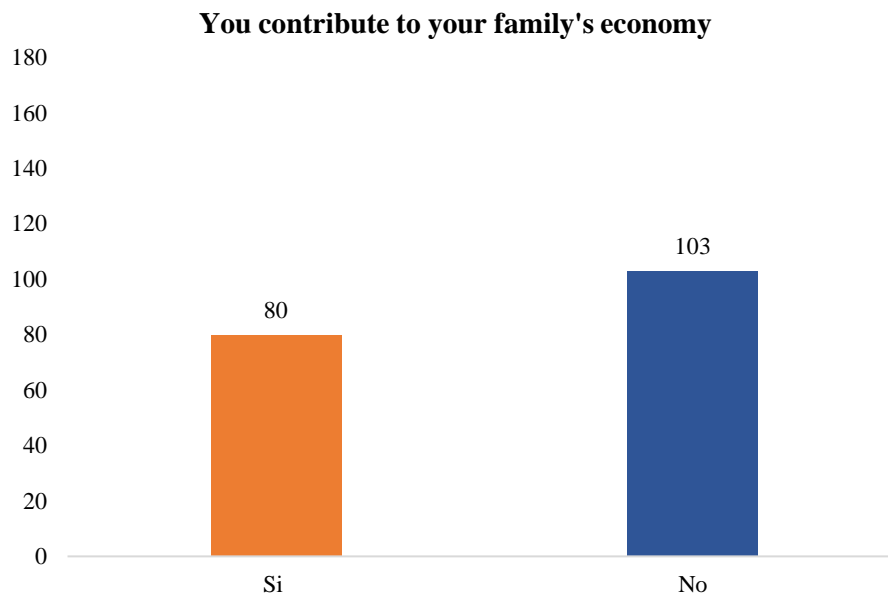
Graphic 3.1



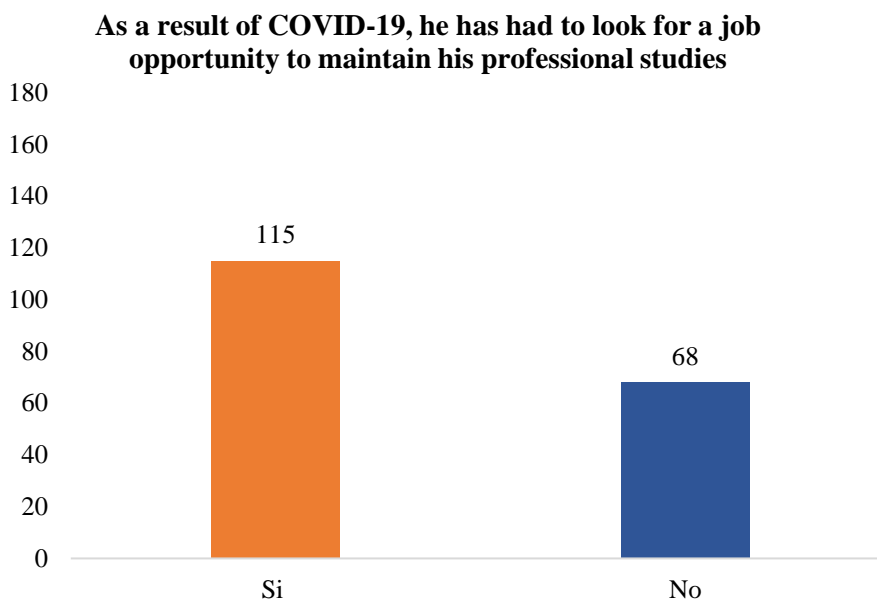
The COVID-19 pandemic seriously affected higher education, with the closure of universities resulting in the non-continuation of learning, the delivery of learning materials and security, as well as students' perception of the value of their degree. Higher education institutions were quick to replace face-to-face classes with online learning, although they often struggled with a lack of experience and time to devise new delivery formats and assignments.

Today, this situation is alarming and worrying for students as their studies are affected from different perspectives, perhaps one of the main consequences is that learning trajectories and study progress are disrupted and the value of higher education institutions is exposed, as due to the economic crisis, students are unlikely to devote full time and money on a consistent basis to take online classes.

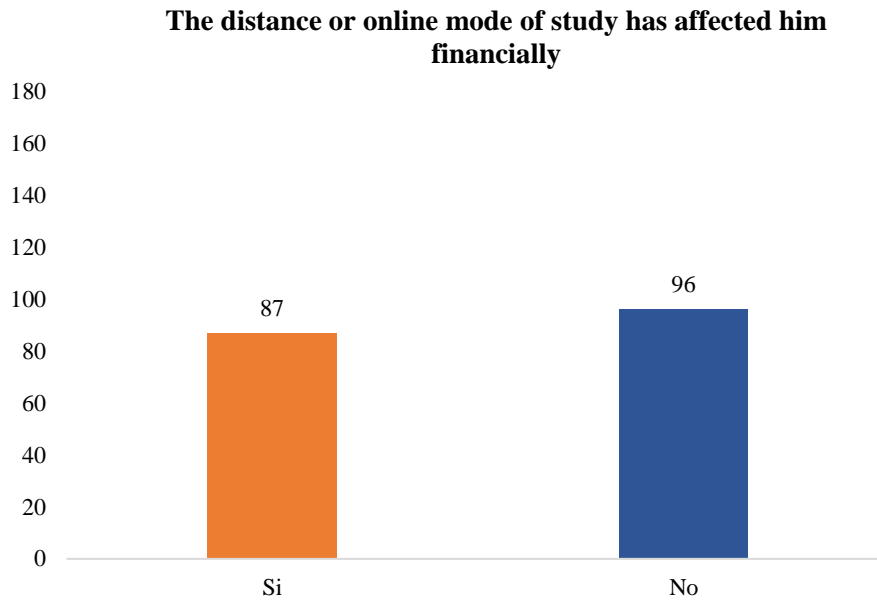
Graphic 3.2



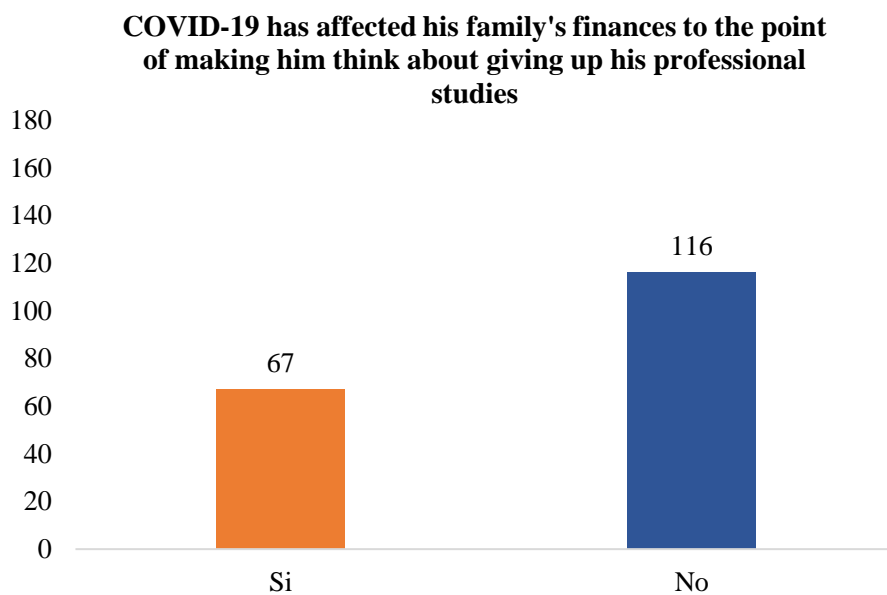
Graphic 3.3



It is very important to mention that most of the students surveyed do not contribute to the family expenses, and according to the results obtained, it is possible to conclude that there is a great risk for those respondents who do have to contribute and who are therefore in a difficult economic situation and consequently are more likely to have poor or no access to the internet, either because they cannot afford to buy a laptop or internet connection or because they live in areas with low connectivity and as a consequence many students do not spend time taking their classes and go out in search of job opportunities that allow them to generate an income to support their families' economy and to be able to somehow maintain their professional studies.

Graphic 3.4

About whether the distance or online mode of study has affected them financially, according to the results observed, it is concluded that it has not been a problem that has affected them significantly with more than half of the students surveyed, but it would be important to take this aspect into consideration since the trends indicate that, if the crisis continues, it could cause a serious problem in the future.

Graphic 3.5

Another important aspect to consider, and perhaps the most important, is that in the face of the COVID 19 pandemic, the vast majority of students have not thought about leaving their professional studies, which leads us to consider and implement strategies that allow students to continue with their studies, providing them with the necessary tools to take better advantage of their studies.

3.8 Discussion and Conclusions

Overall, this crisis has implications that are extremely difficult to grasp, including for education, and has no pre-determined implications. It will be the nature of our collective and systemic responses to these difficulties that will determine how they affect us, the prospects are very uncertain, but if the pandemic did anything, it exposed our vulnerability to crises and revealed how strong the economies we have built can be.

That includes rethinking how the economy will need to evolve to protect itself from adversity and defining the skills, education and training required to support it. It also means working hard to increase the attractiveness and labor market prospects of certain professions, including those considered critical to the common good.

The pandemic that we have been experiencing and that even our authorities at the federal, state and local levels do not have a reasonable strategy to revive the educational landscape at all levels, is leaving a big gap in the quality of education with which our undergraduate students will enter the workplace; while it is true that all economic entities seek educational quality that is reflected in the workplace; Nowadays it is important to understand that we cannot consider that it is enough to give our classes or advice virtually and thus think that we have fulfilled our task towards future generations of students, it is important to consider that implementing strategies that allow our students to continue to have the support as teachers and continue to transmit experience will be useful as a pillar to face the challenges that will be presented to them in the future.

The teaching-learning process in a certain way is questioned, because in most cases we could say that both teachers and students are not closing the educational cycle, and we are not referring to a school or civil calendar period; our vision goes beyond that; that is to say, both parties have not lived together in a face-to-face manner for logical reasons, and this has greatly reduced the quality of assimilation of the student's knowledge, the student's environment with the great diversity of inconveniences that he or she has had to face, such as those analyzed in this article, has been complicated for many, for others it has already become a conflict and for many more it is no longer a priority today, because due to the lamentable conditions we are living in, it is more important for many of our students to look for a job opportunity and support their families than to stay five or six hours in front of a platform and listen to the teacher trying to get their attention with the corresponding subject; That is how stark our reality is today in many of our higher education institutions.

The IES (Institutions of Higher Education) have made efforts to continue teaching courses virtually despite the great lack of budgets and capital to improve the technologies of each of them, it is to recognize the effort of many to try to continue to maintain the level and quality of education of our students, however the need is much greater; a worrying level of school dropout is facing many of our educational institutions, because as we mentioned before, the national health problem has come to revolutionize the conditions of each of our students.

On the other hand, our institutions are becoming more and more vulnerable to the issue of financial conditions to compensate for all the problems that afflict them both academically and administratively, and of course also in terms of employment. It is very important that within these institutions, a great deal of attention is paid to implementing the continuous improvement of all their management, teaching, administrative and service staff, because to the extent that training and human quality is injected into all the staff, it will be to the extent that our HEIs will be able to move forward.

There are many determining factors that local, state and federal governments must consider in the scenario that is still not so encouraging; and of course the proposal is towards the educational part; it is important to understand that our students of higher education in public institutions, which is our case study, are the immediate workforce that will be inserted into the labour market, therefore generating strategies for continuous improvement to minimise dropout levels are of vital importance.

On the other hand, the sensitisation and training of teachers to transmit knowledge to their students is another issue that nowadays we cannot leave aside, unfortunately we are living a very harsh reality, where teaching-learning has become a mechanised process; And we refer to this because with the use of digital platforms, many teachers have become detached from their students, there is no longer a real interest in the problems they are going through and indifference is leading us to the fact that professional training is not fulfilling its mission, which is that all this accumulation of information and knowledge that our students receive in the classroom and nowadays in their homes or public spaces supported by information technologies will allow them in a very short future to the insertion, reinsertion and updating of their work.

On the other hand, HEIs must prepare students as well as possible; of course, as we have already mentioned, through their teaching staff, for activity in a professional field and facilitate their adaptation to the changes in the labour market that may occur throughout their lives, that is to say, in short, to build specific professional and labour profiles highly specialised in certain subjects.

Throughout the Covid-19 pandemic, motivating students in virtual classes has undoubtedly been of great importance and relevance, as a group of unmotivated students is very alarming and risky, as their uncertainty and doubts about continuing their academic training are very vulnerable. The importance and the great role that motivation plays in learning is well known and has been supported by many researchers on the subject.

Unfortunately, the motivational part of the teaching staff has not been seen, has not been encouraged or has not been given much attention in many HEIs, to such an extent that teachers themselves sometimes forget or neglect its importance when exercising their profession both in classrooms and much less nowadays online, of course we cannot put all the blame on the teaching staff of the different institutions; Of course, in this case, higher education students must also do their part to ensure that this motivation is not forgotten day by day, but this responsibility must be shared in a tripartite manner: students-parents-teachers.

Together with the central theme of our research, which is the economic impact, we could not leave aside the motivational factor, as we wish to emphasise that it is a determining factor in the training process of our students; if there is no motivation, the student, even if he or she has the best conditions for training and qualification, will not achieve or reach full fulfilment as a student, much less on a personal level; And much less on a personal and work level, hence the urgent importance of keeping alert with each of our working groups, because if we add the economic detriment for which they have and are going through, adding the poor motivational condition in each of them; the issue of school dropout will continue to increase.

It is time to reconsider and analyse as teachers what areas of opportunity we have to improve and that these allow or help us to train our students in a better way and with a high level of academic quality, because tomorrow we should not complain that unemployment and social problems such as vandalism will continue to increase. A well-trained and well-oriented student knows which path to follow in order to achieve success; because nowadays, as is well known, the demand for work is very great and the supply is very limited. It is important to emphasise to our students that distance learning is important at this time, we are clear that it does not have a better level than classroom training; but adapting to different work systems is something that characterises us as human beings; "adaptability to survive", it is of the utmost importance that our role as teachers is not to make things easy for our students; however, continuous accompaniment can certainly help to prevent our students from leaving or putting their academic training on the back burner as far as possible.

The economy in general in our country has had a very drastic effect on our students; we have clearly analysed this in our case study, of course we cannot ignore this situation of our student population at higher education level; but with all this analysis we can take up many areas of opportunity that have been left by the wayside of this national health condition. The impact of the COVID-19 pandemic not only reached the health system, but also the education system, especially for two reasons: the economic crisis that reduces family income and the lack of conditions for learning through non-classroom education. Thus, with this brief conclusion, these are two major issues that we leave to be analysed and we can see the great scope and consequences that they may continue to have.

It is very true that the impact could be even greater, as the economic effect could last much longer than we imagine, as we must be aware that the recovery of jobs will not occur in the short term, but on the contrary, the great powers themselves are today in a continuous struggle to impose their economic standards, impacting the most vulnerable economies. We could continue to analyse the conditions that have greatly affected our students, but we believe that the most important is the economic factor; since they are limited, they are looking for the best alternative to find a balance for their needs, and of course we know that their food and safety come first; It is very true that we are limited to influence the economic issue in a certain way, but it is also very true that what we have to do as teachers, if we do it as we should, we can mitigate in part the conditions of desertion that our HEIs are going through.

Following the analysis and compilation of research and classroom experience we share that several research studies have presented data suggesting that more than 85% of educators who teach online courses feel that students learn as much as they would in the classroom.

The biggest mistake, experts say, is trying to make online learning "the same" as classroom learning, when in fact it should be very different. Given the spread of the coronavirus outbreak, this sudden global shift to online learning will not stop in a week or two. Universities will need to consider carefully how to assess and manage student learning outcomes, which will lead to a whole new set of challenges. There is the scenario where dissatisfied students who consider online learning to be inferior to face-to-face classes may take action against universities.

Indeed, it is happening in some countries that students affected by the shift to 100% online learning, as a result of coronavirus measures, are requesting a refund of their tuition fees. The perceived ease and usefulness of online education is largely influenced by users' first experiences. This has a significant impact on its ultimate actual adoption. The idea that online education is being implemented rapidly at the expense of quality is something to be concerned about, as online education could be discarded once the coronavirus outbreak is over. Online connectivity must be carefully planned, and faculty members on the front line of this movement need more support than a simple notice of operation justified by a declaration of emergency.

If anything, experts say, the pandemic exposes how online education is still in its infancy. The pandemic quickly shows the collateral effects of institutions run by leaders inexperienced in the field of online education, who are circumstantially charged with formulating policies that treat online education as a crisis management tool. Things might have developed differently if online education had previously been treated as a vital part of normal teaching and learning.

3.9 References

Alex G (2020). Educación en tiempos de crisis sanitaria: Pandemia y educación. Universidad del Magdalena, Santa Martha.

Alicia B (2020). Comisión Económica para América Latina y el Caribe (CEPAL). Coyuntura, escenarios y proyecciones hasta 2030 ante la presente crisis de Covid-19. Retrieved June 4, 2020, from: <https://www.cepal.org/es/presentaciones/coyuntura-escenarios-proyecciones-2030-la-presente-crisis-covid-19>

Bonet, J., Ricciulli, D., Pérez, G., Galvis, L., Haddad, E., Araújo, I., ... y Galvis, L. (2020). Impacto económico regional del Covid-19 en Colombia: un análisis insumo-producto. Documento de Trabajo sobre Economía Regional y Urbana; No. 288.

Brynjolfsson y McAfee (2014). The Second Machine Age. Work, progress, and Prospecty in a Time of Brilliant Tecnologies. New York-London: Norton & Company.

Clavellina, J. L., y Domínguez, R. (2020). Implicaciones económicas de la pandemia por COVID-19 y opciones de política. Índice de riesgo de pérdida de empleo: Retrieved June 1, 2020, from: https://papers.ssrn.com/sol3/papers.cfm?abstract_id=3587200

Fernández, C. (2020). Impacto en el mercado laboral de las medidas de aislamiento para combatir el COVID-19.

Guterres, A. (2020). Solidaridad contra el odio propagado por el coronavirus. Retrieved from: <https://www.un.org/es/coronavirus>.

Gutierrez, A. (2020). Educación en tiempos de crisis sanitaria: Pandemia y educación.

Grupo Banco Mundial Educación. (May, 2020). Retrieved from: <https://pubdocs.worldbank.org/en/143771590756983343/Covid-19-Education-Summary-esp.pdf>

Harari, Y. (March 15, 2020). In the Battle Against Coronavirus, Humanity Lacks Leadership. Time. Retrieved from: <https://time.com/5803225/yuval-noah-harari-coronavirus-humanity-leadership/>

La economía en los tiempos del covid19. Informe semestral de la Región de América Latina y del Caribe. Retrieved June 3, 2020 from: <https://openknowledge.worldbank.org/bitstream/handle/10986/33555/211570SP.pdf>.

OMS (2020). Alocución de apertura del Director General de la OMS en la rueda de prensa sobre la COVID-19 celebrada el 11 de marzo de 2020. Retrieved June 1, 2020 from: <https://www.who.int/es/dg/speeches/detail/who-director-general-s-opening-remarks-at-the-media-briefing-on-covid-19---11-march-2020>

Ordorika, I. Pandemia y educación superior. Scielo. (27 de noviembre de 2020). Retrieved from: http://www.scielo.org.mx/scielo.php?script=sci_arttext&pid=S0185-27602020000200001

Psacharopoulos G., Patrinos H., Collis V., y Vegas E. Publicado en Education for Global Development. (April 30, 2020). Retrieved from: <https://blogs.worldbank.org/es/education/el-costo-del-covid-19-ocasionado-por-el-cierre-de-escuelas>

PNUD (2020). COVID-19: la pandemia. Retrieved from: <https://www.undp.org/content/undp/es/home/coronavirus.html>

<https://blogs.worldbank.org/es/education/el-costo-del-covid-19-ocasionado-por-el-cierre-e-escuelas1>

<https://pubdocs.worldbank.org/en/143771590756983343/Covid-19-Education-Summary-esp.pdf2>

http://www.scielo.org.mx/scielo.php?script=sci_arttext&pid=S0185-276020200002000013

Copyright © 2020 Banco Interamericano de Desarrollo.

Daena: International Journal of Good Conscience. 15(1)1-15. May 2020. ISSN 1870-557X 1 Tiempos de Coronavirus: La Educación en Línea como Respuesta a la Crisis (Times of Coronavirus: Online Education in Response to the Crisis) Abreu, Jose Luis

Chapter 4 Construction element from debris and demolition waste as a post-disaster strategy

Capítulo 4 Elemento constructivo a partir de residuos de escombros y demoliciones como estrategia post desastre

OGURI, Leticia†* & ESCOBAR, Marlem Guadalupe

Tecnológico de Estudios Superiores de Jocotitlán, Architecture, Mexico.

ID 1st Author: *Leticia, Orugi* / **ORC ID:** 0000-0003-3723-9202, **Researcher ID Thomson:** AAX-2427-2021

ID 1st Co-author: *Marlem Guadalupe, Escobar* / **ORC ID:** 0000-0003-3079-3462

DOI: 10.35429/H.2021.9.1.51.69

L. Oguri & M. Escobar

* leticia.oguri@tesjo.edu.mx

A. Ledesma (Coord.). Engineering Science and Technology. Handbooks-©ECORFAN-México, Estado de México, 2021.

Abstract

In Mexico and the world, the events due to natural disasters that occurred in the last decade have led us to reflect on the commitment of Architecture, it is necessary to understand and measure the responsibility of the architect in disaster areas, it is essential to submit to analysis the teaching of architecture as an agent that generates well-being with social responsibility. The problems that derive from natural disasters, have an impact of considerable duration, the impact of an earthquake for example, not only affects the moment of the event itself, but its consequences infer a wide spectrum of affectations. One of the great concerns is the management and final disposal of waste, in the affected areas of Mexico it is a critical situation, which worsens as the volume of waste generation grows, coupled with it, the customary way its disposal is carried out in open-air dumps, which causes great effects on the natural environment. The environmentally adequate final disposal complicates the capacity of the collection services, the infrastructure and the sanitary landfills, however, the need for their correct handling and control opens the possibility of recycling. This article calls for reflection and presents a research project arising from the classroom, which is based mainly on the design of a mold to create modules as a building element (Block) with the use of construction waste and demolition, as recycled aggregates product of rubble and demolitions, one of the objectives of the project is to verify their effectiveness and thus be able to use them in the reconstruction and construction of another alternative housing at low cost.

Earthquake, Debris, Recycling, Recycling, Modules, Social responsibility

Resumen

En México y en el mundo, los eventos por desastres naturales ocurridos en la última década nos han llevado a reflexionar sobre el compromiso de la Arquitectura, es necesario entender y dimensionar la responsabilidad del arquitecto en zonas de desastre, es indispensable someter a análisis la enseñanza de la arquitectura como agente generador de bienestar con responsabilidad social. Los problemas que se derivan de los desastres naturales, tienen un impacto de considerable duración, el impacto de un terremoto por ejemplo, no solo afecta el momento del evento en sí, sino que sus consecuencias infieren un amplio espectro de afectaciones. Una de las grandes preocupaciones es el manejo y disposición final de los residuos, en las zonas afectadas de México es una situación crítica, que se agrava conforme crece el volumen de generación de residuos, aunado a ello, la forma acostumbrada de su disposición se realiza en tiraderos a cielo abierto, lo que provoca grandes afectaciones al entorno natural. La disposición final ambientalmente adecuada complica la capacidad de los servicios de recolección, la infraestructura y los rellenos sanitarios, sin embargo, la necesidad de su correcto manejo y control abre la posibilidad del reciclaje. Este artículo llama a la reflexión y presenta un proyecto de investigación surgido del aula, el cual se basa principalmente en el diseño de un molde para crear módulos como elemento constructivo (Block) con el uso de residuos de construcción y demolición, como agregados reciclados producto de escombros y demoliciones, uno de los objetivos del proyecto es verificar su efectividad y así poder utilizarlos en la reconstrucción y construcción de otra vivienda alternativa a bajo costo.

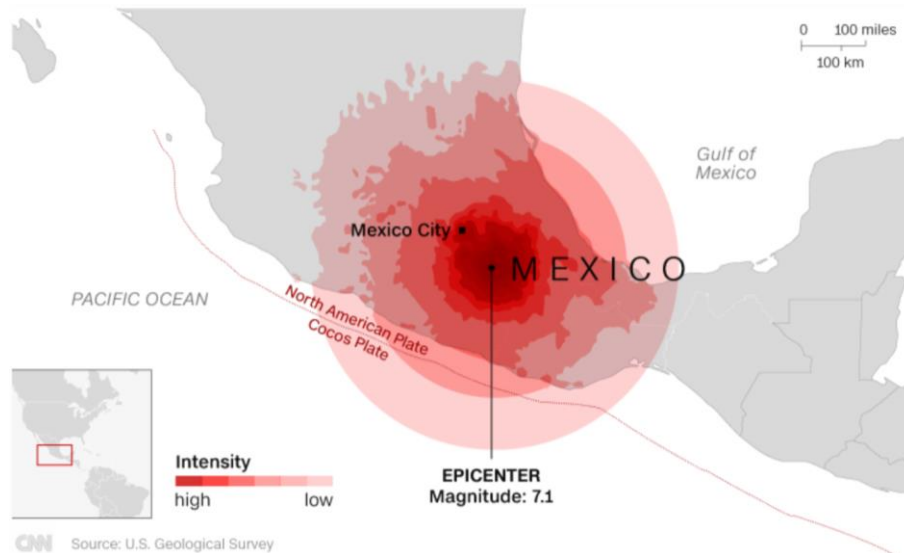
Sismo, Escombros, Reciclaje, Módulos, Responsabilidad social

4.1 Introduction

The earthquakes that have occurred in Mexico and around the world have had an impact not only on the cultural, social and economic spheres, but also on education and architectural practice.

On 19 September 2017 there was an earthquake with a magnitude of 7.1 on the Richter scale with epicentre 120 km south of Mexico City, mainly affecting the States of Mexico, Morelos, Puebla and Mexico City (see figure 4.1), as a result of such movement caused the oceanic tectonic plates of Cocos and North America, to rearrange and fuel the sudden movements of the earth in areas with greater seismicity in Mexico City and other surrounding states, many buildings of more than three levels suffered structural damage in these states, in some cases leaving total collapses due to the deterioration of the buildings themselves or previous deficient construction, although in other cases the damage was only partial or structural, it is known that there is also a serious problem due to lack of compliance with the standards specified in the current building regulations, and consequently, the damage observed is better explained by the lack of compliance with the standards, rather than by possible deficiencies in the current building regulations (Cruz Atienza V, et al, 2017).

Figure 4.1 Location of the epicentre of the earthquake of 19 September 2017



Source: *Mexico had two big earthquakes this month. Here's why*, Faith Karimi, Chandrika Narayan, 2017, <https://edition.cnn.com/2017/09/20/americas/mexico-two-earthquakes-in-one-month/index.html>

As a result of any natural catastrophe, various types of waste are generated, such as special handling waste, which cannot be considered solid urban waste or hazardous waste, since solid urban waste is that which originates from domestic and commercial activity in cities and towns, and hazardous waste is solid materials, These materials are corrosive, reactive, explosive, flammable, flammable, biologically infectious, which if not handled properly and not disposed of properly will generate problems that will have a direct impact on the health of the population and on the environment, soil and water.

Among these special handling wastes are construction and demolition wastes; The Mexican Chamber of the Construction Industry of Mexico attributes this to the fact that there are few entities in the country that have adequate infrastructure for its management, and currently only one recycling plant in operation has been identified, It is also estimated that only 20% of the waste is disposed of in authorised sites, and 3% is recycled, with the rest being disposed of for land levelling, landfills and inappropriately in soils that are optimal for nature preservation and conservation. (CMIC, 2018)

In addition, the extraction and introduction of this type of material not only modifies the soil, but also facilitates the entry of materials or substances into the aquifers that can be carried away by runoff or filtration into the subsoil, and these conditions increase the risk of contamination of water sources, the subsoil and the air.

Therefore, many communities affected by this type of natural phenomenon do not know the proper techniques for the management of debris or waste, and end up disposing of it in rivers or in certain areas a little far from the communities, causing soil contamination, deterioration of the environment and urban image, but above all causing health problems.

In 2017 the SEMARNAT (Ministry of Environment and Natural Resources) released the criteria for the management of construction and demolition waste generated by the 19 September earthquake for the states of Mexico, Morelos, Puebla and Mexico City. This proposal considers the location and operation of final disposal sites, the use and recycling of construction and demolition waste, and finally the clean-up and closure of final disposal sites.

Regarding the use and recycling of debris, it indicates that demolition waste can be used for recycling, obtained by crushing it.

The recycled stone material products can be used in the following projects (SEMARNAT, 2017):

- Sub-base in roads.
- Sub-base in car Parks.
- Embankment construction.
- Landfill.
- Construction of walkways or cycle paths.
- Construction of pipe beds.
- Construction of curb and pavement bases.
- Filling of embankments.
- Hydraulic bases.

Against this backdrop, it is clear that the profession of architect, originally so closely linked to the earth, has changed in recent times due to social, political, economic and educational changes, the introduction of new materials and new practices.

Today, it is necessary to set up awareness-raising programmes aimed at architecture students to reflect on priority issues such as, in this case, shared responsibility in post-disaster situations, seeking to minimise and control waste and, as far as possible, to reincorporate it into the construction chain, since its integral management is a social co-responsibility and requires the joint, coordinated and differentiated participation of producers, distributors, consumers, users of by-products, and the three levels of government as appropriate, under a scheme of market feasibility and environmental, technological, economic and social efficiency.

4.2 Development

In view of the major problem of debris management in post-disaster situations, the use of construction and demolition waste as recycled aggregates in the production of construction elements has attracted attention in recent years.

It has been observed that after natural phenomenological events such as earthquakes, recycled aggregates such as rubble are not suitable for use as high-strength materials, making it possible to make use of low-quality recycled aggregates for the production of concrete blocks.

Faced with this challenge, it has been proposed to create and implement a new building material that incorporates rubble material, through modules that are structurally strong, affordable and contribute to the restoration of housing in affected areas.

In this paper, we report the results of a comprehensive study to assess the feasibility of using crushed bricks, blocks, blocks, brick veneer, tiles, shredded as coarse and fine aggregates in the production of concrete masonry blocks. The effects of crushed aggregate content on the mechanical properties of the non-structural concrete block were quantified. From the results of the experimental tests, it was observed that the incorporation of these crushed waste aggregates had a significant influence on the properties of the blocks.

4.3 Methodology

In view of the great problem that is occurring in our country and in other parts of the world as a result of natural disasters, this research is based on the awareness of the demand for damaged housing and the need to reuse construction and demolition waste such as rubble, to create a new construction element from modules that incorporate fragments of blocks, partitions, ceramics, concrete and other materials with properties that are suitable for reuse in the construction of housing. As can be seen in figure 4.2, there are many tons of this waste material, and it is a material that will contaminate the land surrounding the disaster area and aquifers, as it is dumped clandestinely in these areas, affecting the image and contributing to further environmental deterioration.

Figure 4.2 Jojutla disaster zone, Morelos state, Mexico



Source of reference: Photo taken on site 21 Oct 2018 almost a year after the disaster.

The experimental research method is presented through the manipulation of an untested experimental variable under controlled conditions, in this case, the tests are carried out in a specialised laboratory, with the aim of describing the way or the causes that produce a particular situation or event. The objective of this research is to study the behaviour of the module or construction element through its subjection to various tests, in this way to know and demonstrate its physical properties, in addition, its comparison with analogous elements, makes it possible to detect similarities and to know its virtues and explore new ways to obtain the best use, functionality and sustainability within the standard.

Within the research strategies:

The management of the time and the planning in each one of the stages of the process is of extreme importance to achieve the attainment of the same one, it is for that reason that this investigation has been structured in three periods the first one to short term is the stage of investigation and analysis, being this the theoretical base of all project, the second period to medium term is the practical stage of experimentation where we are subordinated to factors that in some moment can or not interfere in the process as they could be times of tests in laboratory, or physical times of the own element like forged, dried etc. and the last period is the long term, which is the stage of implementation, comparison and elaboration of the product.

Short term:

- Conduct desk and field research.
- Design instruments, surveys, questionnaires and compile photographic archives.
- Analyse information collected both in the literature and in the field.
- Analyse existing prototypes.

In the medium term:

- Select materials from rubble and demolition and granulometries.
- Execute the experimentation of materials to be used, as well as define the samples and proportions.
- Elaborate prototypes with CDW (Construction and Demolition Waste) material.
- Carry out laboratory tests on the materials and the construction element (prototype), carrying out material resistance tests, resistance to compression with universal press.
- Comparison of results.

In the long term:

- Determine the construction processes.

To put forward proposals for improvement in the constructive aspects of the previous prototypes, to study the possibility of integrating new materials and geometries for the reconfiguration of the design of the constructive element and to create the detailed engineering of each prototype, in order to make the product of this research a reliable alternative for contingencies that generate problems with a very high social cost.

- Compare the costs of the product in the current market.
- Construction and Demolition Waste Material.
- Block made from this material.

4.4 Results and discussion

4.4.1 Experimental part

For the development of the project, the process of recycling rubble or waste construction and demolition material caused by the earthquake was used, such as: brick fragments, roof tiles, ceramic tiles, gravel, block fragments and mortar. Basically, it is based on the selection and separation of the material, which is crushed and screened to obtain recycled aggregate materials.

Subsequently, several tests were carried out on mixtures with different proportions of waste materials, cement and water. Checking their adhesion with the cement and other aggregates to create a homogeneous mixture.

At the same time, it was necessary to work on the type of mould to be used, so it was decided to make a solid block and another with cavities.

4.4.2 Materials from debris and demolition waste

The mixture or mortar with which the construction elements were made is composed of Portland cement, water, stone aggregate, which is the rubble and demolition waste previously selected in different granulometries of 3/8" and 3/4", which will later be tested to determine their resistance and can be used as construction material.

4.4.3 Selection and crushing

The rubble and demolition waste RCD was collected and selected with the aim of eliminating residues of rods, wire rods, wire and all impurities not suitable as stone or aggregate material, such as plastic, organic waste, glass, etc.

This selection consisted in the separation of suitable materials, which can be reused and renewed, such as fragments of brick, ceramic tiles, gravel, fragments of blocks and mortars that can adhere to the cement and other aggregates to create a homogeneous mixture with structural properties resistant to those of a commercial block. Finally, the material was subjected to a manual crushing process in order to obtain a similar granulometry to the aggregate commonly used in the manufacture of commercial blocks, which is $\frac{3}{4}$ " gravel and $\frac{3}{8}$ " gravel, which will be replaced by the RCD (fig. 4.3).

Figure 4.3 Material selection and crushing



Source: Photo taken in the concrete laboratory of the Tecnológico de Estudios Superiores de Jocotitlán, Estado de México

4.4.4 Screening and granulometry

The material resulting from the crushing was sieved or mechanically screened with ASTM test sieves to obtain its specific granulometry, which is $\frac{3}{8}$ " and $\frac{3}{4}$ ".

Figure 4.4 Screening of the material and particle size of the stone aggregate or aggregate



Source: Photo taken in the concrete laboratory of the Tecnológico de Estudios Superiores de Jocotitlán, Estado de México

4.4.5 Dosage or proportions

According to bloqueras.org on the dosage for the production of concrete blocks (see table 4.1), we took as a basis for the production of the blocks, replacing the gravel with CDW (construction and demolition waste). The rubble was used, previously crushed and screened, with an aggregate of 3/8" and the proportions of cement were varied, from 0.4, 0.8 and 1.2 kg. For the elaboration of a block or test piece.

Table 4.1 Dosage table to produce concrete blocks

Quantity	Mix m ³	Water litres	Cement kg	Sand kg	Gravel kg.	F+G
60	1	40	50	150	200	0,4
120	2	80	100	300	400	0,4
240	3	160	200	600	800	0,4
480	4	320	400	1200	1600	0,4
960	5	640	800	2400	3200	0,4

Source: <https://bloqueras.org/bloques-concreto/>

On the basis of these data for the elaboration of a block

Table 4.2 Dosage table to produce a concrete block

Quantity	Mix m ³	Water litres	Cement kg	Sand kg	Gravel kg.	F+G
1	0.016	.66	.83	2.5	3.33	0,4

Source: Own elaboration

4.4.6 Mix

Usually, the concrete mixture used to make this type of blocks is a mixture of Portland cement, sand, gravel and water, with the proportions described above, so we proceeded to make the mixtures, having obtained the crushing and selection of each of the materials that had the necessary characteristics and the behaviour of the preliminary mixtures, the experimental design was carried out (mixtures used in the manufacture of the blocks), this design was also based on the principles of handmade manufacture of blocks and bricks, being able to approximate in detail the weights of the materials used. Ten mixtures were designed with variations in proportions and type of material used, the mixtures were defined based on the granulometry of the materials used as aggregates (construction and demolition waste that meet the necessary characteristics of adherence to cement, and the type of material used in the production of the blocks).

Table 4.3 Dosage table to produce RCD mix in percentages

Mix	RCD	Sand	Cal	RP ¹	Cement	Water litres
1	39.21%	16.66%	9.80%	9.80%	24.50%	.66
2	44.44%	35.55%	4.44%	0%	15.55%	.66
3	48.14%	37.03%	3.70%	0%	11.11%	.66
4	58.06%	16.12%	6.45%	0%	19.35%	.66
5	55.81%	13.95%	4.65%	9.30%	16.27%	.66
6	55.31%	14.89%	6.38%	12.76%	10.63%	.66
7	65.35%	16.33%	6.53%	0%	11.76%	.66
8	24.39%	58.53%	4.87%	0%	12.19%	.66
9	65.02%	22.42%	4.48%	0%	8.07%	.66
10	56.45%	32.25%	4.03%	0%	7.25%	.66

Source: Own elaboration

The preparation of this mixture was done mechanically with a mixer with a capacity of 1 bag of cement or 270 litres, the 3/8" RCD waste, cement, lime, sand and water were added, according to the dosage tables (see Table 3). This process requires careful observation of the amount of water needed and the mixing time, which varied from 6 to 8 minutes per mixture according to the observation of the consistency of the mixture.

Plastic waste (rubber).

Figure 4.5 Concrete mixer for the production of concrete mixes



Source: Photo taken in the concrete laboratory of the Tecnológico de Estudios Superiores de Jocotitlán, Estado de México

4.4.7 Preparation of the mould

The proposal for the shape of the mould for the block is the conventional one, for which two commercial moulds were bought, one for a solid block measuring 20cm x 40cm x 20cm (MM⁻¹) and the other for a hollow block measuring 20cm x 40cm x 20cm (MH⁻¹). This is in accordance with the Mexican standard NMX-C-038-ONNCCE, which states that the mould should have a dimension of 20 x 20 x 40 cm.

Figure 4.6 Commercial moulds to produce blocks 20 x 20 x 20 x 40 cm



Source: Photo taken in the concrete laboratory of the Tecnológico de Estudios Superiores de Jocotitlán, Estado de México

The preparations of the moulds were the application of burnt engine oil on the walls, as this will not allow the mixture to adhere nor alter the content of the preparation poured into it. (See fig.4.7).

Figure 4.7 Application of burnt oil to the metal mould



Source: Photo taken in the concrete laboratory of the Tecnológico de Estudios Superiores de Jocotitlán, Estado de México

4.4.8 Pouring the moulds

It is necessary to take care that the mixture is poured immediately into the moulds as it can set very quickly according to the amount of cement and lime, we proceeded to pour the homogeneous mixture and at the same time the air bubbles were eliminated by means of a manual vibration with a rod, putting it in and taking it out constantly, in the emptying it must be taken into account to fill the block completely because if it does not vary in the dimensions of the block, the block must have an adequate compaction, so that it obtains its maximum degree of resistance.

Figure 4.8 Pouring the mixture into the solid mould



Source: Photo taken in the concrete laboratory of the Tecnológico de Estudios Superiores de Jocotitlán, Estado de México

4.4.9 Demoulding

Demoulding is done once the pouring and compacting of the material and the drying of the specimens have been completed, in an appropriate space, free of humidity, with windows that allow air and sunlight to enter.

4.4.10 Waiting time for setting

Waiting time for setting was given for the samples of 28 days to reach the total drying of the samples before proceeding to take them to the laboratory to perform the appropriate tests to see if they comply with the necessary specifications according to NMX-C-038-ONNCCE.

4.4.11 Blocks

According to the Mexican standard NMX-C-404-ONNCCE-2012 which refers to the manufacturing dimension of the solid piece or solid concrete block should have a dimension of 390 mm long, 190 mm, without the thickness of the masonry joint and which should adjust the actual dimension within manufacturing tolerances, for example the common blocks have nominal dimensions of 200mm x 400mm (20cm x 40cm) in height and length respectively.

And the actual dimension is the measurement of each piece obtained by measuring by the test method specified in the Mexican standard NMX-C-038-ONNCCE where it handles tolerances of up to 3mm in any of its dimensions.

4.4.12 Laboratory tests

In order to evaluate the feasibility of the project, it was necessary to submit the new construction material to rigorous laboratory tests to determine compliance with structural requirements and to determine the properties of the structural or standard block in accordance with Mexican standards NMX-C-404 -1997-ONNCCE, and NMX-C-036, NMX-C-037, NMX-C-038, NMX-C-082, NMX-C-185, NMX-C-307.

The tests to which 11 construction elements were subjected (Blocks from sample 01 to 05 are hollow elements, from sample 06 to 11 are samples of solid elements, consisted of breaking load tests (kg), resistance tests (kg/cm^2), as well as the verification of their volumetric weight in the laboratory.

The following are the official reports of the laboratory tests of the hollow and solid blocks of the construction materials laboratory LAMACO Control y calidad S.C. in Santa María Totoltepec, Edo de México.

Figure 4.9 Sample test 01H

LAMACO
CONTROL Y CALIDAD S.C.

REPORTE DE BLOCKS DE CONCRETO LIGERO MACIZO
NORMA MEXICANA
NMX-C-404-1997-ONVCC, NMX-C-636, NMX-C-638, NMX-C-637, NMX-C-639, NMX-C-682, NMX-C-181, NMX-C-307

CLIENTE: TECNOLÓGICO DE ESTUDIOS SUPERIORES DE JOCOTITLÁN

OBRA O PROYECTO Y UBICACIÓN: "ELEMENTO CONSTRUCTIVO TESJO"
TECNOLÓGICO DE ESTUDIOS SUPERIORES DE JOCOTITLÁN CARRETERA TOLUCA-ATLACOMULCO KM 44.8 EJIDO DE SAN JUAN Y SAN AGUSTIN, 80700 JOCOTITLÁN, ESTADO DE MÉXICO

PROVEEDOR: TECNOLÓGICO DE ESTUDIOS SUPERIORES DE JOCOTITLÁN

TIPO: BLOCK HUECO (MUESTRA 1)

LUGAR DE MUESTREO Y EMPLEO: LABORATORIO TESJO

ENSAYE No.	001			
MUESTRA No.	1			
BLOCK No.	001			
ANCHO (cm)	20.0			
LARGO (cm)	40.0			
ALTURA (cm)	19.0			
PESO DEL BLOCK (kg)	12,160			
ÁREA TOTAL (cm ²)	800.0			
ÁREA NETA (cm ²)	443.3			
PESO VOLUMÉTRICO DEL BLOCK (kg/m ³)	1,443.7			
FECHA DE MUESTREO	31/01/2020			
FECHA DE RUPTURA	02/02/2020			
CARGA DE RUPTURA (kg)	14,000			
RESISTENCIA (Kg/cm ²)	17.5			
PORCENTAJE DE ABSORCIÓN (%)	9.8			

COMENTARIOS: LOS ESPECIMENES SE ENSAYARON EN ESTADO SECO.

ELABORÓ: LAMACORRISTA, TEC. EMIGDIO GUADARRAMA BERNAL

REVISÓ: GERENTE TÉCNICO, TEC. VICTORIANO RAMÍREZ TRUJILLO

RECIBÓ: TECNOLÓGICO DE ESTUDIOS SUPERIORES DE JOCOTITLÁN EMPRESA

LCC-PT-03-FIG-01 EDICIÓN 01 2019-01-01 PAGINA 01 DE 01

ARTÍCULO No. 27, Int. 6 Col. La Loma, Santa María Totoltepec, Edo de México. TEL. 01 (722) 1 99 3661 2 12 44 46 044 o 045 722 2 45 07 02 lamaco1366@prodigy.net.mx

Figure 4.10 Sample test 02 H

LAMACO
CONTROL Y CALIDAD S.C.

REPORTE DE BLOCKS DE CONCRETO LIGERO MACIZO
NORMA MEXICANA
NMX-C-404-1997-ONVCC, NMX-C-636, NMX-C-638, NMX-C-637, NMX-C-639, NMX-C-682, NMX-C-181, NMX-C-307

CLIENTE: TECNOLÓGICO DE ESTUDIOS SUPERIORES DE JOCOTITLÁN

OBRA O PROYECTO Y UBICACIÓN: "ELEMENTO CONSTRUCTIVO TESJO"
TECNOLÓGICO DE ESTUDIOS SUPERIORES DE JOCOTITLÁN CARRETERA TOLUCA-ATLACOMULCO KM 44.8 EJIDO DE SAN JUAN Y SAN AGUSTIN, 80700 MUNICIPIO DE JOCOTITLÁN, ESTADO DE MÉXICO

PROVEEDOR: TECNOLÓGICO DE ESTUDIOS SUPERIORES DE JOCOTITLÁN

TIPO: BLOCK HUECO (MUESTRA 2)

LUGAR DE MUESTREO Y EMPLEO: LABORATORIO TESJO

ENSAYE No.	001			
MUESTRA No.	2			
BLOCK No.	001			
ANCHO (cm)	20.0			
LARGO (cm)	40.0			
ALTURA (cm)	21.5			
PESO DEL BLOCK (kg)	12,300			
ÁREA TOTAL (cm ²)	800.0			
ÁREA NETA (cm ²)	395.0			
PESO VOLUMÉTRICO DEL BLOCK (kg/m ³)	1,448.3			
FECHA DE MUESTREO	31/01/2020			
FECHA DE RUPTURA	02/02/2020			
CARGA DE RUPTURA (kg)	12,300			
RESISTENCIA (kg/cm ²)	15.4			
PORCENTAJE DE ABSORCIÓN (%)	8.3			

COMENTARIOS: LOS ESPECIMENES SE ENSAYARON EN ESTADO SECO.

ELABORÓ: LAMACORRISTA, TEC. EMIGDIO GUADARRAMA BERNAL

REVISÓ: GERENTE TÉCNICO, TEC. VICTORIANO RAMÍREZ TRUJILLO

RECIBÓ: TECNOLÓGICO DE ESTUDIOS SUPERIORES DE JOCOTITLÁN EMPRESA

LCC-PT-03-FIG-01 EDICIÓN 01 2019-01-01 PAGINA 01 DE 01

ARTÍCULO No. 27, Int. 6 Col. La Loma, Santa María Totoltepec, Edo de México. TEL. 01 (722) 1 99 3661 2 12 44 46 044 o 045 722 2 45 07 02 lamaco1366@prodigy.net.mx

Figure 4.11 Sample test 03 H

LAMACO
CONTROL Y CALIDAD S.C.

REPORTE DE BLOCKS DE CONCRETO LIGERO MACIZO
NORMA MEXICANA
NMX-C-404-1987-CANICE, NMX-C-404, NMX-C-407, NMX-C-408, NMX-C-409, NMX-C-181, NMX-C-307

CLIENTE:	TECNOLOGICO DE ESTUDIOS SUPERIORES DE JOCOITTLAN
OBRA O PROYECTO Y UBICACION:	"ELEMENTO CONSTRUCTIVO TESJO" TECNOLOGICO DE ESTUDIOS SUPERIORES DE JOCOITTLAN CARRETERA TOLUCA ATLACOMULCO KM 44.8 EJIDO DE SAN JUAN Y SAN AGUSTIN, 80780 MUNICIPIO DE JOCOITTLAN, ESTADO DE MEXICO

A CONTINUACION SE PRESENTAN LOS RESULTADOS DE RESISTENCIA A COMPRESION DE BLOCKS DE CONCRETO QUE SE ENVIARON A LA PRUEBA DE COMPRESION EN EL

PROVEEDOR:	TECNOLOGICO DE ESTUDIOS SUPERIORES DE JOCOITTLAN
TIPO:	BLOCK MACIZO (MUESTRA B)
LUGAR DE MUESTREO Y EMPLEO:	LABORATORIO TESJO

ENVIANTE No.	001		
MUESTRA No.	3		
BLOCK No.	001		
ANCHO (mm)	20.0		
LARGO (mm)	40.0		
ALTURA (mm)	20.0		
PESO DEL BLOCK (kg)	13.790		
AREA TOTAL (cm ²)	800.0		
AREA NETA (cm ²)	423.0		
PESO VOLUMETRICO DEL BLOCK (kg/m ³)	1,818.4		
FECHA DE MUESTREO:	31/01/2020		
FECHA DE RUPTURA:	02/02/2020		
CARGA DE RUPTURA (kg)	10,800		
RESISTENCIA (kg/cm ²)	13.2		
PORCENTAJE DE ABSORCION (%)	13.9		

COMENTARIOS: LOS ESPECIMENES SE ENSAYARON EN ESTADO BECO.

ELABORO:	REVISO:	RECIBO:
TEC. EMANUEL GUADARRAMA BERNAL	TEC. VICTORIANO RAMIREZ TRUJILLO	TECNOLOGICO DE ESTUDIOS SUPERIORES DE JOCOITTLAN EMPRESA

LCC-PT-03-FIG-01 EDICION 01 2018-01-01 PAGINA 01 DE 01

ARTICULO No. 27, Vol. 6 Cof. La Loma, Santa Maria Tototipacapan, Edo de Mexico. TEL: 01 (722) 1 99 3848 2 12 44 46 046 o 046 722 2 45 07 02

Figure 4.12 Sample test 04 H

LAMACO
CONTROL Y CALIDAD S.C.

REPORTE DE BLOCKS DE CONCRETO LIGERO MACIZO
NORMA MEXICANA
NMX-C-404-1987-CANICE, NMX-C-404, NMX-C-407, NMX-C-408, NMX-C-409, NMX-C-181, NMX-C-307

CLIENTE:	TECNOLOGICO DE ESTUDIOS SUPERIORES DE JOCOITTLAN
OBRA O PROYECTO Y UBICACION:	"ELEMENTO CONSTRUCTIVO TESJO" TECNOLOGICO DE ESTUDIOS SUPERIORES DE JOCOITTLAN CARRETERA TOLUCA ATLACOMULCO KM 44.8 EJIDO DE SAN JUAN Y SAN AGUSTIN, 80780 MUNICIPIO DE JOCOITTLAN, ESTADO DE MEXICO

A CONTINUACION SE PRESENTAN LOS RESULTADOS DE RESISTENCIA A COMPRESION DE BLOCKS DE CONCRETO QUE SE ENVIARON A LA PRUEBA DE COMPRESION EN EL

PROVEEDOR:	TECNOLOGICO DE ESTUDIOS SUPERIORES DE JOCOITTLAN
TIPO:	BLOCK MACIZO (MUESTRA B)
LUGAR DE MUESTREO Y EMPLEO:	LABORATORIO TESJO

ENVIANTE No.	001		
MUESTRA No.	4		
BLOCK No.	001		
ANCHO (mm)	20.0		
LARGO (mm)	40.0		
ALTURA (mm)	20.0		
PESO DEL BLOCK (kg)	12.200		
AREA TOTAL (cm ²)	800.0		
AREA NETA (cm ²)	423.0		
PESO VOLUMETRICO DEL BLOCK (kg/m ³)	1,442.1		
FECHA DE MUESTREO:	31/01/2020		
FECHA DE RUPTURA:	02/02/2020		
CARGA DE RUPTURA (kg)	7,600		
RESISTENCIA (kg/cm ²)	8.8		
PORCENTAJE DE ABSORCION (%)	11.8		

COMENTARIOS: LOS ESPECIMENES SE ENSAYARON EN ESTADO BECO.

ELABORO:	REVISO:	RECIBO:
TEC. EMANUEL GUADARRAMA BERNAL	TEC. VICTORIANO RAMIREZ TRUJILLO	TECNOLOGICO DE ESTUDIOS SUPERIORES DE JOCOITTLAN EMPRESA

LCC-PT-03-FIG-01 EDICION 01 2018-01-01 PAGINA 01 DE 01

ARTICULO No. 27, Vol. 6 Cof. La Loma, Santa Maria Tototipacapan, Edo de Mexico. TEL: 01 (722) 1 99 3848 2 12 44 46 046 o 046 722 2 45 07 02

Figure 4.13 Sample test 05 H

LAMACO
CONTROL Y CALIDAD S.C.

REPORTE DE BLOCKS DE CONCRETO LIGERO MACIZO
NORMA MEXICANA
NMX-C-404-1997-04NCCCE, NMX-C-038, NMX-C-037, NMX-C-038, NMX-C-082, NMX-C-185, NMX-C-307

CLIENTE:	TECNOLOGICO DE ESTUDIOS SUPERIORES DE JOCOITTLAN
OBRA O PROYECTO Y UBICACION:	"ELEMENTO CONSTRUCTIVO TESJO" TECNOLOGICO DE ESTUDIOS SUPERIORES DE JOCOITTLAN CARRETERA TOLUCA-ATLACOMULCO KM 44.8 EJIDO DE SAN JUAN Y SAN AGUSTIN, 50700 MUNICIPIO DE JOCOITTLAN, ESTADO DE MEXICO

A CONTINUACION SE PRESENTA A UNICO RESULTADO DE RESISTENCIA A COMPRESION EN BLOCKS DE CONCRETO QUE SE SOMETIERON A LA PRUEBA DE COMPRESION ASIA.

PROVEEDOR:	TECNOLOGICO DE ESTUDIOS SUPERIORES DE JOCOITTLAN
TPO:	BLOCK HUECO (MUESTRA B)
LUGAR DE MUESTREO Y EMPLEO:	LABORATORIO TESJO

ENBAYE No.	001				
MUESTRA No.	5				
BLOCK No.	001				
ANCHO (cm).	20.0				
LARGO (cm).	40.0				
ALTURA (cm).	20.0				
PESO DEL BLOCK (kg).	13,150				
AREA TOTAL (cm ²).	800.0				
AREA NETA (cm ²).	381.5				
PESO VOLUMETRICO DEL BLOCK (kg/m ³).	1,723.5				
FECHA DE MUESTREO.	31/01/2020				
FECHA DE RUPTURA.	02/02/2020				
CARGA DE RUPTURA (kg).	13,150				
RESISTENCIA (kg/cm ²).	18.4				
PORCENTAJE DE ABSORCION (%).	10.6				

COMENTARIOS:	LOS ESPECIMENES SE ENSAYARON EN ESTADO SECO.
--------------	--

ELABORO: LABORATORISTA: TEC. EMIGDO GUADARRAMA BERNAL	REVISO: GERENTE TECNICO: TEC. VICTORIANO RAMIREZ TRUJILLO	RECIBO: TECNOLOGICO DE ESTUDIOS SUPERIORES DE JOCOITTLAN EMPRESA
---	---	---

LCC-PT-03-FIG-01 EDICIÓN 01 2016-01-01 PAGINA 01 DE 01

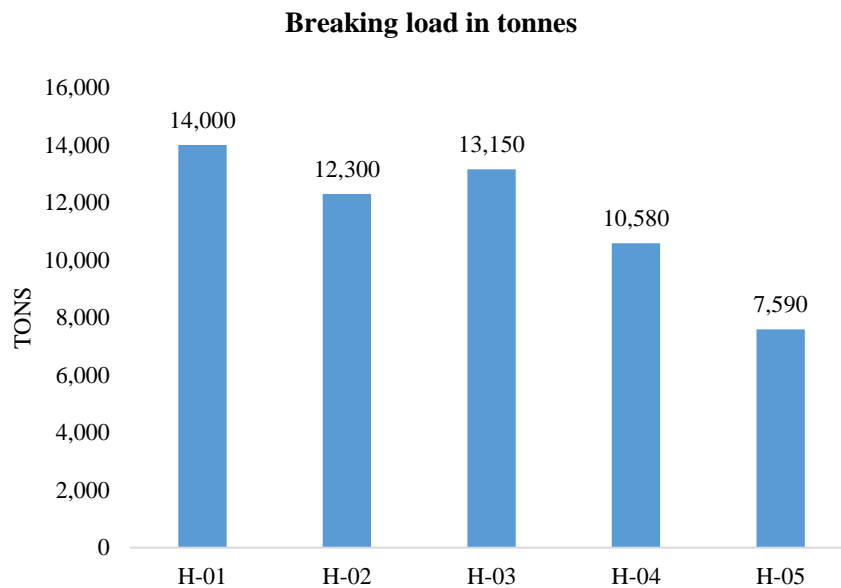
ARTICULO No. 27, Int. 0 Col. La Loma, Santa Maria Totoltepec, Edo de Mexico. lamaco1966@prodigy.net.mx TEL. 01 (722) 1 99 3661 2 12 44 46 044 o 045 722 2 45 07 02

4.4.13 Analysis of the results of the element samples

a. Hollow block

Regarding the tests on the hollow blocks, the laboratory report shows, as shown in graphic 4.1, that Block H-01 obtained the highest resistance to rupture with 14.00 Ton at the maximum degree of rupture.

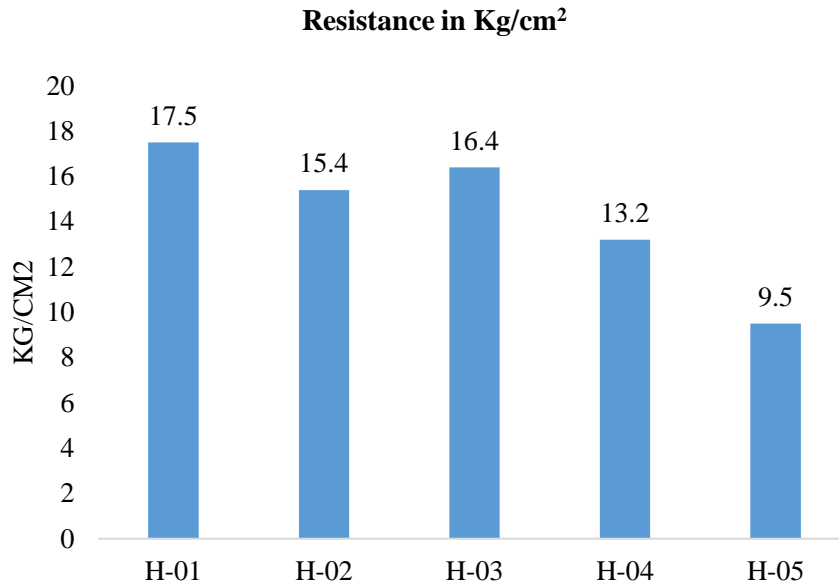
Graphic 4.1 Hollow block breaking load in tonnes



Source: Own elaboration

The data in graphic 4.2, with respect to the resistance test, a point load distributed on the nodding machine is placed on each of the blocks, obtaining a different pressure for each one of them, so it is obtained that in the same way it is block H-01 that obtains greater resistance in comparison to the other blocks.

Graphic 4.2 Hollow block breaking load in tonnes




Source: Own elaboration

From the results of the resistances of the five types of hollow blocks that were made, it is concluded that Block H-01 does not fall within the necessary range to be a non-structural block according to the **PROY-NMX-C-441-ONNCCE-2011** standard (Construction industry - masonry - blocks, partitions or bricks and partitions for non-structural use - specifications and test methods), which specifies that a non-structural block must have a compressive strength of 35 kg/cm².

Solid block

Figure 4.14 Sample test M-06



REPORTE DE BLOCKS DE CONCRETO LIGERO MACIZO
NORMA MEXICANA
NMX-C-441-1987-ONNCCE, NMX-C-436, NMX-C-437, NMX-C-438, NMX-C-462, NMX-C-463, NMX-C-464

CLIENTE:	TECNOLOGICO DE ESTUDIOS SUPERIORES DE JOCOITTLAN	
OBRA O PROYECTO Y UBICACION:	"ELEMENTO CONSTRUCTIVO TESJO" TECNOLOGICO DE ESTUDIOS SUPERIORES DE JOCOITTLAN CARRETERA TOLUCA ATLACONCILCO KM 44.8 GUISO DE SAN JUAN Y SAN AGUSTIN, 85700 MUNICIPIO DE JOCOITTLAN, ESTADO DE MEXICO	
PROVEEDOR:	TECNOLOGICO DE ESTUDIOS SUPERIORES DE JOCOITTLAN	
TIPO:	BLOCK MACIZO (MUESTRA #)	
LUGAR DE MUESTREO Y EMPLEO:	LABORATORIO TESJO	

ENSAYE No.	001	
MUESTRA No.	6	
BLOCK No.	001	
ANCHO (mm)	19.0	
LARGO (mm)	40.0	
ALTURA (mm)	20.0	
PESO DEL BLOCK (kg)	23.000	
AREA TOTAL (cm²)	760.0	
AREA NETA (cm²)	760.0	
PESO VOLUMETRIC DEL BLOCK (kg/m³)	1,616.4	
FECHA DE MUESTREO:	31/01/2020	
FECHA DE RUPTURA:	02/02/2020	
CARGA DE RUPTURA (kg)	20,190	
RESISTENCIA (kg/cm²)	26.6	
PORCENTAJE DE ABSORCIÓN (%)	14.8	

COMENTARIOS:	LOS ESPECIMENES SE ENSAYARON EN ESTADO SECO.
--------------	--

LABORADO <i>[Signature]</i> LABORATORISTA TEC. BRUNO GUADARRAMA BERNAL	REVISADO <i>[Signature]</i> GERENTE TECNICO TEC. VICTORIANO RAMIREZ TRULLIO	RECIBIDO <i>[Signature]</i> TECNOLOGICO DE ESTUDIOS SUPERIORES DE JOCOITTLAN EMPRESA
---	--	---

LCG-PT-03-FIG-01 EDICIÓN 01 2016-01-01
PAGINA 01 DE 01

ARTICULO No. 27, INC. 6 CON. La Loma, Santa María Tenochtitlan, Edo de México. lamaco1986@protonmail.net.mx

TEL. 01 (722) 1 99 9881
2 32 44 48
044 o 045 722 2 40 07 02

Figure 4.15 Sample test M-07

LAMACO
CONTROL Y CALIDAD S.C.

REPORTE DE BLOCKS DE CONCRETO LIGERO MACIZO
NORMA MEXICANA
NMX-C-404-1987-ONRCCO, NMX-C-438, NMX-C-617, NMX-C-638, NMX-C-682, NMX-C-188, NMX-C-307

CLIENTE:	TECNOLOGICO DE ESTUDIOS SUPERIORES DE JOCOTITLAN
OBRA O PROYECTO Y UBICACIÓN:	"ELEMENTO CONSTRUCTIVO TESJO" TECNOLOGICO DE ESTUDIOS SUPERIORES DE JOCOTITLAN CARRETERA TOLUCA ATLACOMULCO KM 44.8 EJIDO DE SAN JUAN Y SAN AGUSTIN, 92700 MUNICIPIO DE JOCOTITLAN, ESTADO DE MEXICO

A continuación se reportan a efectos de información los resultados de ensayos de concreto que se sometieron a la prueba de compresión axial.

PROVEEDOR:	TECNOLOGICO DE ESTUDIOS SUPERIORES DE JOCOTITLAN
TIPO:	BLOCK MACIZO (MUESTRA 7)
LUGAR DE MUESTREO Y EMPLEO:	LABORATORIO TESJO

ENSAYE No:	001	
MUESTRA No:	7	
BLOCK No:	001	
ANCHO (cm):	17.0	
LARGO (cm):	40.0	
ALTURA (cm):	20.0	
PESO DEL BLOCK (kg):	20,000	
AREA TOTAL (cm ²):	700.0	
AREA NETA (cm ²):	700.0	
PESO VOLUMETRICO DEL BLOCK (kg/m ³):	1,428.6	
FECHA DE MUESTREO:	31/01/2020	
FECHA DE RUPTURA:	02/02/2020	
CARGA DE RUPTURA (kg):	18,820	
RESISTENCIA (kg/cm ²):	23.7	
PORCENTAJE DE ABSORCIÓN (%):	12.7	

COMENTARIOS:	LOS ESPECIMENES SE ENSAYARON EN ESTADO SECO.
--------------	--

ELABORO: TEC. EMILIO GUADARRAMA BERNAL	REVISO: TEC. VICTORIANO RAMIREZ TRUJILLO	RECIBO: TECNOLOGICO DE ESTUDIOS SUPERIORES DE JOCOTITLAN EMPRESA
---	---	---

LCC-PT-03-FIG-01 EDICIÓN 01 2016-01-01 PÁGINA 01 DE 01

ARTICULO No. 27, Ave. 6 Cal. La Loma, Santa María Tonoloway, Edo de México. lamacol2006@prodigy.net.mx

TEL. 01 (722) 1 99 3861
2 12 44 46
044 o 045 722 2 45 07 02

Figure 4.16 Sample test 08 M

LAMACO
CONTROL Y CALIDAD S.C.

REPORTE DE BLOCKS DE CONCRETO LIGERO MACIZO
NORMA MEXICANA
NMX-C-404-1987-ONRCCO, NMX-C-438, NMX-C-617, NMX-C-638, NMX-C-682, NMX-C-188, NMX-C-307

CLIENTE:	TECNOLOGICO DE ESTUDIOS SUPERIORES DE JOCOTITLAN
OBRA O PROYECTO Y UBICACIÓN:	"ELEMENTO CONSTRUCTIVO TESJO" TECNOLOGICO DE ESTUDIOS SUPERIORES DE JOCOTITLAN CARRETERA TOLUCA ATLACOMULCO KM 44.8 EJIDO DE SAN JUAN Y SAN AGUSTIN, 92700 MUNICIPIO DE JOCOTITLAN, ESTADO DE MEXICO

A continuación se reportan a efectos de información los resultados de ensayos de concreto que se sometieron a la prueba de compresión axial.

PROVEEDOR:	TECNOLOGICO DE ESTUDIOS SUPERIORES DE JOCOTITLAN
TIPO:	BLOCK MACIZO (MUESTRA 8)
LUGAR DE MUESTREO Y EMPLEO:	LABORATORIO TESJO

ENSAYE No:	001	
MUESTRA No:	8	
BLOCK No:	001	
ANCHO (cm):	20.0	
LARGO (cm):	40.0	
ALTURA (cm):	20.0	
PESO DEL BLOCK (kg):	20,000	
AREA TOTAL (cm ²):	800.0	
AREA NETA (cm ²):	800.0	
PESO VOLUMETRICO DEL BLOCK (kg/m ³):	1,250.0	
FECHA DE MUESTREO:	31/01/2020	
FECHA DE RUPTURA:	02/02/2020	
CARGA DE RUPTURA (kg):	15,670	
RESISTENCIA (kg/cm ²):	24.5	
PORCENTAJE DE ABSORCIÓN (%):	10.0	

COMENTARIOS:	LOS ESPECIMENES SE ENSAYARON EN ESTADO SECO.
--------------	--

ELABORO: TEC. EMILIO GUADARRAMA BERNAL	REVISO: TEC. VICTORIANO RAMIREZ TRUJILLO	RECIBO: TECNOLOGICO DE ESTUDIOS SUPERIORES DE JOCOTITLAN EMPRESA
---	---	---

LCC-PT-03-FIG-01 EDICIÓN 01 2016-01-01 PÁGINA 01 DE 01

ARTICULO No. 27, Ave. 6 Cal. La Loma, Santa María Tonoloway, Edo de México. lamacol2006@prodigy.net.mx

TEL. 01 (722) 1 99 3861
2 12 44 46
044 o 045 722 2 45 07 02

Figure 4.17 Sample test 09 M

LAMACO
CONTROL Y CALIDAD S.C.

REPORTE DE BLOCKS DE CONCRETO LIGERO MACIZO
NORMA MEXICANA
NMX-C-404-1997-CONICCE, NMX-C-438, NMX-C-439, NMX-C-437, NMX-C-438, NMX-C-482, NMX-C-188, NMX-C-307

CLIENTE:	TECNOLOGICO DE ESTUDIOS SUPERIORES DE JOCOTITLAN
OBRA O PROYECTO Y UBICACION:	"ELEMENTO CONSTRUCTIVO TESJO" TECNOLOGICO DE ESTUDIOS SUPERIORES DE JOCOTITLAN CARRETERA TOLUCA ATLACOMULCO KM 44.8 EJIDO DE SAN JUAN Y, SAN AGUSTIN, 50708 MUNICIPIO DE JOCOTITLAN, ESTADO DE MEXICO

SE CONTIENE UN RESUMEN DE LOS RESULTADOS DE RESISTENCIA A COMPRESION DE BLOQUES DE CONCRETO QUE SE SUBMETIERON A LA PRUEBA DE COMPRESION APAL.

PROVEEDOR:	TECNOLOGICO DE ESTUDIOS SUPERIORES DE JOCOTITLAN
TIPO:	BLOCK MACIZO (MUESTRA 9)
LUGAR DE MUESTREO Y EMPLEO:	LABORATORIO TESJO

ENSAYE No.	001			
MUESTRA No.	9			
BLOCK No.	001			
ANCHO (cm)	16.0			
LARGO (cm)	40.0			
ALTURA (cm)	20.0			
PESO DEL BLOCK (kg)	21.900			
AREA TOTAL (cm ²)	640.0			
AREA NETA (cm ²)	640.0			
PESO VOLUMETRICO DEL BLOCK (kg/m ³)	1.716.9			
FECHA DE MUESTREO:	31/01/2020			
FECHA DE RUPTURA:	02/02/2020			
CARGA DE RUPTURA (kg)	26.820			
RESISTENCIA (kg/cm ²)	41.9			
PORCENTAJE DE ABSORCION (%)	16.2			

COMENTARIOS:	LOS ESPECIMENES SE ENSAYARON EN ESTADO SECO.
--------------	--

ELABORO: TEC. ENRIQUE GUADARRAMA BERNAL	REVISO: TEC. VICTORIANO RAMIREZ TRUJILLO	RECIBO: TECNOLOGICO DE ESTUDIOS SUPERIORES DE JOCOTITLAN EMPRESA
--	---	---

LCC-PT-03-FIG-01 EDICION 01 2018-01-01 PAGINA 01 DE 01

ARTICULO No. 27, inc. 6 Col. La Loma, Santa Maria Tototlapepec, Edo de Mexico. lamaco1966@prodigy.net.mx TEL. 01 (722) 1 99 3663 2 12 44 46 044 o 045 722 2 45 07 02

Figure 4.18 Sample test 10 M

LAMACO
CONTROL Y CALIDAD S.C.

REPORTE DE BLOCKS DE CONCRETO LIGERO MACIZO
NORMA MEXICANA
NMX-C-404-1997-CONICCE, NMX-C-438, NMX-C-439, NMX-C-437, NMX-C-438, NMX-C-482, NMX-C-188, NMX-C-307

CLIENTE:	TECNOLOGICO DE ESTUDIOS SUPERIORES DE JOCOTITLAN
OBRA O PROYECTO Y UBICACION:	"ELEMENTO CONSTRUCTIVO TESJO" TECNOLOGICO DE ESTUDIOS SUPERIORES DE JOCOTITLAN CARRETERA TOLUCA ATLACOMULCO KM 44.8 EJIDO DE SAN JUAN Y, SAN AGUSTIN, 50708 MUNICIPIO DE JOCOTITLAN, ESTADO DE MEXICO

SE CONTIENE UN RESUMEN DE LOS RESULTADOS DE RESISTENCIA A COMPRESION DE BLOQUES DE CONCRETO QUE SE SUBMETIERON A LA PRUEBA DE COMPRESION APAL.

PROVEEDOR:	TECNOLOGICO DE ESTUDIOS SUPERIORES DE JOCOTITLAN
TIPO:	BLOCK MACIZO (MUESTRA 10)
LUGAR DE MUESTREO Y EMPLEO:	LABORATORIO TESJO

ENSAYE No.	001			
MUESTRA No.	10			
BLOCK No.	001			
ANCHO (cm)	19.0			
LARGO (cm)	40.0			
ALTURA (cm)	20.0			
PESO DEL BLOCK (kg)	24.150			
AREA TOTAL (cm ²)	760.0			
AREA NETA (cm ²)	760.0			
PESO VOLUMETRICO DEL BLOCK (kg/m ³)	1.588.8			
FECHA DE MUESTREO:	31/01/2020			
FECHA DE RUPTURA:	02/02/2020			
CARGA DE RUPTURA (kg)	15.320			
RESISTENCIA (kg/cm ²)	20.2			
PORCENTAJE DE ABSORCION (%)	10.6			

COMENTARIOS:	LOS ESPECIMENES SE ENSAYARON EN ESTADO SECO.
--------------	--

ELABORO: TEC. ENRIQUE GUADARRAMA BERNAL	REVISO: TEC. VICTORIANO RAMIREZ TRUJILLO	RECIBO: TECNOLOGICO DE ESTUDIOS SUPERIORES DE JOCOTITLAN EMPRESA
--	---	---

LCC-PT-03-FIG-01 EDICION 01 2018-01-01 PAGINA 01 DE 01

ARTICULO No. 27, inc. 6 Col. La Loma, Santa Maria Tototlapepec, Edo de Mexico. lamaco1966@prodigy.net.mx TEL. 01 (722) 1 99 3663 2 12 44 46 044 o 045 722 2 45 07 02

Figure 4.19 Sample test 11 M

LAMACO
CONTROL Y CALIDAD S.C.

REPORTE DE BLOCKS DE CONCRETO LIGERO MACIZO
NORMA MEXICANA
NMX-C-404-1987 CNMCC, NMX-C-636, NMX-C-637, NMX-C-638, NMX-C-681, NMX-C-196, NMX-C-387

CLIENTE:	TECNOLOGICO DE ESTUDIOS SUPERIORES DE JOCOITTLAN
OBRA O PROYECTO Y UBICACIÓN:	"ELEMENTO CONSTRUCTIVO TESJO" TECNOLOGICO DE ESTUDIOS SUPERIORES DE JOCOITTLAN CARRETERA TOLUCA-ATLACOMULCO KM 44.8 EJIDO DE SAN JOAN Y SAN AGUSTIN, 50780 MUNICIPIO DE JOCOITTLAN, ESTADO DE MEXICO
PROVEEDOR:	TECNOLOGICO DE ESTUDIOS SUPERIORES DE JOCOITTLAN
TIPO:	BLOCK MACIZO (MUESTRA 11)
LUGAR DE MUESTREO Y EMPLEO:	LABORATORIO TESJO

ENSAYE No.	001
MUESTRA No.	11
BLOCK No.	001
ANCHO (mm)	20.0
LARGO (mm)	40.0
ALTURA (mm)	20.0
PESO DEL BLOCK (kg)	26,700
AREA TOTAL (cm ²)	800.0
AREA META (cm ²)	800.0
PESO VOLUMETRICO DEL BLOCK (kg/m ³)	1,806.3
FECHA DE MUESTREO:	21/01/2020
FECHA DE RUPTURA:	02/02/2020
CARGA DE RUPTURA (kg)	19,160
RESISTENCIA (kg/cm ²)	24.0
PORCENTAJE DE ABSORCIÓN (%)	13.6

COMENTARIOS: LOS ESPECIMENES SE ENSAYARON EN ESTADO SECO.

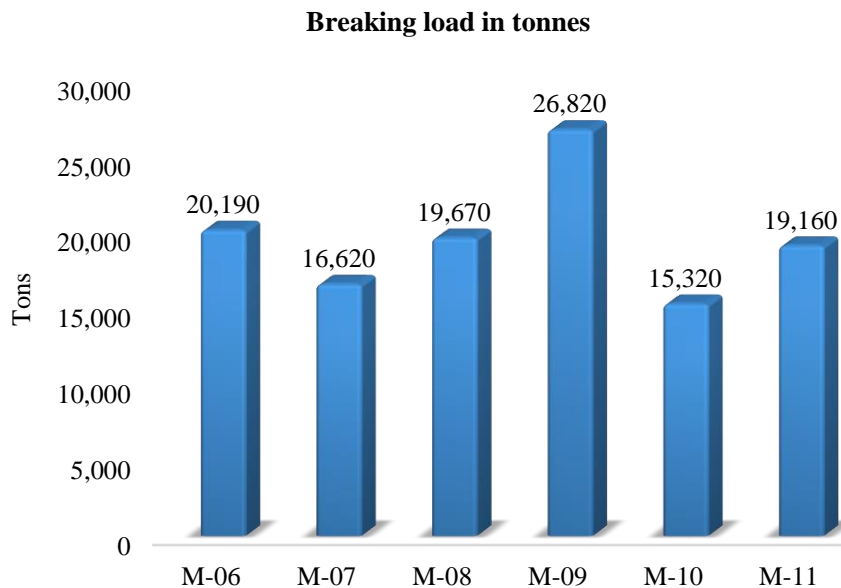
ELABORADO: *[Signature]* REVISADO: *[Signature]* RECIBIDO: *[Signature]*
 LAMACONISTA: TEC. ERICSSO GUADARRAMA BERNAL. GERENTE TÉCNICO: TEC. VICTORIANO RAMIREZ TRUJILLO. TECNOLÓGICO DE ESTUDIOS SUPERIORES DE JOCOITTLAN EMPRESA

LCC-PT-63-FIG-01 EDICIÓN 01 2018-01-01 PÁGINA 01 DE 01

ARTÍCULO No. 27, Ins. 6 Cdt. La Loma, Santa María Totontepec, Edo de México. lamaco1766@prodiata.net.mx TEL. 01 (722) 1 99 3663 2 12 44 46 044 o 045 722 2 45 07 02

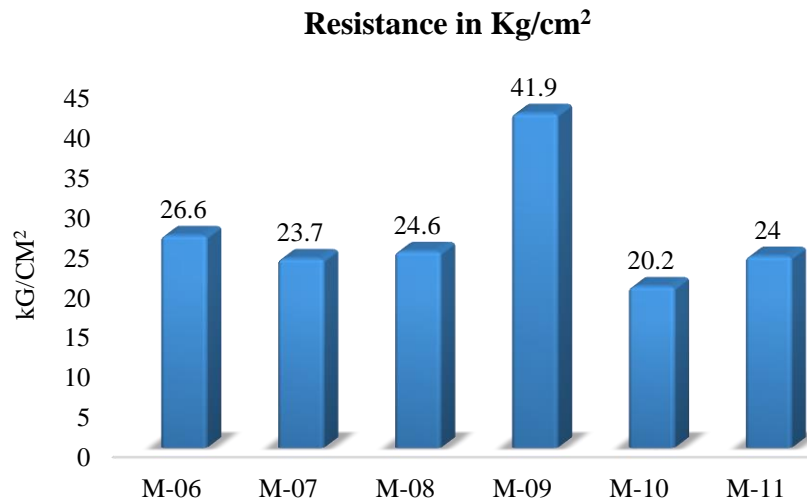
The report of the laboratory tests carried out on the solid Block (see graphic 4.3) indicates that the prototype called Block M-09 obtained the highest compressive strength with 26,820 kg, at the maximum degree of rupture. On the other hand, the average of the six blocks as a whole is 20.45 kg.

Graphic 4.3 Breaking load of solid block in tonnes



Source: Own elaboration

The data in graphic 4.4 simplifies the strength results of the six solid block samples we made. Similarly, the M-09 block obtained the highest strength compared to the other prototypes.

Graphic 4.4 Resistance of the solid block in tons

Source: Own elaboration

Concluding that Block M-09 falls within the necessary range with 41.9 kg/cm² to be a non-structural block according to the NMX-E-441-ONNCEE standard, which specifies that a non-structural block must have a compressive strength of 35 kg/cm². The average strength of these six blocks is 36.56 kg/cm².

4.5 Conclusions

Obtaining the results of the laboratory tests, it has been concluded that the module elaborated with rubble material shows real resistance characteristics, and that it is possible to create a hollow or solid non-structural block with average resistance for minor constructions of one to two levels maximum.

It is inferred that the result can be superior by using special moulds for its production, and also by using vibro-compaction it will increase its resistance up to 60 kg/cm², which would result in a block with a possible resistance greater than that of a conventional block and therefore present the same, or better benefits than a commercial one.

In Mexico, the construction industry needs to modernise and manage applicable standards for the management of construction and demolition waste. It has been observed that other underdeveloped countries do this and minimise the generation of waste in their cities, as well as helping to reduce the volume of waste in open air dumps, linked to the production of carbon dioxide and care for the environment, which is the main concern in the world today. Finally, it is intended that the project, more than being innovative, will be useful in the future plans of a federal regulation for the adequate management of construction and demolition waste and will serve to promote projects of this type for the academic and professional community.

As a substantive function articulated with teaching and research, interaction between the academic community and society is promoted, with the aim of establishing processes of creation and transformation of society, with the generation of proposals and solutions to the major problems that occur in our country and the satisfaction of needs faced by the community.

However, the concept of linkage is to address the main elements that are defined as:

The presence and academic interaction that an educational institution contributes to society must be critical and creative, leading to achievements in teaching and research. By being aware of the needs of the environment, academic activity is resized as a whole, as a form of ethical-pedagogical learning, which allows the articulation of the theoretical, methodological and professional aspects through the intervention of interdisciplinary programmes to meet the needs and problems of social, housing, industrial, agricultural and other sectors.

4.6 References

Cámara mexicana de la industria de la Construcción. *Plan de Manejo de Residuos de la construcción*. Pag 12-69. Retrieved from: <http://www.cmic.org.mx>

Cruz Atienza, Víctor Manuel, Krishna Singh, Shri, Ordaz Schroeder, Mario, Coordinación de Ingeniería Sismológica, Instituto de Ingeniería, UNAM Departamento de Sismología, Instituto de Geofísica, UNAM.

Karimi Faith & Chandrika Narayan, Chandrika, CNN, Updated 1920 GMT (0320 HKT) September 20, 2017, Mexico had two major earthquakes this month. Here's why, <https://edition.cnn.com>

Norma Mexicana NMX-C-038-ONNCCE.

SEMARNAT. (2017). *Criterios para el manejo de los residuos de construcción y demolición generados por el sismo del 19 de septiembre para los estados de México, Morelos, Puebla y Ciudad de México*. México: Gobierno de México.

Chapter 5 Structural characterisation of copper oxide by X-ray diffraction

Capítulo 5 Caracterización estructural de óxido de cobre por difracción de rayos-X

LÓPEZ, Roberto†*, NAMIGTLE, Jesús and MASTACHE, Jorge

Tecnológico de Estudios Superiores de Jocotitlán. Department of Mechatronics Engineering. Carretera Toluca-Atlacomulco KM 44.8, Ejido de San Juan y San Agustín, Jocotitlán, 50700 México.

ID 1st Author: *Jorge, López* / **ORC ID:** 0000-0001-8341-3684, **CVU CONACYT ID:** 233228

ID 1st Co-author: *Jesús, Namigtle* / **ORC ID:** 0000-0002-0908-4592, **CVU CONACYT ID:** 624757

ID 2nd Co-author: *Jorge, Mastache* / **ORC ID:** 0000-0001-6104-6764, **CVU CONACYT ID:** 612069

DOI: 10.35429/H.2021.9.1.70.96

R. López, J. Namigtle and J. Mastache

* roberto.lopez@tesjo.edu.mx

A. Ledesma (Coord.). Engineering Science and Technology. Handbooks-©ECORFAN-México, Estado de México, 2021.

Abstract

In this work, the study of the structural characterization of copper oxide by the X-ray diffraction technique is presented. To obtain layers of copper oxide, sputtering and thermal oxidation techniques were combined. The average crystal size was calculated for the sputtered copper samples. For the copper oxide films obtained by thermal oxidation, both the crystal size and the texture coefficient were calculated. The crystalline quality was poor for layers obtained by sputtering. Thermal oxidation carried out on these films transformed its structure to the copper oxide phase known as cupric oxide.

Copper oxide, X-ray diffraction, Average crystal size

Resumen

En este trabajo se presenta el estudio de la caracterización estructural del óxido de cobre mediante la técnica de difracción de rayos X. Para la obtención de capas de óxido de cobre se combinaron las técnicas de sputtering y oxidación térmica. Se calculó el tamaño medio de los cristales para las muestras de cobre pulverizadas. Para las películas de óxido de cobre obtenidas por oxidación térmica, se calculó tanto el tamaño de los cristales como el coeficiente de textura. La calidad cristalina era pobre para las capas obtenidas por sputtering. La oxidación térmica realizada en estas películas transformó su estructura en la fase de óxido de cobre conocida como óxido cúprico.

Óxido de cobre, Difracción de rayos-X, Tamaño promedio de cristal

5.1 Introduction

Nowadays, technology has presented great advances in conjunction with research and experimentation, covering needs by exploiting natural resources to the maximum. Copper has been used since antiquity for its physical and chemical properties that enhance it taking countless technological applications. Together with its oxides (CuO) and (Cu₂O), it maintains a more sophisticated development in its use in areas such as electronics, optoelectronics, etc. Among its advantages is the cost-effective reusability at the end of its useful life. The alloys are generally hard, strong and corrosion resistant. Thin films have achieved great specialisation in their study. They are formed by the growth of atoms or molecules that impinge on the surface of a substrate, with a thickness ranging from 1-100 nm. They can be manufactured by different methods depending on the material to be deposited and are used in optoelectronic devices, wear-resistant coatings, insulation, conductivity of electronic circuits, microelectronics such as semiconductor heterostructures and electrodes, among others. The production of CuO films is possible through a combination of methods such as sputtering and thermal oxidation. Because sputtering is a technique capable of producing thin films of almost any material and any type of substrate capable of withstanding high temperatures, it has been one of the most widely used. There are two types of sputtering (reactive and non-reactive). Reactive sputtering uses a mixture of gases, usually a reactive gas (hydrogen) and an inert gas (argon), which react with the target used in the deposition inside the chamber. In contrast to the non-reactive method, only the inert gas is used or the vacuum is simply evaporated and the target is deposited on the undisturbed substrate. The present work focuses specifically on non-reactive sputtering performed under vacuum without the use of an inert gas. When a material exhibits a number of properties useful for performing a certain function, analysis is carried out by a technique or method. Numerous structural characterisation techniques have been used in the field of materials and nanomaterials. X-ray diffraction is the most widely used analytical technique for the structural characterisation of samples, whereby it is possible to observe crystalline structures. This technique has excelled in different areas such as chemistry, mineralogy, biology and areas related to materials science, resulting in a positive impact on their study. The phenomenon occurs when a wave encounters an obstacle or an opening in its propagation of a size comparable to its wavelength. This tool has a wide range of data of relevant interest to analyse and study the determination of the geometry of each cell. The technique offers different utilities such as studying the deterioration, restoration and treatment of materials, as well as their properties and composition. The properties of materials are conditioned by the nature of the atoms that compose them and the way in which they bond with others, seeking maximum stability and a configuration with the lowest possible energy. Thus, many materials have a certain arrangement and organisation of atoms.

The so-called crystalline materials are composed of a spatial network of atoms distributed periodically and without any gaps, there are 14 possible types of Bravais networks. From the following work it is expected to show the importance of the experimental conditions used to obtain CuO. This is done by the combination of two techniques used in the synthesis due to the efficiency they offer together. In addition to optimising the production process in order to obtain samples analysed by means of a non-destructive structural characterisation technique.

5.2 Experimental methodology

The production of CuO deposits needs to fulfil certain criteria in order to offer high optimisation and excellent properties when used in different areas of study. This work focuses on the two aforementioned techniques to obtain CuO. The process of obtaining CuO is shown below.

Deposition of Cu using the sputtering technique

In this process, the deposition is carried out using the sputtering technique with the equipment (Agar auto sputter coater model 108A), using a Cu target with a purity of 99.9%. The Cu is deposited on the substrate forming nanostructures and subsequently thin films. Vacuum was performed in the chamber with a vacuum pump at 0.12 mb. Depending on the target-substrate distance and the deposition time the sample turns different shades.

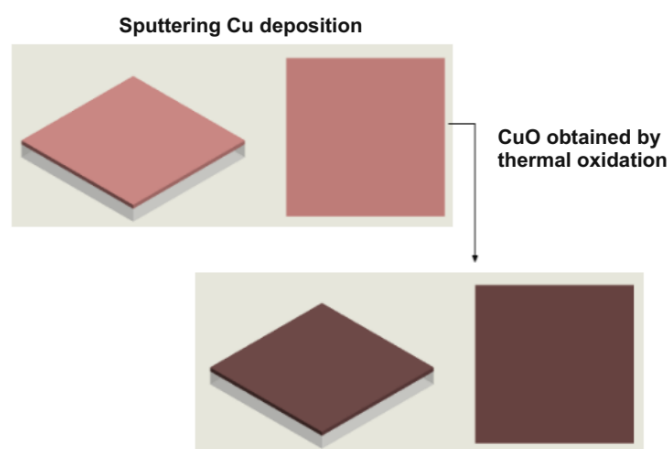
Thermal oxidation of Cu

This technique is complementary to sputtering. In this stage, the Cu deposit is placed inside a muffle at a high temperature (the temperatures used in oxidation are 500°C and 900°C). The equipment is composed of a closed chamber covered by a refractory material that allows a uniform heat delivery to the interior. The Cu undergoes an oxidation process as a result of the temperature used.

Obtaining CuO by the combination of two techniques sputtering and thermal oxidation for samples with short deposition time at 30 mm target-substrate distance

Deposition was carried out at a 30 mm target-substrate distance in a short deposition time, the sample takes a light colour even if it goes through the oxidation process using a muffle. The Cu deposit does not show much difference compared to the unoxidised sample. The diagram in figure 5.1 shows the process of obtaining CuO.

Figure 5.1 Production of CuO films by sputtering and thermal oxidation with 30 mm target-substrate spacing in a short deposition period



5.3 Results

XRD Cu diffractograms

Figure 5.2 shows the diffractograms obtained by XRD. The measurement time and the number of steps that have been executed during the analysis define the clarity and accuracy of the diffraction peaks. The number of steps executed was 3001 steps. In the four diffractograms, a curve appears between $2\theta = 22^\circ$ and 32° indicating the reading of an amorphous "substrate" material where the copper was deposited.

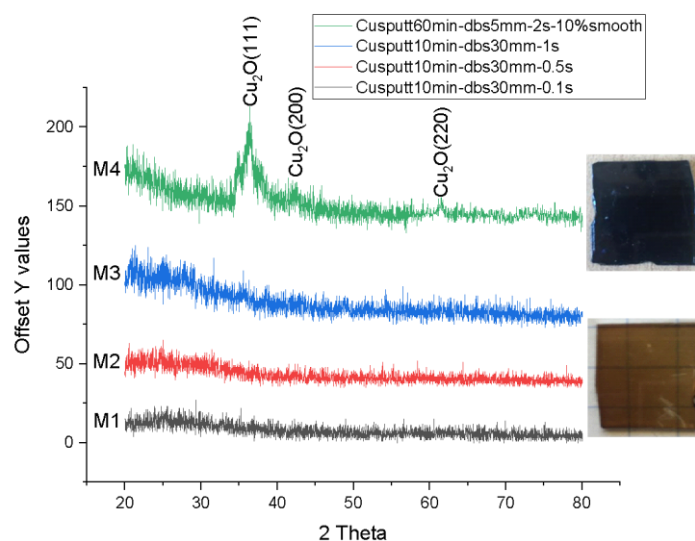
Copper was sputtered for 10 minutes, deposited on a glass substrate by means of a copper target at a target-substrate distance of 30 mm. As a result, a film was obtained which at first sight is not continuous. It presents the phenomenon of transmission, so it is possible to observe the background where it is positioned (M1, M2 and M3). In M1 the analysis was carried out at 0.1 s for each step, this diffractogram does not show any representative peak. The analysis was carried out again increasing the measurement time to 0.5 s for each step represented in the M2 diffractogram where an improvement is noticeable, however, it does not show outstanding peaks, so it was decided to carry out a new XRD analysis at 1 s representative of the M3 diffractogram where the copper peaks are not present.

Normally the standard time in the equipment is 0.1 s for each step; sufficient time for a crystalline material to show its representative peaks. In the diffractograms they do not stand out in comparison to the noise, which is why they were not followed up, and possible influencing factors are presented below:

- The layer is not continuous, so the peaks are not distinguishable in the diffractogram.
- The layer may be very thin (the copper film shows the transmission phenomenon).
- The material (copper) may have low crystallinity.

M4 is a comparative analysis of a Cu deposit for 60 minutes, using a Cu target at a target-substrate distance of 5 mm analysed by XRD for 2s. Smooth at 10% was performed to smooth the excess noise presented in the diffractogram, improving the definition of the peaks. The deposited layer is dark due to the increased deposition time, decreased white-substrate distance and longer XRD analysis time. The analysis shows three peaks at $2\theta = 36.38^\circ$, 42.42° and 61.48° corresponding to (111), (200) and (220) planes of the Cu₂O structure (PDF 00-005-0667). The presence of Cu₂O in the Cu deposit is due to the possible O-Cu reaction inside the chamber even after vacuum pumping, being an easily oxidised metal, the reaction is evident. The average crystal size taken from the most intense peak (111) corresponding to $2\theta = 36.38^\circ$ is 8.25 nm. Having a small crystal size, Cu nanostructures are considered where thin films are not yet formed.

Figure 5.2 XRD diffractograms obtained from Sputtering; M1; Cu deposition for 10 min using a Cu blank at a 30 mm blank-substrate distance analysed at 0.1 s, M2; Cu deposition for 10 min using a Cu blank at a 30 mm blank-substrate distance analysed at 0.5 s, M3; Cu deposition for 10 min using a Cu blank at a 30 mm blank-substrate distance analysed at 1 s. M4 Cu deposition for 60 min using a Cu blank at a 5 mm blank-substrate distance analysed at 2 s. Each running 3001 steps.



Calculation of Scherrer's Eq. (1) (Patterson, 1939), for the (111) plane of the diffractogram of the M4 Cu deposit.

T = Glass size to be calculated

$K = 0.94$

$\lambda = 0.15402 \text{ nm}$

$B = 1.04656$

$\theta_B = 16.18$

- Conversion of units

(°) gradians to (rad) radians

$1^\circ = 0.0174533 \text{ rad.}$

$$\frac{(1.04656)(\pi)}{180} = 0.01826591782 \quad (1)$$

- Replacement

$$T = \frac{(0.94)(0.15402 \text{ nm})}{(0.01826591782) \cos(16.18)} \quad (2)$$

$$T = \frac{0.1447788 \text{ nm}}{0.01754242333} \quad (3)$$

$T = 8.2530 \text{ nm}$

The crystal size for the (111) plane is 8.2530 nm.

Calculation of Scherrer's Eq. (1) (Patterson, 1939), for the (200) plane of the diffractogram of the Cu M4 deposit.

- Data

T = Crystal size to be calculated

$K = 0.94$

$\lambda = 0.15402 \text{ nm}$

$B = 1.48975$

$\theta_B = 21.21$

Conversion of units

(°) gradians to (rad) radians

$1^\circ = 0.0174533 \text{ rad.}$

$$\frac{(1.48975)(\pi)}{180} = 0.02600104253 \quad (4)$$

Replacement

$$T = \frac{(0.94)(0.15402 \text{ nm})}{(0.02600104253) \cos \cos (21.21)} \quad (5)$$

$$T = \frac{0.1447788 \text{ nm}}{0.02423974939} \quad (6)$$

$$T = 5.9727 \text{ nm}$$

The crystal size for the (200) plane is 5.9727 nm.

Calculation of Scherrer's Eq. (1) (Patterson, 1939), for the (220) plane of the diffractogram of the Cu deposit M4

Data

T= Crystal size to be calculated

K= 0.94

λ = 0.15402 nm

B= 0.98597

θ_B = 30.74

Conversion of units

(°) gradians to (rad) radians

1° = 0.0174533 rad.

$$\frac{(0.98597)(\pi)}{180} = 0.01720842283 \quad (7)$$

- Replacement

$$T = \frac{(0.94)(0.15402 \text{ nm})}{(0.01720842283) \cos \cos (30.74)} \quad (8)$$

$$T = \frac{0.1447788 \text{ nm}}{0.01479056432} \quad (9)$$

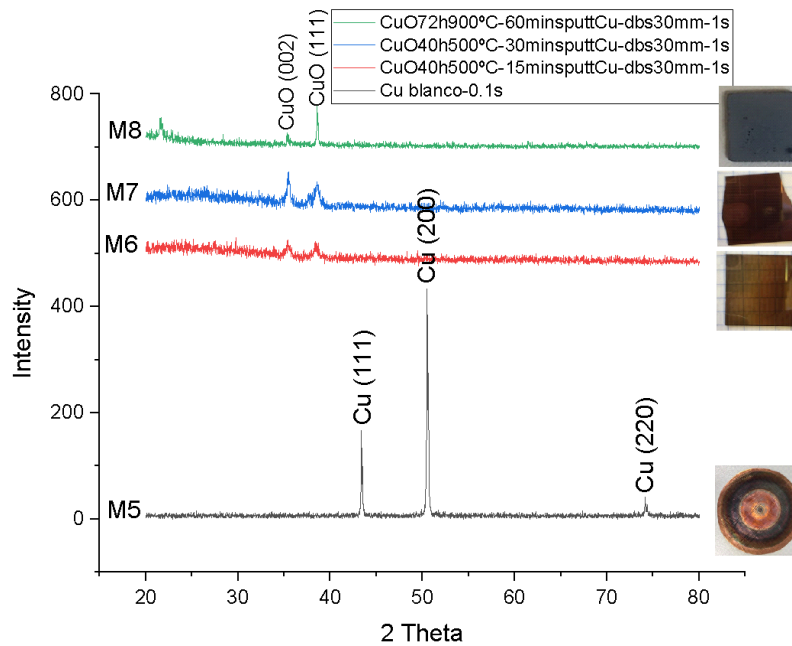
$$T = 9.7885 \text{ nm}$$

The crystal size for the (220) plane is 9.7885 nm.

XRD diffractogram of CuO

Figure 5.3 shows the diffractograms obtained by XRD, the number of steps executed for each diffractogram was 3001 steps. The M5 diffractogram is representative of the copper target (a target is the material to be evaporated by ion bombardment and then deposited on a substrate). It is possible to observe an erosion pattern due to the sputtering process it has undergone during its lifetime. Diffractogram M6 is a deposit of copper by sputtering for 15 minutes and then oxidised for 40 h at 500°C, the film obtained is thin, presents low crystallinity and shows the transmission phenomenon. The diffractogram M7 represents the deposit by sputtering for 30 minutes and then oxidised for 40 h at 500°C, the deposit obtained is not very translucent due to the increase in mass (Cu) which influences the definition and width of the peaks. The M8 diffractogram is a sputtering deposit for 60 minutes on a quartz substrate and then oxidised at 900°C in a muffle. The sample obtained takes on a grey colour due to the significant increase in deposition. The 4 samples analysed were obtained at a target-substrate distance of 30 mm.

Figure 5.3 Diffractograms obtained by XRD. M5; representative of the copper blank analysed by XRD for 0.1s, M6; Cu deposited for 15 min at a blank-substrate distance of 30mm and subsequently oxidised for 40 h at 500°C analysed by XRD for 1s (CuO). M7; Cu deposition for 15 min at a target-substrate distance of 30 mm and subsequently oxidised for 40 h at 500°C analysed by 1s XRD (CuO). M8; Cu deposit for 60 min at a target-substrate distance of 5 mm and subsequently oxidised for 72 h at 900°C analysed by XRD for 1 s (CuO)



The M5 diffractogram shows the Cu target used in the sputtering in which the characteristic Cu peaks located at $2\theta = 43.38^\circ$, 50.50° and 74.18° respective to the (111), (200) and (220) planes stand out. The calculated TC value of the most intense peak is 2.1994 which indicates that it is preferentially oriented towards the (200) plane. The average crystal size taken from the highest peak (200) is 39.8764 nm.

The M6 diffractogram is the result of a CuO deposit. The Cu was deposited by sputtering for 15 min on a glass substrate, then subjected to a thermal process (muffle) for 40 h at 500°C resulting in copper oxidation. XRD analysis was used to determine the phases present in the film in which there are two peaks at $2\theta = 35.38^\circ$ and 38.42° corresponding to (002) and (111) planes of the CuO structure (PDF 00-045-0937). The diffractogram does not show a great difference in the intensity of the peaks, so it does not have a preferential orientation, so it was checked by estimating the texture coefficient, which gave a result of 0.97393, less than 1. The average size of the crystal taken from the most intense peak (002) is 13.9357 nm, which indicates the presence of nanostructures. The M7 diffractogram is the result of a CuO deposit (the sample turns a darker colour due to a higher amount of mass (Cu) being oxidised compared to the sample obtained for 15 min). Cu was deposited by sputtering for 30 min on a glass substrate, then subjected to a thermal process (muffle) for 40 h at 500°C, resulting in copper oxidation. XRD analysis was used to determine the phases present in the deposit where it shows two peaks at $2\theta = 35.38^\circ$ and 38.42° corresponding to (002) and (111) planes of the CuO structure (PDF 00-045-0937). The peaks are at the same 2θ position of the M4 diffractogram but this time the peaks are more intense and their width decreases. There is a little noticeable difference in the intensity of the (111) plane at $2\theta = 38.42^\circ$ with respect to the other peak, that is why the preferential orientation was estimated and the result was 1.0807 greater than 1, which corresponds to the preferential orientation towards the (111) plane. The average crystal size taken from the most intense peak (002) is 21.1260 nm which indicates the formation of a thin film. The M8 diffractogram represents the CuO deposit. The Cu was deposited by Sputtering for 60 minutes on a quartz substrate, then it was subjected to a thermal process (muffle) for 72 h at 900°C as a result the oxidation is obtained. XRD analysis at 1 s for each step was used to determine the phases present in the deposit. Three peaks are presented in which only two were identified at $2\theta = 35.36^\circ$ and 38.60° corresponding to (002) and (111) planes of the CuO structure (PDF 00-045-0937).

Texture coefficient comparison

Table 5.1 shows the results obtained by calculating Eq. (2) Texture coefficient. The CuO M6 (15 min deposit by Sputtering with a thermal process "oxidation" by a muffle for 40 h at 500°C) does not show preferential orientation as a tiny amount of Cu is oxidised whereas the diffractogram M7 (copper deposit for 30 min by Sputtering with a thermal process "oxidation" by a muffle for 40 h at 500°C) doubles the Cu deposit i.e., more mass (Cu) is oxidised, so the peaks are better defined and start to have a preferential orientation towards the (002) plane. The diffractogram of the M8 (deposit for 60 minutes oxidised for 72 h at 900°C) already presents a preferential orientation towards the plane (002) due to the improvement of obtaining, on the other hand they are not compared with the diffractogram M5 where the texture coefficient is higher because it is the Cu target having an excellent crystalline structure due to the definition of the peaks.

Table 5.1 Preferential orientation calculated using Eq. (2) Texture Coefficient

Diffractogram	Texture coefficient	Preferential orientation
M5 (white de Cu-0.1s)	2.1994	Preferentially oriented towards the plane (200)
M6 (CuO40h500°C-15minSputtCu-dbs30mm-1s)	0.9739	No preferential orientation
M7 (CuO40h500°C-30minSputtCu-dbs30mm-1s)	1.08076	Preferentially oriented towards the plane (002)
M8 (CuO72h900°C-60minsputt-dbs30mm-1s)	1.5135	Preferably oriented towards the plane (002)

Crystal size comparison

Table 5.2 shows the average crystal size of the diffraction peaks, which is inversely proportional to the width of the diffraction peaks (the wider the peak, the smaller the crystal size). The diffractogram M6 represents the smallest crystal size, because the peaks are too wide and not very intense, the sample contains a combination of CuO nanostructures without forming a thin film, whereas in the diffractogram M8, because of the longer Cu deposition time, more particles were deposited. The deposit already forms a CuO thin film.

Table 5.2 Average crystal size calculated by Eq. (2) Scherrer

Diffractogram	Map	Average crystal size (nm)
M5 (white de Cu-1s)	(111)	49.6264
	(200)	39.8764
	(220)	31.8092
M6 (CuO40h500°C-15minSputtCu-dbs30mm-1s)	(002)	13.9357
	(111)	15.2728
M7 (CuO40h500°C-30minSputtCu-dbs30mm-1s)	(002)	21.1260
	(111)	19.0288
M8 (CuO72h900°C-60minsputt-bds30mm-1s)	(002)	38.9619
	(111)	53.0491

Calculations of the texture coefficient and crystal size for the diffractograms in figure 8

Calculation of Eq. (2) Texture coefficient (R, Lopez, & Leyva Porras, 2021) for copper target M5

- Data:

TC= texture coefficient

I= measured relative intensities of each plane (hkl) in the XRD pattern of the characterised sample.

Map (111)	Map (200)	Map (220)
30.03	100	8.22

I_0 = intensity of the same plane taken from the standard reference data (PDF 00-004-0836 for CuO)

Map (111)	Map (200)	Map (220)
100	46	20

$n =$ number of diffraction peaks: 3

- Replacement

$$= \frac{100}{46} \left\{ \left(\frac{1}{3} \right) \left(\frac{38.03}{100} + \frac{100}{46} + \frac{8.22}{20} \right) \right\}^{-1} \quad (10)$$

$$TC = \frac{100}{46} \left(\frac{1}{\left(\frac{38.03}{100} + \frac{100}{46} + \frac{8.22}{20} \right)} \right) \quad (11)$$

$$TC = \frac{100}{46} \left(\frac{1}{(2.9652)} \right) \quad (12)$$

$$TC = \frac{50}{23} \left(\frac{1}{0.9884} \right) \quad (13)$$

$$TC = \left(\frac{50}{22.7332} \right) \quad (14)$$

$$TC = 2.1994 \quad (15)$$

$TC > 1$, the calculated value of the strongest peak is 2.1994, which indicates that the CuO film is preferentially oriented in the (200) plane.

Calculation of Scherrer's Eq. (1) (Patterson, 1939), for the (100) plane of the diffractogram of copper target *M5*

Data

$T =$ Crystal size to be calculated

$K = 0.94$

$\lambda = 0.15402$ nm

$B = 0.17989$

$\theta_B = 21.6903$

Conversion of units:

(°) gradians to (rad) radians

$1^\circ = 0.0174533$ rad.

$$\frac{(0.17989)(\pi)}{180} = 3.139672791 \times 10^{-3} \quad (16)$$

- Replacement

$$T = \frac{(0.94)(0.15402 \text{ nm})}{(3.139672791 \times 10^{-3}) \cos(21.6903)} \quad (17)$$

$$T = \frac{0.1447788 \text{ nm}}{2.917368746 \times 10^{-3}} \quad (18)$$

$T = 49.6264$ nm

The crystal size for the (100) plane is 46.6264 nm.

Calculation of Scherrer's Eq. (1) (Patterson, 1939), for the (200) plane of the diffractogram of the copper blank *M5*

Data:

T= Crystal size to be calculated

K= 0.94

$\lambda = 0.15402$ nm

B= 0.23001

$\theta_B = 25.2564$

Conversion of units:

(°) gradians to (rad) radians

1° = 0.0174533 rad.

$$\frac{(0.23001)(\pi)}{180} = 4.014431813 \times 10^{-3} \quad (19)$$

- Replacement

$$T = \frac{(0.94)(0.15402 \text{ nm})}{(4.014431813 \times 10^{-3}) \cos(21.6903)} \quad (20)$$

$$T = \frac{0.1447788 \text{ nm}}{3.630682206 \times 10^{-3}} \quad (21)$$

$$T = 39.8764 \text{ nm}$$

The crystal size for the (200) plane is 39.8764 nm.

Calculation of Scherrer's Eq. (1) (Patterson, 1939), for the (220) plane of the diffractogram of the copper blank M5

Data

T= Crystal size to be calculated

K= 0.94

$\lambda = 0.15402$ nm

B= 0.32691

$\theta_B = 37.0882$

Conversion of units

(°) gradians to (rad) radians

1° = 0.0174533 rad.

$$\frac{(0.32691)(\pi)}{180} = 5.705655858 \times 10^{-3} \quad (22)$$

- Replacement

$$T = \frac{(0.94)(0.15402 \text{ nm})}{(5.705655858 \times 10^{-3}) \cos(37.0882)} \quad (23)$$

$$T = \frac{0.1447788 \text{ nm}}{4.551448133 \times 10^{-3}} \quad (24)$$

$$T = 31.8092 \text{ nm}$$

The crystal size for the (220) plane is 31.8072 nm.

Calculation of Eq. (2) Texture coefficient (R, Lopez, & Leyva Porras, 2021) for CuO *M6*.

- Data

TC = texture coefficient

I = measured relative intensities of each plane (hkl) in the XRD pattern of the characterised sample.

Map (002)	Map (100)
100	95.87

I_0 = intensity of the same plane taken from the standard reference data (PDF 00-045-0937 for CuO)

Map (002)	Map (100)
100	91

n = number of diffraction peaks: 2

- Replacement.

$$= \frac{100}{100} \left\{ \left(\frac{1}{2} \right) \left(\frac{100}{100} + \frac{95.87}{91} \right) \right\}^{-1} \quad (25)$$

$$TC = \frac{100}{100} \left(\frac{1}{\left(\frac{100}{100} + \frac{95.87}{91} \right)} \right) \quad (26)$$

$$TC = 1 \left(\frac{1}{\left(1 + \frac{95.87}{91} \right)} \right) \quad (27)$$

$$TC = 1 \left(\frac{1}{(2.0535)} \right) \quad (28)$$

$$TC = 1 \left(\frac{1}{1.0267} \right) \quad (29)$$

$$TC = \left(\frac{1}{1.0267} \right) \quad (30)$$

$$TC = 0.97393 \quad (31)$$

$TC < 1$, is not a textured film because it does not have a preferential orientation.

Calculation of Scherrer's Eq. (1) (Patterson, 1939), for the (002) plane for CuO *M6*

Data

T = Crystal size to be calculated

K = 0.94

λ = 0.15402 nm

$$B = 0.62479$$

$$\theta_B = 17.69$$

Conversion of units:

(°) gradians to (rad) radians

$$1^\circ = 0.0174533 \text{ rad.}$$

$$\frac{(0.62479)(\pi)}{180} = 0.01090464263 \quad (32)$$

- Replacement

$$T = \frac{(0.94)(0.15402 \text{ nm})}{(0.01090464263) \cos(17.69)} \quad (33)$$

$$T = \frac{0.1447788 \text{ nm}}{0.01038901148} \quad (34)$$

$$T = 13.9357 \text{ nm}$$

The crystal size for the (002) plane is 13.9357 nm.

Calculation of Scherrer's Eq. (1) (Patterson, 1939), for the (111) plane for CuO M6

Data

T = Crystal size to be calculated

$$K = 0.94$$

$$\lambda = 0.15402 \text{ nm}$$

$$B = 0.57516$$

$$\theta_B = 19.21$$

Conversion of units

(°) gradians to (rad) radians

$$1^\circ = 0.0174533 \text{ rad.}$$

$$\frac{(0.57516)(\pi)}{180} = 0.01003843573 \quad (35)$$

- Replacement.

$$T = \frac{(0.94)(0.15402 \text{ nm})}{(0.01003843573) \cos(19.21)} \quad (36)$$

$$T = \frac{0.1447788 \text{ nm}}{9.479485166 \times 10^{-3}} \quad (37)$$

$$T = 15.2728 \text{ nm}$$

The crystal size for the (100) plane is 15.2728 nm.

Calculation of Eq. (2) Texture coefficient (R, Lopez, & Leyva Porras, 2021) for CuO M7

Data

TC = coeficiente de textura

I = measured relative intensities of each plane (hkl) in the XRD pattern of the characterised sample.

Map (002)	Map (111)
100	77.4

I_0 = intensity of the same plane taken from the standard reference data (PDF 00-045-0937 for CuO).

Map (002)	Map (111)
100	91

n = number of diffraction peaks: 2.

- Replacement.

$$= \frac{100}{100} \left\{ \left(\frac{1}{2} \right) \left(\frac{100}{100} + \frac{74.4}{91} \right) \right\}^{-1} \quad (38)$$

$$TC = \frac{100}{100} \left(\frac{1}{\left(\frac{100}{100} + \frac{74.4}{91} \right)} \right) \quad (39)$$

$$TC = 1 \left(\frac{1}{\left(1 + \frac{74.4}{91} \right)} \right) \quad (40)$$

$$TC = 1 \left(\frac{1}{(1.8505)} \right) \quad (41)$$

$$TC = 1 \left(\frac{1}{0.925274} \right) \quad (42)$$

$$TC = \left(\frac{1}{0.925274} \right) \quad (43)$$

$$TC = 1.0807 \quad (44)$$

$TC > 1$ The calculated value of the strongest peak is 1.0807, which indicates that the CuO film is preferentially oriented in the (111) plane.

Calculation of Scherrer's Eq. (1) (Patterson, 1939), for the (002) plane for CuO $M7$

Data

T = Crystal size to be calculated

K = 0.94

λ = 0.15402 nm

B = 0.41228

θ_B = 17.75

Conversion of units:

(°) gradians to (rad) radians

$$1^\circ = 0.0174533 \text{ rad.}$$

$$\frac{(0.41228)(\pi)}{180} = 7.19564344 \times 10^{-3} \quad (45)$$

- Replacement.

$$T = \frac{(0.94)(0.15402 \text{ nm})}{(7.19564344 \times 10^{-3}) \cos(17.75)} \quad (46)$$

$$T = \frac{0.1447788 \text{ nm}}{6.853100588 \times 10^{-3}} \quad (47)$$

$$T = 21.1260 \text{ nm}$$

The crystal size for the (002) plane is 21.1260 nm.

Calculation of Scherrer's Eq. (1) (Patterson, 1939), for the (111) plane for CuO M7

Data

T = Crystal size to be calculated

$$K = 0.94$$

$$\lambda = 0.15402 \text{ nm}$$

$$B = 0.46183$$

$$\theta_B = 19.27$$

Conversion of units:

(°) gradians to (rad) radians

$$1^\circ = 0.0174533 \text{ rad.}$$

$$\frac{(0.46183)(\pi)}{180} = 8.060454084 \times 10^{-3} \quad (48)$$

- Replacement.

$$T = \frac{(0.94)(0.15402 \text{ nm})}{(8.060454084 \times 10^{-3}) \cos(19.27)} \quad (49)$$

$$T = \frac{0.1447788 \text{ nm}}{7.608858109 \times 10^{-3}} \quad (50)$$

$$T = 19.0288 \text{ nm}$$

The crystal size for the (002) plane is 19.0288 nm.

Calculation of Eq. (2) Texture Coefficient (R, Lopez, & Leyva Porras, 2021) for the M8

Data

TC = texture coefficient

I = measured relative intensities of each plane (hkl) in the XRD pattern of the characterised sample

Map (002)	Map (111)
35.32	100

I_0 = intensity of the same plane taken from the standard reference data (PDF 00-004-0836 for CuO).

Map (002)	Map (111)
100	91

n = number of diffraction peaks: 2

- Replacement.

$$= \frac{100}{91} \left\{ \left(\frac{1}{2} \right) \left(\frac{100}{91} + \frac{35.32}{100} \right) \right\}^{-1} \quad (51)$$

$$TC = \frac{100}{91} \left(\frac{1}{\left(\frac{100}{91} + \frac{35.32}{100} \right)} \right) \quad (52)$$

$$TC = \frac{100}{91} \left(\frac{1}{(1.452101099)} \right) \quad (53)$$

$$TC = \frac{100}{91} \left(\frac{1}{0.7260505495} \right) \quad (54)$$

$$TC = \left(\frac{100}{66.0706091} \right) \quad (55)$$

$$TC = 1.5135 \quad (56)$$

$TC > 1$, the calculated value of the strongest peak is 1.5135, which indicates that the CuO film is preferentially oriented in the (111) plane.

Calculation of Scherrer's Eq. (1) (Patterson, 1939), for the (002) plane of the diffractogram M8

Data

T = Crystal size to be calculated

$K = 0.94$

$\lambda = 0.15402 \text{ nm}$

$B = 0.22346$

$\theta_B = 17.6800$

Conversion of units:

(°) gradians to (rad) radians

$1^\circ = 0.0174533 \text{ rad.}$

$$\frac{(0.22346)(\pi)}{180} = 3.900112747 \times 10^{-3} \quad (57)$$

- Replacement.

$$T = \frac{(0.94)(0.15402 \text{ nm})}{(3.900112747 \times 10^{-3}) \cos \cos (17.6800)} \quad (58)$$

$$T = \frac{0.1447788 \text{ nm}}{3.71590087 \times 10^{-3}} \quad (59)$$

$$T = 38.9619 \text{ nm}$$

The crystal size for the (002) plane is 38.9619 nm.

Calculation of Scherrer's Eq. (1) (Patterson, 1939), for the (111) plane of the diffractogram M8

Data

T = Crystal size to be calculated

$$K = 0.94$$

$$\lambda = 0.15402 \text{ nm}$$

$$B = 0.16568$$

$$\theta_B = 19.3005$$

Conversion of units:

(°) gradians to (rad) radians.

$$1^\circ = 0.0174533 \text{ rad.}$$

$$\frac{(0.16568)(\pi)}{180} = 2.891661505 \times 10^{-3} \quad (60)$$

- Replacement.

$$T = \frac{(0.94)(0.15402 \text{ nm})}{(2.891661505 \times 10^{-3}) \cos(19.3005)} \quad (61)$$

$$T = \frac{0.1447788 \text{ nm}}{2.72914454 \times 10^{-3}} \quad (62)$$

$$T = 53.0491 \text{ nm}$$

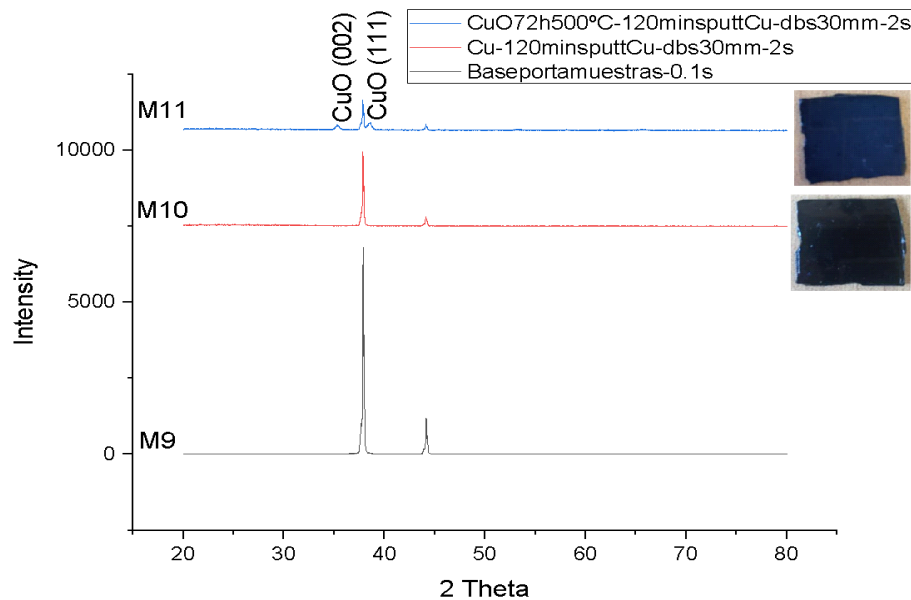
The crystal size for the (111) plane is 53.0491 nm.

Diffractogram of the sample holder, Cu and CuO deposit by XRD

Figure 5.4, M9 represents an XRD analysis of the base of the sample holder for 0.1 s. M10 is a Cu deposit by means of a Cu target deposited on a glass substrate by sputtering for 2 h, then analysed by XRD for 2 s. The sample takes a dark colour due to the CuO. The sample takes a dark colour due to the long deposition time. M11 is a Cu deposit by sputtering Cu target for 120 min deposited on a glass substrate, then oxidised in a flask for 72 h at 500°C and analysed by XRD for 2 s. The sample obtained from the Cu sputtering was oxidised in a flask for 72 h at 500°C and analysed by XRD for 2 s. The sample obtained from the Cu sputtering was then oxidised in a flask for 72 h at 500°C.

The sample obtained from the oxidation has similarity compared before oxidation.

Figure 5.4 Diffractogram obtained by XRD. M9; sample holder base analysed for 0.1 sec. M10; Cu deposition by Sputtering for 120 min, analysed for 2s. M11; (CuO) Cu deposition by Sputtering for 120 min, with 72 hours of thermal oxidation by muffle at 500°C and analysed for 2s (CuO)



Cu was sputtered for 120 min by sputtering deposited on a glass substrate and then XRD analysis was performed for 2s (M10), the intense peaks are found at $2\theta = 37.88^\circ$ and 44.14° . When characterising the diffraction peaks from standard reference data for Cu no similarity in the positions was found. Subsequently, an analysis of the M9 sample holder base was carried out for 0.1 s, presenting similarity in the diffraction peaks found at $2\theta = 37.86^\circ$ and 44.12° . The peaks present higher intensity compared to the M9 diffractogram considering that the analysis time was shorter. Due to the similarity it is possible that both diffractograms present the measurement of the sample holder base, when having interference to the Cu deposit the peaks decrease their intensity. Possible reasons why the sample was not read by XRD:

- The Cu target has low or no crystallinity.
- The Cu layer is not continuous.

Some authors previously reported that the deposition rate should not exceed a limit such that the overgrowth layer is deposited before atomic hopping to an equilibrium position is possible, resulting in non-crystalline nuclei formed on the substrate surface. The diffractogram of M11 is representative of Cu deposition by sputtering for 120 min deposited on a glass substrate and subsequently oxidised in a flask for 72 h at 500°C and analysed by XRD for 2 s. The increased analysis time was possible due to the increase of analysis time. The increase in analysis time it was possible to observe four peaks at $2\theta = 35.34^\circ$, 37.84° , 38.56° and 44.12° . Only two peaks $2\theta = 35.34^\circ$ and 38.56° corresponding to (002) and (111) planes of the CuO structure (PDF 00-045-0937) could be identified. Due to the thermal process that the Cu deposit underwent, CuO was visible in the M11 diffractogram. The two remaining peaks $2\theta = 37.84^\circ$ and 44.12° are attributed to the measurement of the base of the sample holder because it presents the same peaks seen previously in M9 and M10. The presence of the sample holder peaks meant that texture coefficient and crystal size calculations were not performed because it is not of interest to study the material (aluminium) of the sample holder.

XRD diffractogram of CuO

Figure 5.5 shows the different diffractograms obtained by XRD, M12 is a Cu deposit using a Cu target (at a target-substrate distance of 30 mm) by the sputtering technique for 120 min deposited on a glass substrate, subsequently oxidised in a flask for 72 h at 500°C and analysed by XRD for 1 s (with pink base). M13 is a Cu deposit by sputtering Cu target for 120 min deposited on a glass substrate, then oxidised in a flask for 72 h at 500°C and analysed by XRD for 3 s (pink based). M14 is a Cu deposit using a Cu target (at a target-substrate distance of 5 mm) by the sputtering technique for 45 min deposited on a glass substrate, subsequently oxidised in a fume cupboard for 72 h and analysed by XRD for 0.1 s.

Figure 5.5

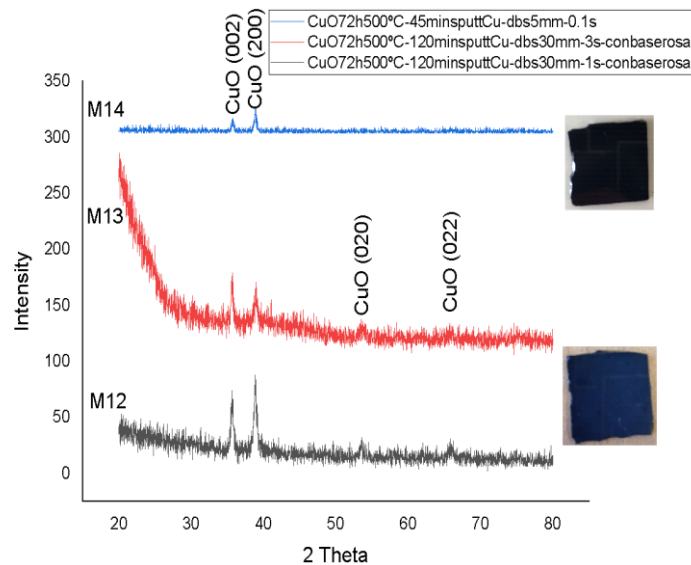


Figure 5.5 Diffractogram obtained by XRD. M12; Cu deposit sputtered for 120 min (30 mm blank-substrate distance), with 72 hours of thermal oxidation by muffle at 500°C and analysed for 1 s (with pink base) (CuO). M13; Cu deposition by sputtering for 120 min (30 mm blank-substrate distance), with 72 h thermal oxidation by flask at 500°C and analysed for 3 s (pink basis) (CuO). M14; Cu deposit by sputtering for 45 min, (target-substrate distance 5 mm), subsequently oxidised at 72 h by a muffle at 500°C and analysed for 0.1 s (CuO). Due to the diffractograms obtained with sample holder reading, a pink base was included between the sample holder and the deposit in M12 and M13 in order to obtain only the CuO analysis. The diffractogram of M12 is representative of Cu deposition by sputtering for 120 min deposited on a glass substrate at a target-substrate distance of 30 mm, then oxidised in a flask for 72 h at 500°C and analysed by XRD for 1 s (for this analysis a pink base was included to avoid reading the sample holder). Four peaks are shown at $2\theta = 35.64^\circ$, 38.90° , 53.62° and 65.86° low intensity corresponding to (002), (200), (020) and (022) planes of the CuO structure (PDF 00-045-0937). The texture coefficient calculated for the M12 diffractogram is 1.0310, because it is greater than 1 it is considered a textured film oriented towards the (200) plane. The average crystal size taken for the most intense peak (200) is 20.7663, due to the crystal size it is already considered a thin film. The diffractogram of M13 is representative of Cu deposition by sputtering for 120 min deposited on a glass substrate at a white-substrate distance of 30 mm, then oxidised in a flask for 72 h at 500°C and analysed by XRD for 3 s (for this analysis a pink base was included to avoid reading the sample holder). Four peaks are shown at $2\theta = 35.62^\circ$, 38.84° , 53.48° and 65.72° with a small intensity, these peaks are the same as those seen in M12 corresponding to (002), (200), (020) and (022) planes of the CuO structure (PDF 00-045-0937). The texture coefficient calculated for the diffractogram of M13 is 0.2416, because it is less than 1 it does not have a preferential orientation. The average crystal size taken for the most intense peak (002) is 22.7857, due to the crystal size it is already considered a thin film. The diffractogram of M14 is representative of Cu deposition by sputtering for 45 minutes on a glass substrate at a target-substrate distance of 5 mm to decrease the deposition time. Subsequently it is oxidised for 72 h at 500°C and by XRD analysed for 0.1 s. The deposit is similar to the one obtained during 120 min at 30 mm with the only difference that the last two peaks (020) and (022) are not found in this diffractogram. Two peaks were found at $2\theta = 35.78^\circ$ and 38.92° corresponding to (002) and (200) planes of the CuO structure (PDF 00-045-0937) similar to those found in M12 and M13. The texture coefficient calculated for the diffractogram of M14 is 1.7174, because it is greater than 1 it is considered a textured film oriented towards the (200) plane. The average crystal size taken for the most intense peak (200) is 25.5054, due to the crystal size it is already considered a thin film. The largest average crystal size belongs to the diffractogram of M14 due to the white-substrate arrangement in the sputtering deposition. Calculation of Eq. (2) Texture Coefficient (R, Lopez, & Leyva Porras, 2021) for the M12

Data

$TC =$ texture coefficient

$I =$ measured relative intensities of each plane (hkl) in the XRD pattern of the characterised sample

Map (002)	Map (200)	Map (020)	Map (022)
81.22	100	31.53	33.73

I_0 = intensity of the same plane taken from the standard reference data (PDF 00-004-0836 for CuO)

Map (002)	Map (200)	Map (020)	Map (022)
100	28	6	8

n = number of diffraction peaks: 4

- Replacement.

$$= \frac{100}{28} \left\{ \left(\frac{1}{4} \right) \left(\frac{100}{28} + \frac{81.22}{100} + \frac{31.53}{6} + \frac{33.73}{8} \right) \right\}^{-1} \quad (63)$$

$$TC = \frac{100}{28} \left(\frac{1}{\frac{1}{4} \left(\frac{100}{28} + \frac{81.22}{100} + \frac{31.53}{6} + \frac{33.73}{8} \right)} \right) \quad (64)$$

$$TC = \frac{100}{28} \left(\frac{1}{\frac{1}{4}(13.85487857)} \right) \quad (65)$$

$$TC = \frac{100}{28} \left(\frac{1}{3.463719643} \right) \quad (66)$$

$$TC = \left(\frac{(100)(1)}{(28)(3.463719643)} \right) \quad (67)$$

$$TC = \left(\frac{100}{96.9841499} \right) \quad (68)$$

$$TC = 1.0310 \quad (69)$$

$TC > 1$, the calculated value of the most intense peak is 1.0310, which indicates that the CuO film is preferentially oriented in the (200) plane.

Calculation of Scherrer's Eq. (1) (Patterson, 1939), for the (002) plane of the diffractogram M12

Data

T = Crystal size to be calculated

$K = 0.94$

$\lambda = 0.15402$ nm

$B = 0.46062$

$\theta_B = 17.8127$

Conversion of units:

(°) gradians to (rad) radians.

$1^\circ = 0.0174533$ rad.

$$\frac{(0.46062)(\pi)}{180} = 8.039335601 \times 10^{-3} \quad (70)$$

- Replacement.

$$T = \frac{(0.94)(0.15402 \text{ nm})}{(8.039335601 \times 10^{-3}) \cos \cos (17.8127)} \quad (71)$$

$$T = \frac{0.1447788 \text{ nm}}{7.653942795 \times 10^{-3}} \quad (72)$$

$$T = 18.9155 \text{ nm}$$

The crystal size for the (002) plane is 18.9155 nm.

Calculation of Scherrer's Eq. (1) (Patterson, 1939), for the (200) plane of the diffractogram M12

Data

T = Crystal size to be calculated

$$K = 0.94$$

$$\lambda = 0.15402 \text{ nm}$$

$$B = 0.42355$$

$$\theta_B = 19.4191$$

Conversion of units:

(°) gradians to (rad) radians.

$$1^\circ = 0.0174533 \text{ rad.}$$

$$\frac{(0.42355)(\pi)}{180} = 7.392342047 \times 10^{-3} \quad (73)$$

- Replacement.

$$T = \frac{(0.94)(0.15402 \text{ nm})}{(7.392342047 \times 10^{-3}) \cos \cos (19.4191)} \quad (74)$$

$$T = \frac{0.1447788 \text{ nm}}{6.971805583 \times 10^{-3}} \quad (75)$$

$$T = 20.7663 \text{ nm}$$

The crystal size for the (200) plane is 20.7663 nm.

Calculation of Scherrer's Eq. (1) (Patterson, 1939), for the (020) plane of the diffractogram M12

Data

T = Crystal size to be calculated

$$K = 0.94$$

$$\lambda = 0.15402 \text{ nm}$$

$$B = 0.57$$

$$\theta_B = 26.81$$

Conversion of units:

(°) gradians to (rad) radians

$$1^\circ = 0.0174533 \text{ rad.}$$

$$\frac{(0.57)(\pi)}{180} = 9.948276736 \times 10^{-3} \quad (76)$$

- Replacement.

$$T = \frac{(0.94)(0.15402 \text{ nm})}{(9.948276736 \times 10^{-3}) \cos(26.81)} \quad (77)$$

$$T = \frac{0.1447788 \text{ nm}}{8.878996989 \times 10^{-3}} \quad (78)$$

$$T = 16.3057 \text{ nm}$$

The crystal size for the (020) plane is 16.3057 nm.

Calculation of Scherrer's Eq. (1) (Patterson, 1939), for the (022) plane of the diffractogram M12

Data

T = Crystal size to be calculated

$$K = 0.94$$

$$\lambda = 0.15402 \text{ nm}$$

$$B = 0.8921$$

$$\theta_B = 32.93$$

Conversion of units:

(°) gradians to (rad) radians.

$$1^\circ = 0.0174533 \text{ rad.}$$

$$\frac{(0.8921)(\pi)}{180} = 0.01557025679 \quad (79)$$

- Replacement.

$$T = \frac{(0.94)(0.15402 \text{ nm})}{(0.01557025679) \cos(32.93)} \quad (80)$$

$$T = \frac{0.1447788 \text{ nm}}{0.01306866684} \quad (81)$$

$$T = 11.0783 \text{ nm}$$

The crystal size for the (022) plane is 11.0783 nm.

Calculation of Eq. (2) Texture coefficient (R, Lopez, & Leyva Porras, 2021) for M13

Data:

TC = texture coefficient

I = measured relative intensities of each plane (hkl) in the XRD pattern of the characterised sample.

Map (002)	Map (200)	Map (020)	Map (022)
100	81.23	45.26	40.85

I_0 = intensity of the same plane taken from the standard reference data (PDF 00-004-0836 for CuO).

Map (002)	Map (200)	Map (020)	Map (022)
100	28	6	8

n = number of diffraction peaks: 4.

- Replacement.

$$= \frac{100}{100} \left\{ \left(\frac{1}{4} \right) \left(\frac{100}{100} + \frac{81.23}{28} + \frac{45.26}{6} + \frac{40.85}{8} \right) \right\}^{-1} \quad (82)$$

$$TC = \frac{100}{100} \left(\frac{1}{\frac{1}{4} \left(\frac{100}{100} + \frac{81.23}{100} + \frac{45.26}{6} + \frac{40.85}{8} \right)} \right) \quad (83)$$

$$TC = \frac{100}{100} \left(\frac{1}{\frac{1}{4} (16.55065476)} \right) \quad (84)$$

$$TC = \frac{100}{100} \left(\frac{1}{4.13766369} \right) \quad (85)$$

$$TC = 1 \left(\frac{1}{4.13766369} \right) \quad (86)$$

$$TC = 1(0.2416) \quad (87)$$

$$TC = 0.2416 \quad (88)$$

$TC < 1$, the calculated value of the most intense peak is 0.2416, which indicates that the CuO film has no preferential orientation towards any plane.

Calculation of Scherrer's Eq. (1) (Patterson, 1939), for the (002) plane of the diffractogram M13

Data

T = Crystal size to be calculated

$K = 0.94$

$\lambda = 0.15402$ nm

$B = 0.38244$

$\theta_B = 17.8387$

Conversion of units:

(°) gradians to (rad) radians

$1^\circ = 0.0174533$ rad.

$$\frac{(0.38244)(\pi)}{180} = 6.674837191 \times 10^{-3} \quad (89)$$

- Replacement.

$$T = \frac{(0.94)(0.15402 \text{ nm})}{(6.674837191 \times 10^{-3}) \cos \cos (17.8387)} \quad (90)$$

$$T = \frac{0.1447788 \text{ nm}}{6.353929014 \times 10^{-3}} \quad (91)$$

$$T = 22.7857 \text{ nm}$$

The crystal size for the (002) plane is 22.7857 nm.

Calculation of Scherrer's Eq. (1) (Patterson, 1939), for the (200) plane of the diffractogram M13

Data

T = Crystal size to be calculated

$$K = 0.94$$

$$\lambda = 0.15402 \text{ nm}$$

$$B = 0.55168$$

$$\theta_B = 19.4787$$

Conversion of units:

(°) gradians to (rad) radians

$$1^\circ = 0.0174533 \text{ rad.}$$

$$\frac{(0.55168)(\pi)}{180} = 9.628632417 \times 10^{-3} \quad (92)$$

- Replacement.

$$T = \frac{(0.94)(0.15402 \text{ nm})}{(9.628632417 \times 10^{-3}) \cos \cos (19.4787)} \quad (93)$$

$$T = \frac{0.1447788 \text{ nm}}{9.077542651 \times 10^{-3}} \quad (94)$$

$$T = 15.9491 \text{ nm}$$

The crystal size for the (200) plane is 15.9491 nm.

Calculation of Scherrer's Eq. (1) (Patterson, 1939), for the (020) plane of the diffractogram M13

Data

T = Crystal size to be calculated

$$K = 0.94$$

$$\lambda = 0.15402 \text{ nm}$$

$$B = 0.89178$$

$$\theta_B = 26.74$$

Conversion of units:

(°) gradians to (rad) radians

$$1^\circ = 0.0174533 \text{ rad.}$$

$$\frac{(0.89178)(\pi)}{180} = 0.0155644972 \quad (95)$$

- Replacement.

$$T = \frac{(0.94)(0.15402 \text{ nm})}{(0.0155644972) \cos (26.74)} \quad (96)$$

$$T = \frac{0.1447788 \text{ nm}}{0.01389999075} \quad (97)$$

$$T = 10.4157 \text{ nm}$$

The crystal size for the (020) plane is 10.4157 nm.

Calculation of Scherrer's Eq. (1) (Patterson, 1939), for the (022) plane of the diffractogram M13

Data

T = Crystal size to be calculated

$$K = 0.94$$

$$\lambda = 0.15402 \text{ nm}$$

$$B = 0.45722$$

$$\theta_B = 32.86$$

Conversion of units:

(°) gradians to (rad) radians.

$$1^\circ = 0.0174533 \text{ rad.}$$

$$\frac{(0.45722)(\pi)}{180} = 7.979994406 \times 10^{-3} \quad (98)$$

- Replacement.

$$T = \frac{(0.94)(0.15402 \text{ nm})}{(7.979994406 \times 10^{-3}) \cos (32.86)} \quad (99)$$

$$T = \frac{0.1447788 \text{ nm}}{6.703186261 \times 10^{-3}} \quad (100)$$

$$T = 21.5985 \text{ nm}$$

The crystal size for the (022) plane is 21.5985 nm.

Calculation of Eq. (2) Texture coefficient (R, Lopez, & Leyva Porras, 2021) for M14

Data

TC = texture coefficient

I = measured relative intensities of each plane (hkl) in the XRD pattern of the characterised sample

Map (002)	Map (200)
58.75	100

I_0 = intensity of the same plane taken from the standard reference data (PDF 00-004-0836 for CuO)

Map (002)	Map (200)
100	28

n = number of diffraction peaks: 2

- Replacement.

$$= \frac{100}{28} \left\{ \left(\frac{1}{2} \right) \left(\frac{100}{100} + \frac{81.23}{28} \right) \right\}^{-1} \quad (101)$$

$$TC = \frac{100}{28} \left(\frac{1}{\left(\frac{100}{28} + \frac{58.75}{100} \right)} \right) \quad (102)$$

$$TC = \frac{100}{28} \left(\frac{1}{(4.158928571)} \right) \quad (103)$$

$$TC = \frac{100}{28} \left(\frac{1}{2.079464286} \right) \quad (104)$$

$$TC = \left(\frac{(100)(1)}{(28)(2.079464286)} \right) \quad (105)$$

$$TC = \left(\frac{100}{58.225} \right) \quad (106)$$

$$TC = 1.7174 \quad (107)$$

$TC > 1$, the calculated value of the strongest peak is 1.7174, indicating that the textured CuO film is preferentially oriented in the (200) plane.

Calculation of Scherrer's Eq. (1) (Patterson, 1939), for the (002) plane of the diffractogram M14

Data

T = Crystal size to be calculated

K = 0.94

λ = 0.15402 nm

B = 0.36913

θ_B = 17.8899

Conversion of units:

(°) gradians to (rad) radians.

1° = 0.0174533 rad.

$$\frac{(0.36913)(\pi)}{180} = 6.442533868 \times 10^{-3} \quad (108)$$

- Replacement.

$$T = \frac{(0.94)(0.15402 \text{ nm})}{(6.442533868 \times 10^{-3}) \cos \cos (17.8889)} \quad (109)$$

$$T = \frac{0.1447788 \text{ nm}}{6.131028139 \times 10^{-3}} \quad (110)$$

$$T = 23.6141 \text{ nm}$$

The crystal size for the (002) plane is 23.6141nm.

Calculation of Scherrer's Eq. (1) (Patterson, 1939), for the (200) plane of the diffractogram M14

Data

T = Crystal size to be calculated

K = 0.94

λ = 0.15402 nm

B = 0.34485

θ_B = 19.4189

Conversion of units:

(°) gradians to (rad) radians.

1° = 0.0174533 rad.

$$\frac{(0.34485)(\pi)}{180} = 6.018767926 \times 10^{-3} \quad (111)$$

- Replacement.

$$T = \frac{(0.94)(0.15402 \text{ nm})}{(6.018767926 \times 10^{-3}) \cos \cos (19.4189)} \quad (112)$$

$$T = \frac{0.1447788 \text{ nm}}{5.676378501 \times 10^{-3}} \quad (113)$$

$$T = 25.5054 \text{ nm}$$

The crystal size for the (200) plane is 25.5054 nm.

5.4 Conclusions

By combining two techniques, sputtering and thermal oxidation, it was possible to obtain samples with different thicknesses according to the time employed in the deposition. After the arrangement of the system with a target-substrate distance of 5 mm, deposits similar to those of 120 minutes were obtained in a shorter time, optimising the process. According to the diffractograms, it was observed that the material to be deposited, called "white", determines the characteristics of the deposits made. If this material does not have a crystalline structure, the diffraction peaks corresponding to this material will be null. If the deposit is not well placed in the sample holder of the XRD diffractometer, it will not be read at depth, in addition to including in the diffractograms the reading of the material of which the sample holder is made, interfering with the analysis. The calculations made for the texture coefficient and average crystal size present the parameters of the crystalline structure of each XRD diffractogram analysed. Confirming if it is a film according to the average crystal size and if it is textured towards a preferential plane. In conclusion, controlling the experimental conditions in the synthesis of CuO determines the properties of the thin films, as well as the future use in a device.

5.5 References

- Betancourth G, D., Gómez C, J. F., Mosquera, J., & Tirado Mejía , L. (2010). X-ray Diffraction Analysis on Rocks from Emerald Mining Region. *Scientia et Technica*.
- Duque Jaramillo , J., Llano Sánchez, L. E., & Villazón Amaris, H. (2006). Crystalline structure of copper, mechanical microscopic properties and processing.
- Korkmaz, S., Gecici, B., Korkmaz, D., Mohammadigharehbagh, R., Pat, S., Ozen, S., . . . Hafizittin, H. (2016). Morphology, composition, structure and optical properties of CuO/Cu₂O thin films prepared by RF sputtering method.
- Lung Chu, C., Chun Lu, H., Yang Lo, C., You Lai, C., & Hsiang Wang, Y. (2009). Physical properties of copper oxide thin films prepared by dc reactive magnetron sputtering under different oxygen partial pressures.
- Marroquín, E. Y. (2008). Extinción de la difracción de rayos X en la medición de figuras polares de plata de alta pureza.
- Patterson, A. L. (1939). The Scherrer for X-Ray Particle Size Determination . *APS physics*.
- Payá, J. M. (2020). Tratamiento de emisiones de COVs en la industria química farmacéutica mediante oxidación térmica regenerativa. (PDF 00-045-0937).
- Pérez, M. (2012). Técnicas de caracterización petrológicas (I): microscopía óptica de polarización (MOP) y difracción de rayos X (DRX).
- Prasanth, D., Sibin, k., & Barshilia, C. (2019). Optical properties of sputter deposited nanocrystalline CuO thin films.
- R, López, R., & Leyva Porras, C. (2021). Cupric oxide (CuO)/zinc oxide (ZnO) heterojunction diode with low turn-on voltage. *ScienceDirect*.
- Rodríguez Reyes, P. (2012). Síntesis y caracterización de nanopartículas de cobre y óxido de cobre y su incorporación en una matriz polimérica y el estudio de sus propiedades antibacterianas. *Centro de investigación de química aplicada*.
- Stuart, R. V. (1983). *Vacuum Technology, Thin Films, and Sputtering. An Introduction*.
- Subramanian, B., Anu Priya, K., Thanka Rajan, S., Dhandapani, P., & Jayachandran, M. (2014). Antimicrobial activity of sputtered nanocrystalline CuO impregnated fabrics.
- Wasa, K., Kanno, I., & Kotera, H. (2012). *Sputtering Deposition Technology. Fundamentals and Applications for functional Thin Film, Nanomaterials, and MEMS*.

Chapter 6 Redesign of a fatigue machine guide plate based on topology optimization

Capítulo 6 Rediseño de una placa guía de una máquina de fatiga con base en optimización topológica

SOTO-MENDOZA, Gilberto†*, MARTÍNEZ-GARCÍA, José', EDMUNDO-MASTACHE, Jorge' and HERNÁNDEZ-GÓMEZ, Luis Héctor''

†Tecnológico Nacional de México. Tecnológico de Estudios Superiores de Jocotitlán. Department of Mechatronics Engineering. Toluca-Atlacomulco Highway KM 44.8, Ejido de San Juan y San Agustín, Jocotitlán, 50700 Mexico.

''Instituto Politécnico Nacional. ESIME Zacatenco Unit. Graduate Studies and Research Section. Building 5, 3rd. floor. Professional Unit Adolfo López Mateos. Col. Lindavista. Alc. Gustavo A. Madero. 07738 Mexico City. Mexico.

ID 1st Author: *Gilberto, Soto-Mendoza* / **ORC ID:** 0000-0001-7357-9445, **CVU CONACYT ID:** 635154

ID 1st Co-author: *José, Martínez-García* / **ORC ID:** 0000-0002-7797-1062, **CVU CONACYT ID:** 612069

ID 2nd Co-author: *Jorge, Edmundo-Mastache* / **ORC ID:** 0000-0001-6104-6764, **Researcher ID Thomson:** H-1187-2018, **CVU CONACYT ID:** 544943

ID 3rd Co-author: *Luis Héctor, Hernández-Gómez* / **ORC ID:** 0000-0003-2573-9672, **CVU CONACYT ID:** 5107

DOI: 10.35429/H.2021.9.1.97.113

G. Soto, J. Martínez, J. Edmundo and L. Hernández

* gilberto.soto@tesjo.edu.mx

A. Ledesma (Coord.). Engineering Science and Technology. Handbooks-©ECORFAN-México, Estado de México, 2021.

Abstract

Machinery components are subjected to dynamic loads. In particular, the fatigue machines must be designed for these types of conditions. On the other hand, the industry demands that it is sought to consume the least amount of raw material for its construction, that is, to optimize. In general, optimization tasks have been carried out mostly by trial and error. In the present work, a redesign of a guide plate of a fatigue machine was carried out based on Topology Optimization. For this purpose, Static Structural, Topology Optimization, Fatigue and Modal Analysis were carried out. With this, a new design is obtained with a reduction in its raw material of 61%. The component was designed for infinite life so that it will not compromise its structural integrity throughout the life of the equipment operation.

Analysis, MEF, Natural frequency, Fatigue

Resumen

Los componentes de las máquinas están sometidos a cargas dinámicas. En particular, las máquinas de fatiga deben ser diseñadas para este tipo de condiciones. Por otro lado, la industria exige que se busque consumir la menor cantidad de materia prima para su construcción, es decir, optimizar. En general, las tareas de optimización se han llevado a cabo mayoritariamente por ensayo y error. En el presente trabajo, se realizó un rediseño de una placa guía de una máquina de fatiga basado en la Optimización Topológica. Para ello, se ha realizado un análisis estructural estático, de optimización topológica, de fatiga y modal. Con ello se obtiene un nuevo diseño con una reducción en su materia prima del 61%. El componente fue diseñado para una vida infinita, de manera que no comprometa su integridad estructural a lo largo de la vida de operación del equipo.

Análisis, MEF, Frecuencia natural, Fatiga

6.1 Introduction

An issue of relevance for mechanical components that are subjected to loads that change over time is fatigue. Fatigue occurs in a component when it is subjected to variable loads, which can be dynamic (uniformly varying loads) or random (seismic loads, wind loads, etc.). Fatigue failures represent a very high economic cost. These costs come from fatigue failures of land vehicles, trains, aircraft, bridges, cranes, offshore oil well structures, as well as a variety of machinery and equipment. They also involve human lives (Budynas & Nisbett, 2019), (Ugural, 2015). A fatigue testing machine allows measuring the fatigue resistance property of the material. Knowing this property, the number of cycles the material can be subjected to while retaining its structural integrity can be determined. Fatigue tests can be tension, compression, bending, torsion or a combination of stresses (Fatigue Test, 2021).

Today, machinery designers are required to minimise the cost of their designs. This is in order to be more competitive in the marketplace. It is a difficult challenge. One way to reduce cost is to remove material, to design leaner components. However, this has as a consequence an impact on the strength of the mechanical elements that make it up, its natural frequency is reduced, among others. The traditional way to optimise the product is to do it by trial and error. Such a technique is costly and time-consuming (Chen & Liu, 2018). With technological development, software has emerged that allows the mechanical behaviour of machines to be simulated. It is essential, that the designer has the scientific knowledge and is able to manipulate these programs to be much more efficient and competitive.

The programs that have been developed are mostly based on the Finite Element Method. They can be used to analyse the mechanical behaviour of complex geometries that cannot be obtained or would be time-consuming with traditional techniques. Additionally, analyses can be coupled to consider various phenomena. In this paper, a methodology is presented to optimise a mechanical component subjected to variable loads by means of numerical simulation. This involves static-structural analysis, topology optimisation studies, fatigue analysis and modal analysis in order to ensure its structural integrity during operation by obtaining a design with a lower weight than that proposed in the traditional way.

Computer Aided Design and Computer Aided Engineering programmes will be used for this purpose. These programmes have taken on another dimension in the training of today's engineers and have generated a link with industry that demands ever faster responses. There is a model focused on the cooperation of industry and universities to standardise and certify human resources (Lukač, 2011).

In addition, surface meshing and sub-modelling will be used to reduce the consumption of computational resources required for simulation. These techniques are very useful when academic licences are available that are limited in the number of nodes or elements that can be solved.

Section two gives a general description of the type of fatigue machine where the component to be optimised is located, as well as its overall dimensions. Then, in section three, the methodology followed to optimise the component is presented. In this section, only a general explanation is given; in the subsequent sections, each of its stages is covered.

It is essential to understand the theoretical basis of the phenomenon to be studied and not just see the programme as a black box. You must have the engineering knowledge to know what is intended to be obtained from the simulation and to verify that the results are reliable. The fact is that there may be several particular cases in which the results do not match reality and you may fall into error due to lack of experience. Topic four presents the theoretical basis of the studies carried out.

Section five deals with the numerical simulation. It starts with a structural analysis coupled to the topology optimisation study. With the stl model delivered by the optimisation, a redesign of the original part is created and the static simulation is performed again. Given that the component is subjected to fatigue loads, this analysis is carried out with the aim of achieving an infinite life. To ensure that the stress results do not vary with mesh size, a mesh sensitivity analysis is carried out and to reduce computational cost, the sub-modelling technique is used.

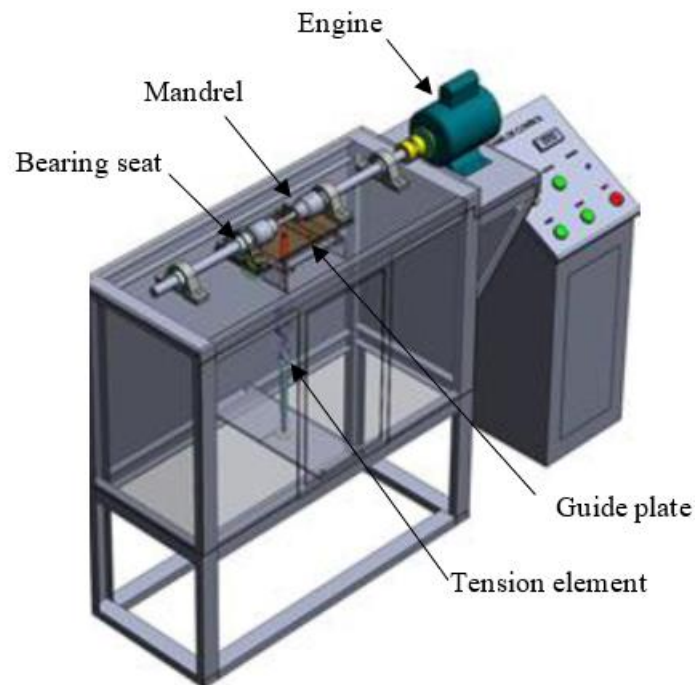
In section six, the results of deformation, mass, fatigue and natural frequencies are analysed. The original guide plate component is compared with the proposed new design. Finally, conclusions are drawn.

6.2 Description of the problem

One of the needs of educational institutions is to have infrastructure in their laboratories to complement the training of engineers, giving the opportunity to perform experiments. Materials testing is a key area. Among the tests performed is fatigue strength. This material property is essential for the design of machinery.

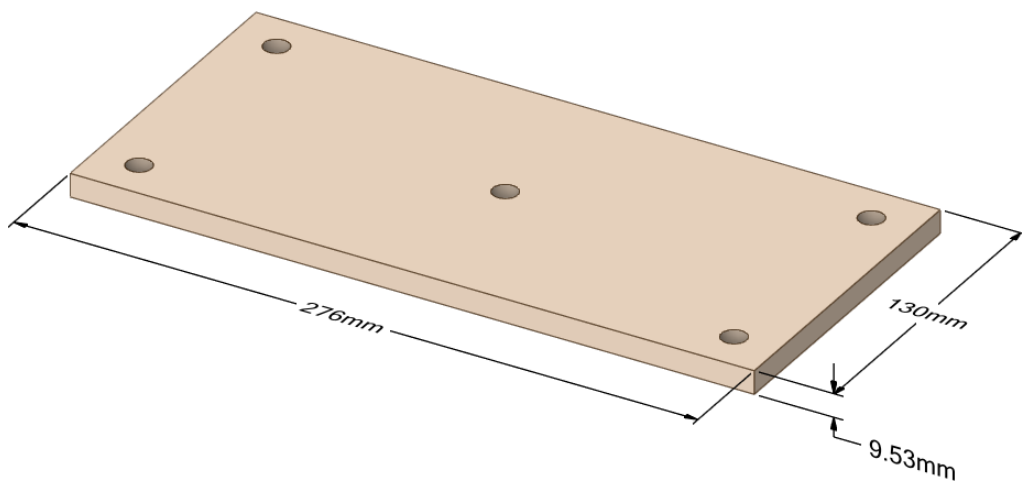
Many institutions lack such equipment. Some others have encouraged thesis work in the design of such academic equipment to fill this need. Some examples are Universidad de los Andes (Londoño, 2019), Escuela Superior Politécnica De Chimborazo (Castagneto, 2020), Universidad Católica Santo Toribio de Mogrovejo (Olivera, 2019), among others.

The common design form of these teams is shown in Figure 6.1.

Figure 6.1 Fatigue machine

Source: (Simbaña & Chango, 2012)

Machine components must be designed according to the operating conditions. The case study requires a fatigue analysis and a modal analysis because it is subjected to dynamic loads. The idea of building a component using as little material as possible without losing its functionality involves several challenges, although numerical simulation tools help to this end with a shorter execution time than the traditional trial-and-error way. This paper presents the redesign of a fatigue machine guide plate based on topology optimization. **Figure 6.2** shows the overall dimensions of the guide plate of the case study.

Figure 6.2 Guide plate dimensions

6.3 Methodology

The design of a machine depends to a large extent on the creativity of the designer, on the ideas he or she has to perform the desired function. The following methodology is focused on optimising components that are subjected to variable loads and are intended to be lightweight. The stages for this purpose are:

1. Create a crude model
2. Determine the operating conditions of the component
3. Structural simulation
4. Simulation from a topology optimization perspective

5. Creation of the new model on the basis of topology optimization
6. Structural analysis of the new design
7. Fatigue study
8. Modal analysis
9. Analysis of results

The following section begins with the theoretical basis for the type of analysis required for the case study.

6.4 Theoretical basis

6.4.1 Structural analysis

The use of the Finite Element Method (FEM) has grown in engineering. It allows structural analysis of complex geometries among other types of analysis. In general, its stages are as follows:

- The model (geometry) is created in some Computer Aided Design (CAD) software.
- The mechanical properties of the material are defined.
- The model is discretised (mesh generation).
- Boundary conditions are applied.
- The solve simulation is run.
- Finally, the required results such as deformation, stresses, etc. are sought (post-processing).

For a linear structural analysis we have the following equation:

$$[K]\{D\} = \{F\} \quad (1)$$

Where:

$\{D\}$ = Displacement vector

$\{F\}$ = Force vector

$\{K\}$ = Stiffness matrix of the structure

In the case study, several structural analyses are carried out. It is assumed that the design will work in the linear zone of the material, so Equation 1 is the one that the program will be solving.

6.4.2 Optimisation

The requirement to obtain a strong mechanical component using the least amount of material in order to make it lighter and/or reduce costs has led to the development of new technologies. The typical way to perform optimisation is through trial and error, but this procedure is deficient because of the cost and time consumed to execute it. Nowadays, numerical simulation has become a powerful tool in engineering and thanks to more powerful computers, a large number of calculations involving these techniques can be solved. Numerical optimisation compared to the traditional technique is more productive and economical (Chen & Liu, 2018).

There are two perspectives in numerical optimisation. The first is topology optimization and the second is parametric optimisation. The designer must optimise from different perspectives considering the process involved in the design itself.

The aim of topology optimization is to find the ideal distribution of the defined material in a given space considering the loads and boundary conditions. With this it is possible to obtain a good initial design concept. This type of optimisation should be used in the early stages of design.

Parametric optimisation, on the other hand, focuses on determining the shape and dimension of the structure in question. The design variables are usually length, thickness, etc. and the state variables are stress, deformations, etc.

6.4.3 Fatigue analysis

Fatigue occurs in a component when it is subjected to variable loads, which can be dynamic (uniformly varying loads) or random (seismic loads, wind loads, etc.). Among the serious accidents due to fatigue failure is the British Comet Jet in 1954, this caused the Comet flights to be suspended and the production of the British jet was stopped (The Aircraft Accidents That Revolutionised Aircraft Design - BBC News World, 2014). Fatigue study is essential in the design of mechanical components subjected to varying loads because of the economic impact of failure.

There are different approaches to fatigue study. The method of interest for this study is the stress-life method. This method is the most traditional, it is easy to implement and there is a lot of experience. However, it is only applied to elastic stresses, it is limited to low and high cycle stresses. In low cycle applications it is less accurate. It relies on stress-life (S-N) curves (Budynas & Nisbett, 2019). The case study is high cycling.

6.4.3.1 Fatigue terminology

Among the terminology found in fatigue we have:

Stress range

$$\sigma_r = \sigma_{max} - \sigma_{min} \quad (2)$$

Mean stress

$$\sigma_m = \frac{\sigma_{max} + \sigma_{min}}{2} \quad (3)$$

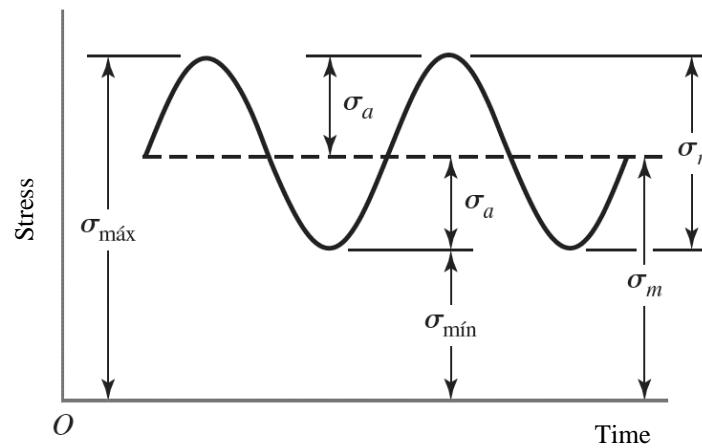
Alternating stress

$$\sigma_a = \left| \frac{\sigma_{max} - \sigma_{min}}{2} \right| \quad (4)$$

Investment ratio (stress ratio)

$$R = \frac{\sigma_{min}}{\sigma_{max}} \quad (5)$$

Figure 6.3 illustrates these parameters. The horizontal axis represents the time and the vertical axis the applied stress. The illustration shows a sinusoidal behaviour, however, it does not necessarily have to be that way. The purpose of the graph is to illustrate the terminology: Maximum stress, minimum stress, alternating stress and stress range.

Figure 6.3 Fatigue terminology

Source: (Budynas & Nisbett, 2019)

6.4.3.2 Mean stress different from zero

In practical cases, you have different stress ratios, i.e. the mean stress is different from zero. In general, laboratory tests typically start from a mean stress equal to zero. The effect of the mean stress is that, if it increases, the amplitude of the equivalent fatigue stresses decreases. There are several theories of fatigue failure for non-zero mean stress including: Sodeberg, Goodman, Gerber, Langer, etc. Goodman's criterion is perhaps the most widely used for the design of machinery components subjected to cyclic loading (Mott et al., 2018). In this study we will look for the component to have infinite life and the Goodman criterion (Equation 6) will be used. It is important to emphasise that Dowling's research indicates that this criterion is not accurate when finite life is estimated and other criteria are suggested (Dowling et al., 2009).

$$\frac{S_a}{S_e} + \frac{S_m}{S_{ut}} = 1 \quad (6)$$

Where:

Sa = Alternating strength.

Se = Fatigue strength limit

Sm = Mean stress

Sut = Ultimate stress

6.4.4 Modal analysis

In order to determine the behaviour of structures subjected to loads that change over time, structural-dynamic analyses are carried out. In these, the inertia and damping of the structure play an essential role. There are several types of such analyses such as: Random, Transient, Modal, among others. In the present work a modal analysis is carried out in order to obtain the natural frequencies and the modes of vibration of the system.

Equation 7 is used to obtain the natural frequency and modes of vibration of the system. It is assumed that the vibration is free, the mass and stiffness matrices are constant (Howard & Cazzolato, 2015).

$$[M]\{\ddot{u}\} + [K]\{u\} = \{0\} \quad (7)$$

Where:

$[M]\{\ddot{u}\}$ = Inertial force

$[K]\{u\}$ = Elastic force

$[M]$ = Mass matrix

$[C]$ = Damping matrix

$[K]$ = Stiffness matrix

$\{\ddot{u}\}$ = Acceleration vector

$\{\dot{u}\}$ = Velocity Vector

$\{u\}$ = Displacement vector

(t) = Time

The oscillation is assumed to be harmonic of the form:

$$\{u\} = \{\phi\}_n \cos \omega_n t \quad (8)$$

Substituting the value into the above equation converts it to:

$$(-\omega_n^2[M] + [K])\{\phi\}_n = \{0\} \quad (9)$$

$\{\phi\}_n$ = The eigenvector representing the modes of vibration of the natural frequencies.

ω_n = It is the natural circular frequency

A trivial solution is $\{\phi\}_n = 0$, the following series of solutions corresponds to Equation 10.

$$|[K] - \omega_n^2[M]| = 0 \quad (10)$$

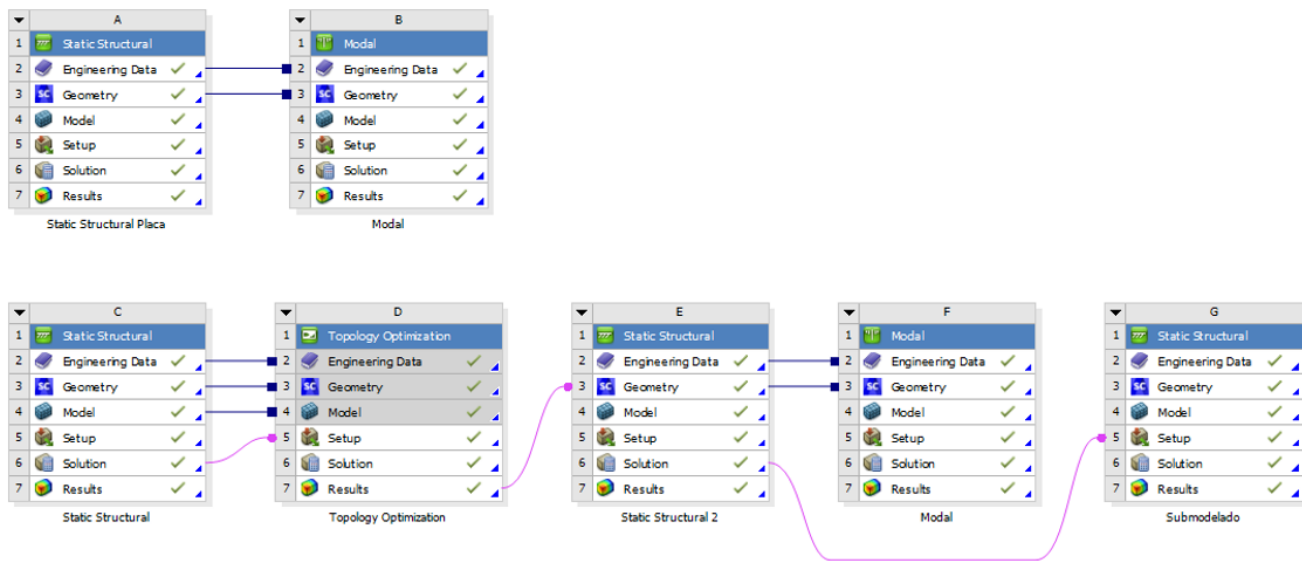
With the natural circular frequencies (eigenvalues) the natural frequency f_n can be obtained (Equation 11).

$$f_n = \frac{\omega_n}{2\pi} \quad (11)$$

6.5 Numerical simulation

The numerical simulation was performed in ANSYS® Student, a free software, but it is limited to the number of elements or nodes it can solve. For structural analyses the number of nodes or elements, whichever is reached first, is 128 000 (Download Ansys Student | Workbench-Based Simulation Tools, 2021).

The general scheme that was realised on the Workbench platform is shown in Figure 6.4. Workbench is the platform where all the modules offered by ANSYS® are located. In addition, it allows coupling the modules.

Figure 6.4 Diagram of the analyses in ANSYS® Workbench

Following the methodology, the following steps are taken:

6.5.1 Creating a crude model

To start the simulation, the geometrical model is required. Geometries can be lines (in this case a cross section is indicated), surfaces or volumes. It should always be simplified in order to use less computational resources. In the case of the study we start with a surface as we intend to build the model with plates. Figure 6.5 shows this surface with its dimensions. The thickness considered is 4.76 mm (3/16"). In addition, the SpaceClaim program was used to prepare the geometry for the simulation by splitting the edges. This allows to select where the boundary conditions are to be applied.

Figure 6.5 Initial geometry

6.5.2 Determination of the operating conditions of the component

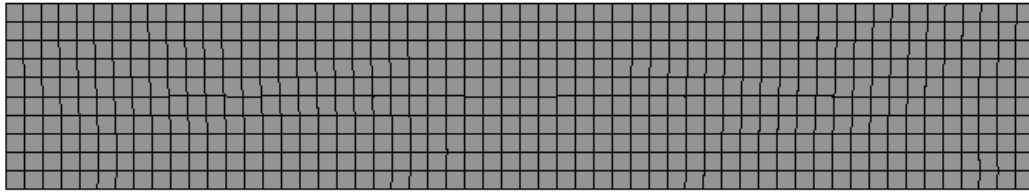
The component is attached to two bearing housings fixed with bolts (see Figure 6.1). A maximum vertical force of 490.5 N is applied to induce a bending moment in the specimen. The component is to be constructed from a structural steel with the following properties:

- Young's modulus = 200 GPa
- Poisson Ratio = 0.3
- Yield stress = 250 MPa
- Ultimate stress = 460 MPa

6.5.3 Structural simulation

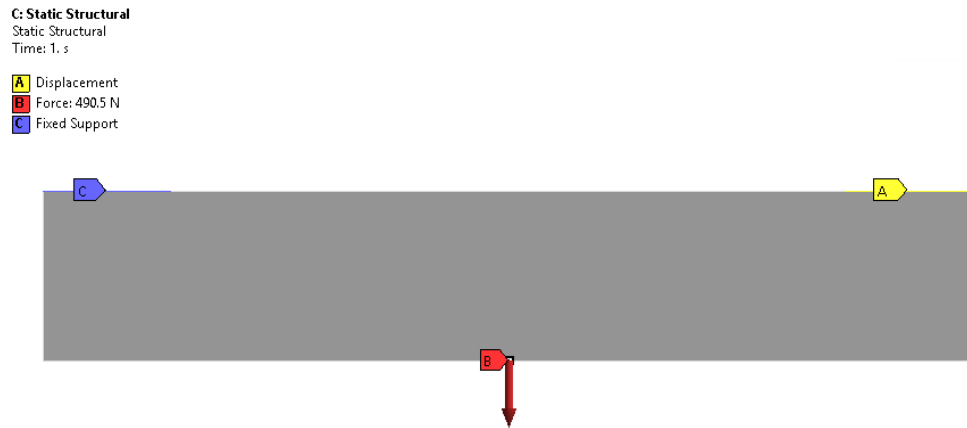
Once the material has been assigned to the model and the boundary conditions are ready to be assigned, the mesh is generated (see Figure 6.6). For structural analysis it is recommended that the mesh quality "Element Quality" is not less than 0.2. A mesh size control of 5 mm was used. The number of nodes is 627 and the number of elements is 560. Its minimum mesh quality is 0.96 and the average is 0.98. The closer to one the better. This first analysis is coupled with the topology optimization analysis.

Figure 6.6 Mesh



The boundary conditions are: on the left side a fixed support "Fix support" and on the right side a displacement constraint "Displacement" in Y-direction. The load is a vertical force of 490.5 N in the vertical direction (see Figure 6.7).

Figure 6.7 Border conditions



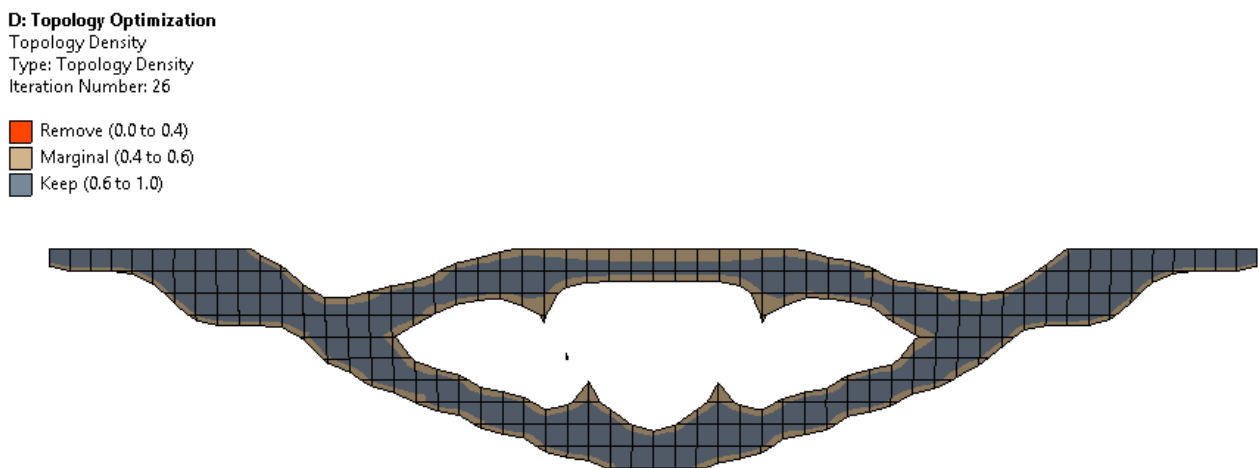
6.5.4 Simulation from topology optimization perspective

The idea of this simulation is to obtain the material distribution in such a way that the component is as rigid as possible, i.e. that it deforms as little as possible under the load to which it is subjected. The process requires the following:

- Optimisation region. The entire component is given and boundary conditions are excluded.
- Objective. In this case, the model is to be as rigid as possible. This option is indicated as "Compliance".
- Restriction. It is indicated to reduce the mass to 1 30% for this case, this parameter can be adjusted to see different distribution options.

The topology optimization analysis is coupled to the structural analysis (see Figure 6.4). The result of this simulation is shown in Figure 6.8.

Figure 6.8 topology optimization



6.5.5 Creation of the new model based on topology optimization

Based on the topology optimization, a new geometry is created (see Figure 6.9). The topology optimization model can be exported to STL format and worked with from any design program. In this work, the SpaceClaim module was used continuously and the optimisation result was coupled with the geometry of the following structural analysis (see Figure 6.4). The new design is shown in Figure 6.10.

Figure 6.9 Model based on topological optimisation

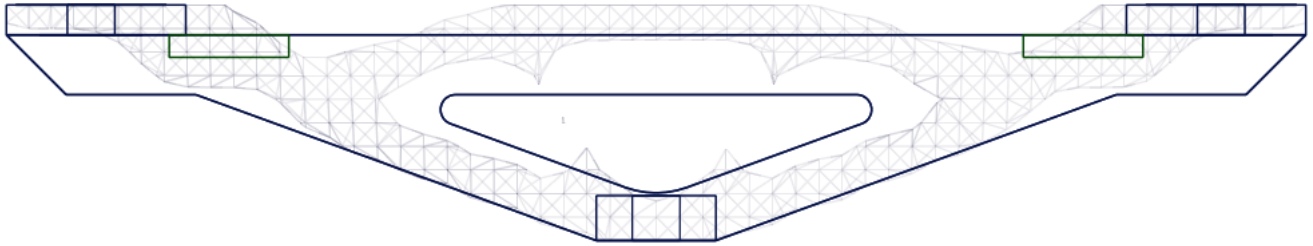
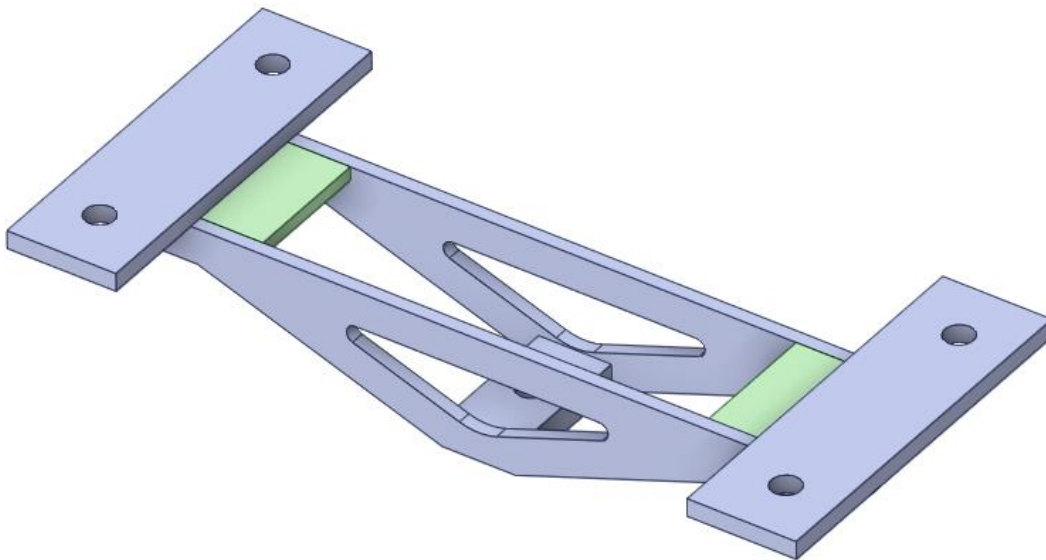
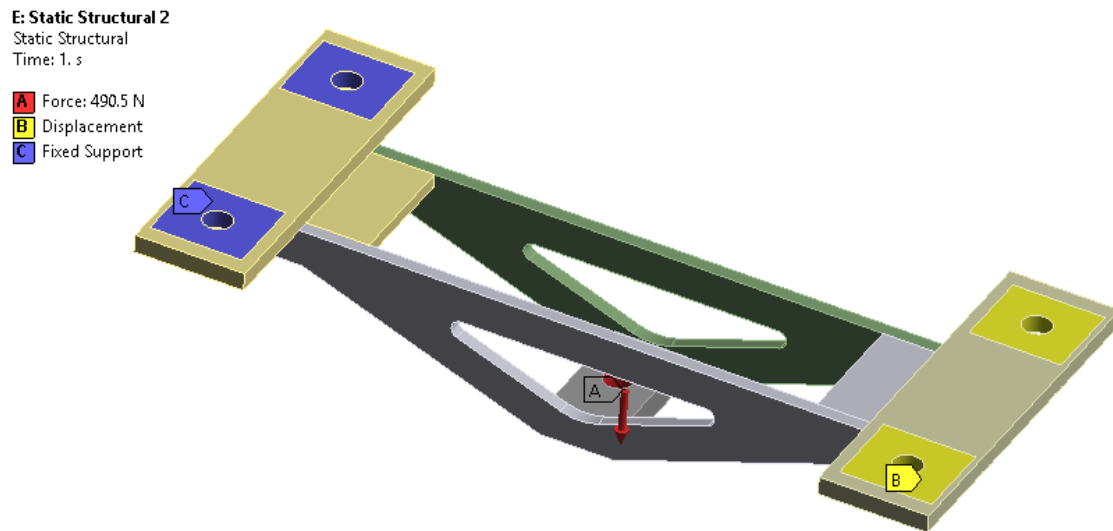


Figure 6.10 New model

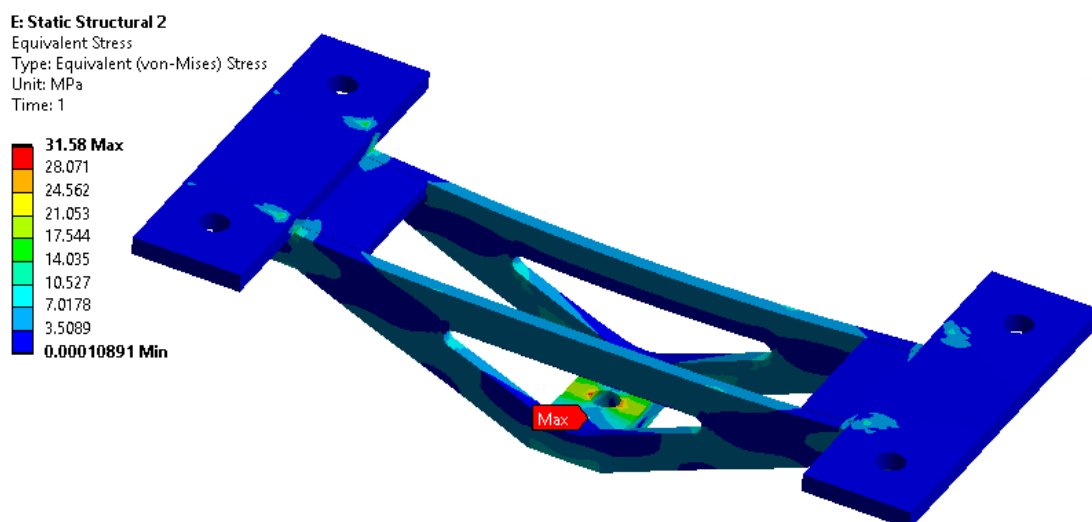


6.5.6 Structural analysis of the new design

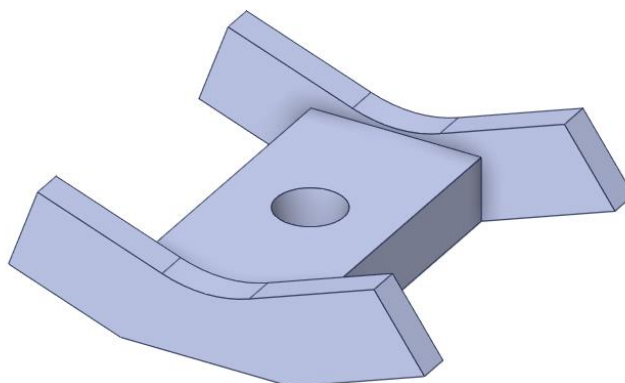
The same process as in section 6.5.3 for the structural analysis is followed again. Only now surfaces are selected instead of edges and lines for the boundary conditions (see Figure 6.11).

Figure 6.11 Model boundary conditions

The static failure theory used is that of von Mises, as this is a ductile material. The highest indicated stress is at the bottom near the borehole (see Figure 6.12). However, this may change with the mesh size. So, a mesh sensitivity analysis is performed. The drawback that can occur is the limit of nodes that can be solved by the student licence. There are several techniques that can be used to reduce the computational cost such as symmetry and sub-modelling.

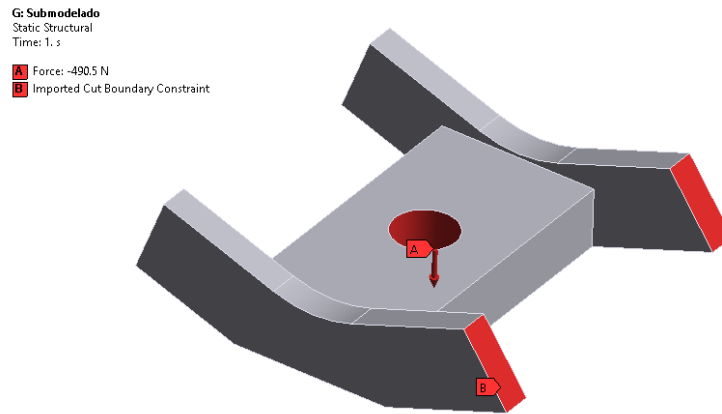
Figure 6.12 von Mises Stress

Sub-modelling consists of selecting the region of the geometry where further refinement is required. It must take into account the area where it cuts. It must not have stresses that change drastically. The solution of the static study has to be coupled with the setup of a new structural study (see Figure 6.4). The geometry of the new study corresponds to the refinement region (see Figure 6.13).

Figure 6.13 Geometry for sub-modelling

For the boundary conditions, the constraints in the shear zone are imported and the vertical load is applied to the borehole (see Figure 6.14).

Figure 6.14 Sub-model boundary conditions



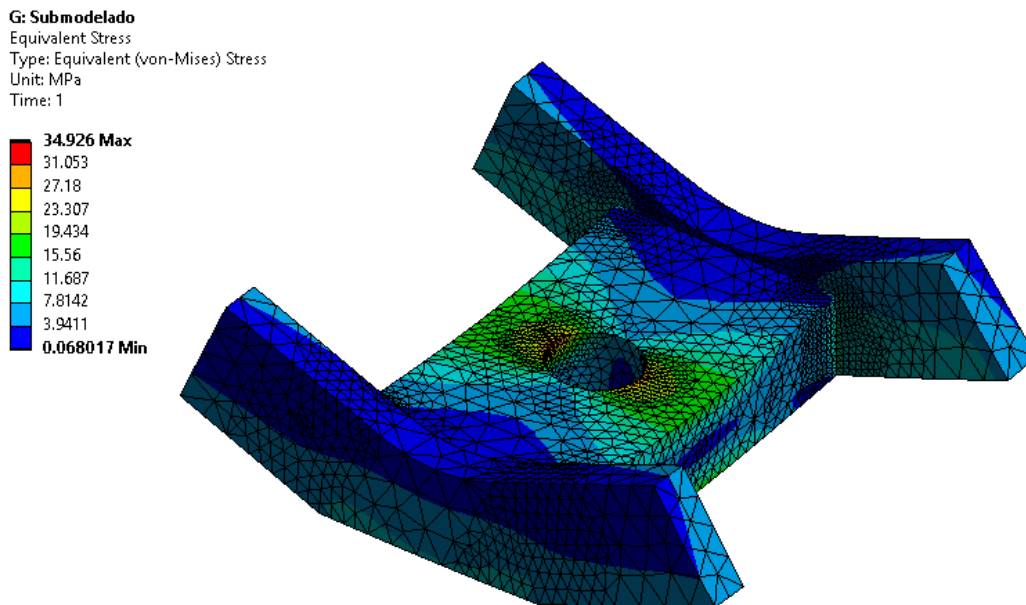
The simulation run is continued and the von Mises forces are obtained. Then, the convergence condition is appended to the von Mises results. It is indicated that the results should not vary by more than 5 %. You can adjust this value according to your requirements. This value indicates that if the stress results of each run with mesh refinement are within the range the simulation stops. The results are said to converge. Table 6.1 shows this process with the number of nodes required. A considerable increase in the number of nodes is observed which implies a longer calculation time.

Table 6.1 Mesh sensitivity analysis

Corrida	von Mises (MPa)	Change (%)	Nodes	Elements
1	31.822		8816	5206
2	34.35	7.6407	48744	32369
3	34.926	1.6616	126821	87808

The result indicates that the maximum von Mises stress is 34.9 MPa (see Figure 6.15). This is below the yield stress of the material. Therefore, it will not fail under static loading. The next study is the fatigue analysis. Since the component is subjected to cyclic loading.

Figure 6.15 von Mises Stress in the sub-model

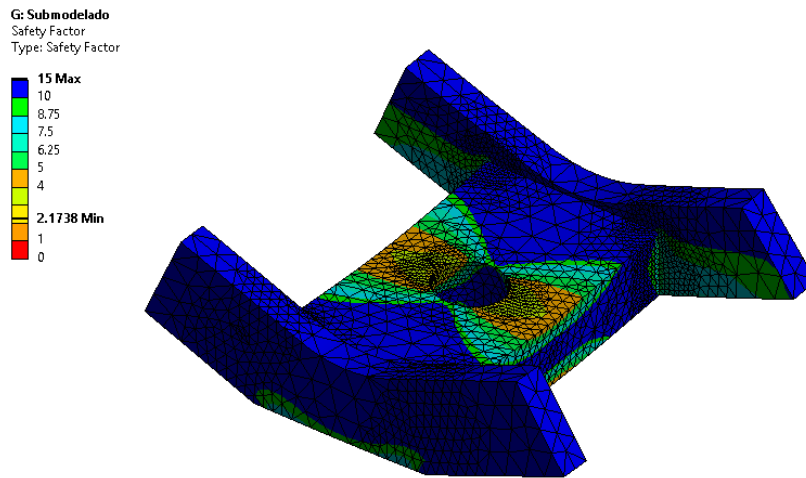


6.35.7 Fatigue study

The fatigue failure theory used is Goodman's (Equation 6). The stress ratio is 0 "Zero based". A correction factor for surface finish, size and reliability of 0.48 is considered. Infinite life is sought. Under these conditions, the fatigue safety factor is obtained (see Figure 6.16).

The minimum safety factor considered for this component is 2 as it is subjected to dynamic loads. The factor of safety obtained from the fatigue study is 2.17. The results indicate that it will not fail due to fatigue.

Figure 6.16 Fatigue safety factor



6.5.8 Modal analysis

The component must not operate at its natural frequency as this would result in high stresses that would compromise the structural integrity of the component. For this reason, these values are determined. Figure 6.17 and 6.18 show the first two modes of vibration. The first natural frequency is 596 Hz and the second is 1350 Hz.

Figure 6.17 First vibration mode

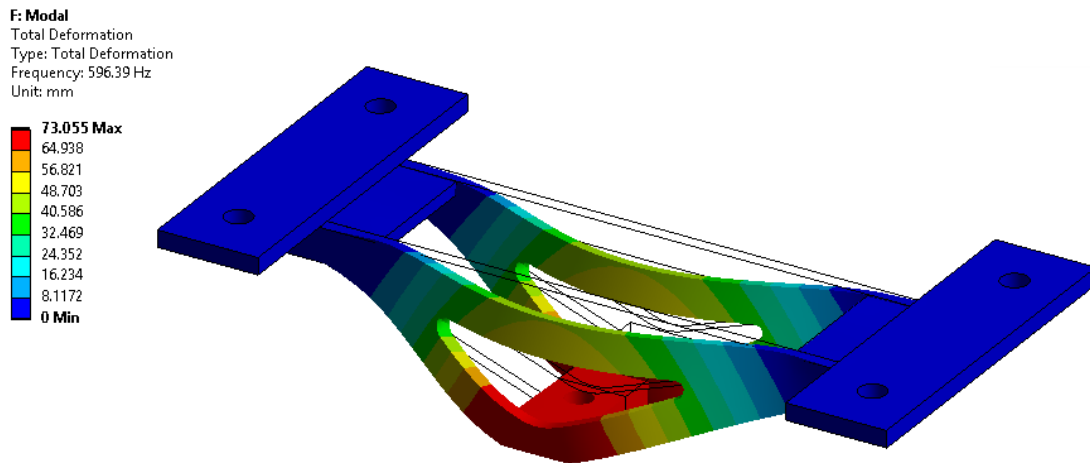
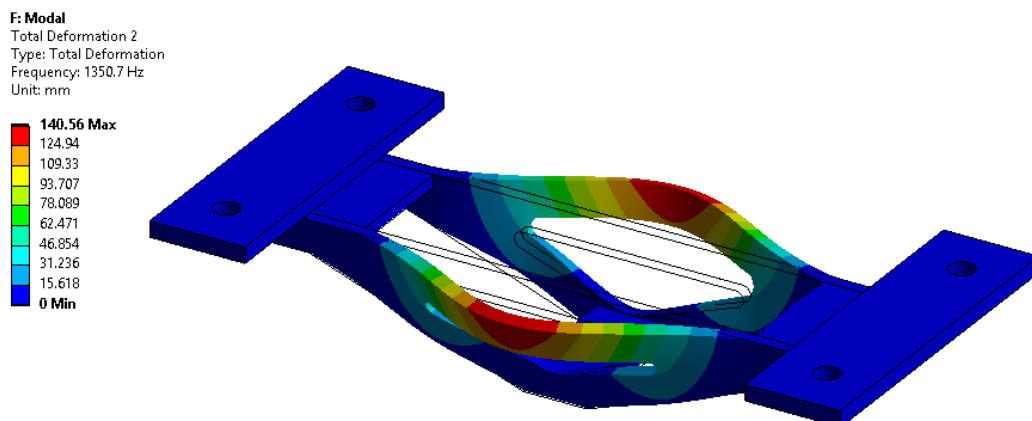


Figure 6.18 Second vibration mode



6.6 Analysis of results

6.6.1 Deformation

Structural and fatigue analyses are performed on the guide plate (original component). The boundary conditions used are the same as those used in the previous sections. Figure 6.19 shows the deformation of the plate which is at the centre and has a maximum value of 0.0166 mm. Figure 6.20 shows the maximum deformation of the new model which is 0.0153mm. Both results are very similar.

Figure 6.19 Plate deformation

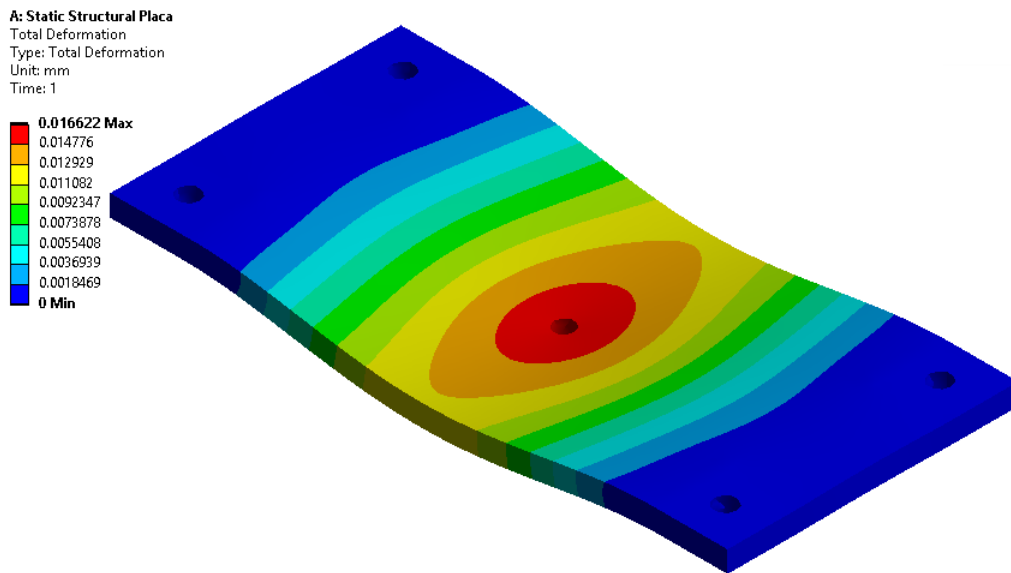
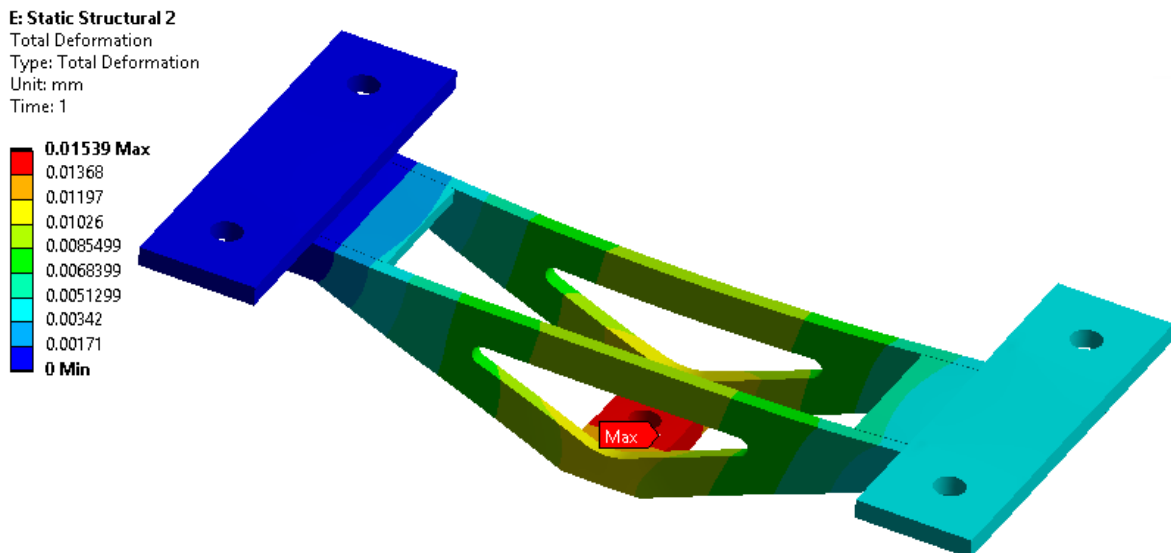


Figure 6.20 Deformation of the new model



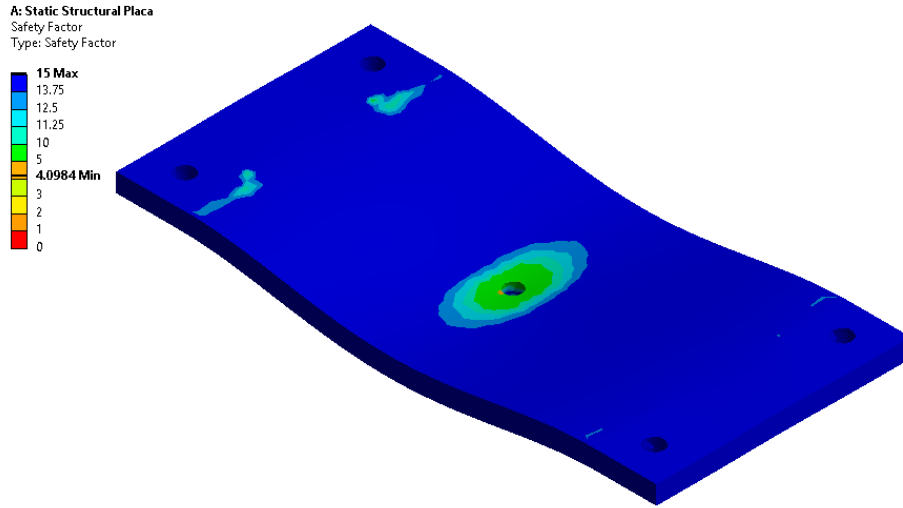
6.6.2 Mass

On the other hand, if we analyse the mass of each component we have for the plate a mass of 2.65 kg and for the new model a mass of 1.05 kg. As can be seen there is a considerable variation. This indicates that the new model is much lighter. The weight of the new design represents 39 % of the original model.

6.6.3 Fatigue

Figure 6.21 shows the minimum fatigue safety factor of the plate of 4.09 which is higher than that shown in Figure 6.16 of 2.17. Therefore, the fatigue strength of the plate is higher. However, the new design meets the required factor of safety.

Figure 6.21 Fatigue plate safety factor



6.6.4 Natural frequencies

Figure 6.22 and Figure 6.23 show the first vibration modes of the plate which are: 1007 Hz and 1556 Hz. Both are high. In the proposed model the first natural frequency is reached at 596 Hz. This is lower than that of the plate. Even so, it is still high as it corresponds to about 35760 rpm and the two-pole AC motor has an approximate speed of 3600 rpm.

Figure 6.22 First plate vibration mode

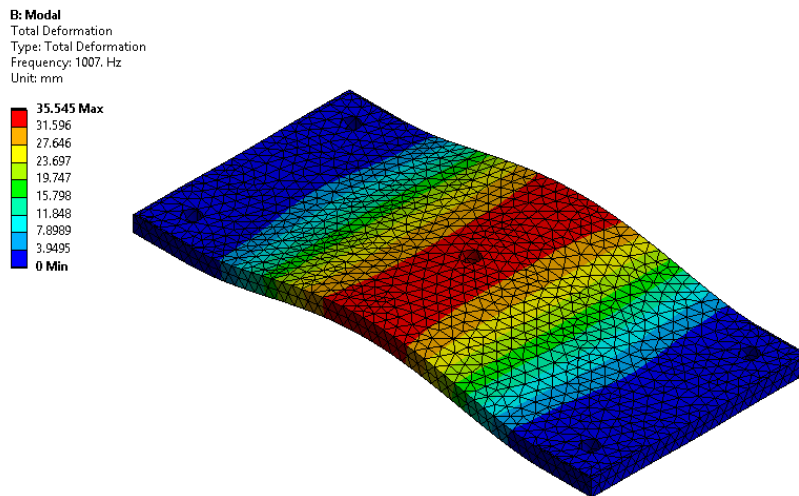
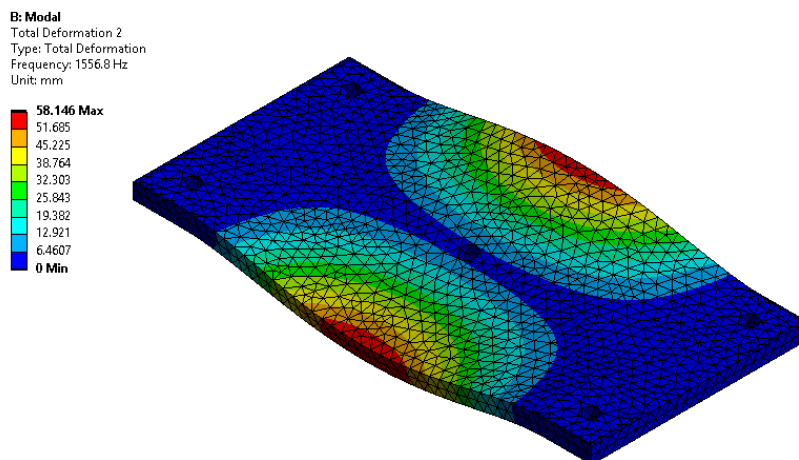


Figure 6.23 Second vibration mode of the plate



6.7 Conclusions

The same analyses were carried out under the same loading conditions for both designs. The differences in deformation are very similar and can be considered negligible ($0.0166 - 0.0153 = 0.0013\text{mm}$). As for the fatigue safety factor, it is noticeable. It can be said that the plate is in excess and the new design complies with the required safety factor. On the other hand, the modal analysis indicates that the new design reaches its first natural frequency (576 Hz) before the plate. This is still a high value compared to the revolutions of AC motors. Therefore, the redesign will not have any problems. The variable that was noticeable between the two models was the change in mass. The redesign contains a mass of 39 % with respect to the board (original model). Optimisation by topology is very useful if you need to find the least amount of material to create a component. However, it can give complex shapes. Manufacturing processes must be taken into account to adjust and build a new design. Manufacturing costs must be assessed as the weight of the material is not the only factor in this.

6.8 References

- Budynas, R., & Nisbett, K. (2019). *Shigley's Mechanical Engineering Design*. McGraw-Hill Education.
- Castagneto, L. A. (2020). *Escuela Superior Politécnica De Chimborazo*. Escuela Superior Politécnica De Chimborazo, Ecuador.
- Chen, X., & Liu, Y. (2018). *Finite Element Modeling and Simulation with ANSYS Workbench* (2nd ed.). CRC Press. <https://www.routledge.com/Finite-Element-Modeling-and-Simulation-with-ANSYS-Workbench-Second-Edition/Chen-Liu/p/book/9781138486294>
- Dowling, N., Calhoun, C., & ARCARI, A. (2009). Mean Stress Effects in Stress-life Fatigue and the Walker Equation. *Fatigue & Fracture of Engineering Materials & Structures*, 32, 163–179. <https://doi.org/10.1111/j.1460-2695.2008.01322.x>
- Download Ansys Student / Workbench-based Simulation Tools. (2021). <https://www.ansys.com/academic/students/ansys-student>
- Fatigue Test*. (2021). <https://www.testresources.net/applications/test-types/fatigue-test/>
- Howard, C. Q., & Cazzolato, B. S. (2015). *Acoustic analyses using MATLAB® and ANSYS®*. CRC Press.
- Londoño, B. S. (2019). *Diseño y construcción de banco de pruebas para estudios de fatiga en flexión rotativa*. Universidad de los Andes, Colombia.
- Los accidentes aéreos que revolucionaron el diseño de los aviones - BBC News Mundo*. (2014). https://www.bbc.com/mundo/noticias/2014/04/140421_accidentes_avion_seguridad_vert_fut_rg
- Lukač, D. (2011). New dimensions in the CAE/CAD standardisation and certification process in the industrial and the educational sector. *International Journal of Knowledge and Learning*, 7(1–2), 145–155. <https://doi.org/10.1504/IJKL.2011.043897>
- Mott, R. L., Vavrek, E. M., & Wang, J. (2018). *Machine elements in mechanical design* (6th ed.). Pearson.
- Olivera, M. F. (2019). *Diseño y construcción de máquina de ensayos flexo rotativa para el estudio de la fatiga mediante el método esfuerzo vida para la sede valle Jequetepeque de UNT*. Universidad Católica Santo Toribio de Mogrovejo, Chiclayo.
- Simbaña, R. M., & Chango, D. M. (2012). *Diseño y construcción de una máquina para realizar ensayo de fatiga por flexión rotativa utilizando PC*. Escuela Politécnica del Ejército Extensión Latacunga.
- Ugural, A. C. (2015). *Mechanical Design of Machine Components* (Taylor & Francis Group (Ed.); 2nd ed.). CRC Press.

Chapter 7 Noise level evaluation in the resin figures manufacturing process

Capítulo 7 Evaluación del nivel de ruido en el proceso de fabricación de figuras de resina

GARCÍA-SANCHEZ, Viviano†', MALDONADO-ONOFRE, Daniel*'', MIER-QUIROGA, Luis Antonio'' and COUTIÑO-MORENO, Elvis''

†' *Instituto Tecnológico de Toluca, State of Mexico, Mexico.*

'' *Tecnológico de Estudios Superiores de Jocotitlán, Department of Electromechanical Engineering, State of Mexico, Mexico.*

''' *Tecnológico de Estudios Superiores de Jocotitlán*

ID 1st Author: *Viviano, García-Sánchez*

ID 1st Co-author: *Daniel, Maldonado-Onofre* / ORC ID: 0000-0002-6078-2206

ID 2nd Co-author: *Luis Antonio, Mier-Quiroga* / ORC ID: 0000-0001-8290-4115

ID 3rd Co-author: *Elvis, Coutiño-Moreno* / ORC ID: 0000-0003-2455-2574

DOI: 10.35429/H.2021.9.1.114.128

V. García, D. Maldonado, T. De la Mora, L. Mier and E. Coutiño

* daniel.maldonado@tesjo.edu.mx

A. Ledesma (Coord.). Engineering Science and Technology. Handbooks-©ECORFAN-México, Estado de México, 2021.

Abstract

The investigation allowed the evaluation of the levels of noise in dedicated factories to the manufacture of decorative resin figures, located in a population of the north of the Municipality of Toluca State Capital of Mexico. The study was developed with the objective to count on a reference mechanism to prevent risks to the health derived from the level with exhibition to the noise generated in this type of facilities, in such a way that the proprietors can protect to their personnel guaranteeing the development of their activities and not see themselves involved in labor demands. The investigation was limited the study of a single factory solely that is representative of the activities that are made normally in all the factories located in the zone, of which exist more than 50. For the measurements of the noise level, an integrating sound level meter was used type 2, of mark CEL Instruments® model CEL-328 and for the calibration of this was used an acoustic calipers mark CEL Instruments®, model CEL-282, series 2/11616221; the measurements and calibration were made taking in account the effective legislation in the matter of noise according to the Official Norm Mexicana NOM-011- STPS-2001, Conditions of Security and Hygiene in the Centers of Work Where Noise Is generated. Of the analysis of results it was observed that the level of noise in the areas of rectified and music, was with a NSCEAT, greater of 90 dB and in the remaining areas was smaller, but require of preventive measures since all presented/displayed 80 a greater NSCE of dB. In general the level of exhibition to the noise (NER) of the factory is of 86,6 dB, this value according to the norm applied in this study is necessary to implement some measures that allow to diminish the levels of noise with the purpose of avoiding labor diseases derived from the noise.

Noise level analysis, Noise, Risk

Resumen

La investigación permitió evaluar los niveles de ruido en talleres dedicados a la fabricación de figuras decorativas de resina, ubicados en una población del norte del Municipio de Toluca Estado de México. El estudio se desarrolló con el objetivo de contar con un mecanismo de referencia para prevenir riesgos a la salud derivados del nivel con exposición al ruido generado en este tipo de instalaciones, de tal manera que los propietarios puedan proteger a su personal garantizando el desarrollo de sus actividades y no se vean involucrados en demandas laborales. La investigación se limitó al estudio de una sola fábrica que es representativa de las actividades que se realizan normalmente en todas las fábricas ubicadas en la zona, de las cuales existen más de 50. Para las mediciones del nivel de ruido, se utilizó un sonómetro integrador tipo 2, de marca CEL Instruments® modelo CEL-328 y para la calibración de éste se utilizó un calibrador acústico marca CEL Instruments®, modelo CEL-282, serie 2/11616221; las mediciones y calibración se realizaron tomando en cuenta la legislación vigente en materia de ruido de acuerdo a la Norma Oficial Mexicana NOM-011- STPS-2001, Condiciones de Seguridad e Higiene en los Centros de Trabajo donde se genera Ruido. Del análisis de resultados se observó que el nivel de ruido en las áreas de rectificado y música, fue con un NSCEAT, mayor de 90 dB y en las áreas restantes fue menor, pero requieren de medidas preventivas ya que todas presentaron 80 un NSCE mayor de dB. En general el nivel de exposición al ruido (NER) de la fábrica es de 86,6 dB, este valor según la normativa aplicada en este estudio es necesario implementar algunas medidas que permitan disminuir los niveles de ruido con la finalidad de evitar enfermedades laborales derivadas del ruido.

Análisis del nivel de ruido, Ruido, Riesgo

7.1 Introduction

The field of occupational health and safety is very broad, ranging from the conditions of facilities and production processes to the behaviour of workers. Work activity is limited by factors capable of causing alterations in the work environment and, therefore, in the worker's health (Alexandry, 1978).

It is important to consider that, for good human performance, the worker must not exceed his or her limits of resistance and remain in adequate conditions in the workplace. One of the main areas of opportunity in occupational hygiene is the study of physical agents such as temperature, lighting, vibrations and the most common of all, noise. Noise has become so common in people's daily lives that we hardly recognise its effects until we have been adversely affected by it.

Noise is defined as an unpleasant and annoying sound. This phenomenon depends on several factors, such as frequency, intensity, duration, exposure time, age of the worker and individual susceptibility.

Noise causes damage to human beings, such as headache, bad mood, insomnia, stress, irritability, central nervous system disorders, hypertension, etc. These affect the quality of life of workers.

The research allowed the evaluation of noise levels in workshops dedicated to the manufacture of decorative resin figures, located in a town in the north of the Municipality of Toluca, capital of the State of Mexico. This study was developed with the objective of having a reference mechanism to prevent health risks derived from the level of exposure to noise generated in this type of installations, so that the owners can protect their personnel by guaranteeing the development of their activities and not be involved in labour lawsuits. The study was limited to the study of only one workshop, which is representative of the activities that are normally carried out in all the workshops located in the area, of which there are more than 50. For the noise level measurements, a CEL Instruments® model CEL-328 type 2 integrating sound level meter was used, and for its calibration, a CEL Instruments® model CEL-282, series 2/11616221 acoustic calibrator was used; the measurements and calibration were carried out taking into account the current legislation on noise in accordance with the Official Mexican Standard NOM-011- STPS-2001, Safety and Hygiene Conditions in Workplaces Where Noise is Generated.

The results obtained from the analysis of the noise level evaluation in the workshop showed that the grinding and music areas had a NSCEAT of 90.1 and 91.7 dB(A) respectively, and the remaining areas had a NSCEAT of 78.8 dB(A), moulding 78.8 dB(A), casting 81.5 dB(A), finishing 82.4 dB(A), decorating 83.3 dB(A) and compressors 85.4 dB(A), as can be seen the noise level was lower, but it is necessary to take preventive measures since they all gave a NSCEAT greater than 80 dB.

In general the noise exposure level (NER) of the workshop is 86.6 dB, this value according to the standard applied in this study is below 90 dB which is recommended by the regulations that were taken as a reference for an 8-hour working day, but as it resulted in a value greater than 85 dB (A), it is necessary to implement preventive measures to reduce noise levels in order to avoid occupational diseases caused by noise.

7.2 Development

The research carried out is of a cross-sectional type as the study was carried out at a defined time and moment, in this case in an eight-hour working day with three periods of observation or reading, as proposed by the standard, we will also only limit ourselves to observing the events or phenomenon under study without intervening in them, so the research will be non-experimental. Furthermore, the study is descriptive in nature, as it seeks to develop an image or representation of the characteristics of the noise generated by the tools used in this type of workshop, as well as the measurement of the particular variables of this physical phenomenon, for its analysis, emphasising the independent study of each characteristic, but it is possible in some way to integrate the decisions of two or more characteristics in order to determine how the phenomenon is or how it manifests itself.

Thus, at no point is it intended to establish the relationship between these variables. However, the results can be used to predict some phenomenon that can be originated by the studied variable, such as in this case that workers can develop some occupational disease related to high noise levels (Astete and Kitamura, 1978).

North of the city of Toluca there is a population dedicated to the elaboration of resin figures, in which there are approximately 50 workshops dedicated to this activity, directly employing approximately ten people per workshop, and another large number who benefit indirectly from the sale and resale of these articles, making it a very important economic activity in the region, since these pieces are sold all over the country.

Due to the large number of sources of employment that this activity directly generates, it is necessary that it is carried out in such a way that the workers work with safety and hygiene measures that prevent the risks of suffering accidents or occupational diseases (ASIG, 2007) (Atallah, 2007) that could be caused by the processes used in the manufacture of the resin figurines (Figure 7.1).

Figure 7.1 Typical workshop for the manufacture of resin figures in the village of San Andrés Cuexcontitlán



A first effort to determine the health and safety conditions existing in these workshops is to carry out a study of the level of exposure to noise, taking as a reference the regulations in force in Mexico.

For this reason, a tour of the area was carried out in order to obtain authorisation to carry out the study; however, there was very little collaboration from the workshop owners, fortunately one of them agreed to carry out the study.

The workshop where the research was carried out is a typical workshop in the area, since practically all the workshops carry out the same processes and use the same tools and working conditions, so the study is representative of all the other workshops in the area.

In order to carry out the evaluation of the noise level generated in the workshop, a previous visit was made to the workshop to obtain a series of data relating to the production process, such as: the machinery used, the main noise emitting sources figure 7.2, the number of workers exposed and the use of hearing protection equipment.

Figure 7.2 NSCEAT measurement with an integrating sound level meter in the resin pouring area



Once the area to be evaluated had been previously surveyed, the noise exposure level (NER) was determined, for which the following aspects were taken into account.

7.3 Results

The desired confidence level was determined on the basis of the following three considerations:

$X = \sigma$ or 66% confidence.

$X = 2\sigma$ or 95% confidence

$X = 3\sigma$ or 99% confidence

Taking a selection decision of 2σ for this study.

The characteristics of the investigated phenomenon were estimated. For this purpose, the probability of the event occurring (p) or not occurring (q) was determined; when insufficient information is available on the probability of the event, it is assigned the maximum values:

$$P=0.50 \quad q=0.50$$

The maximum acceptable degree of error in the research results was determined. This can be up to 10%; normally the most advisable is to work with variables of 2 to 6%, as variations of more than 10% reduce the validity of the information too much.

The finite sample size formula is applied when it is known how many elements the population has (Branco, 2007) (Campanhole 1993).

For finite populations the sample is:

$$n = \frac{Z^2 p q N}{N e^2 + Z^2 p q} \quad (1)$$

Where:

Z=confidence level; (95%-5%).

N=universe; 50

P=probability in favour;(0.50)

q=probability against;(0.50)

e=estimation error; 5%.

$$n = \frac{\text{n=sample size}}{50 * (0.05)^2 + (1.96)^2(1 - 0.5) * 0.5}$$

$$n = \frac{1.96^2 * (1 - 0.5) * 0.5 * 50}{0.125 + 0.9604} = \frac{48.02}{1.0854} = 44.24$$

Therefore the sample size is 44 workshops, but as mentioned above it was difficult to convince the owners of these to agree to carry out the study, therefore it is recommended for further research on the topic to expand the sample size, however for our study we selected a non-probabilistic sample selection method, This is the case of decisional sampling, which is characterised by the fact that the field researcher uses his or her criteria to select the elements of the sample based on a clear definition of the target population, as in this case study, so a representative workshop was selected from the 50 workshops that work in the area (Munch, 2005).

These workshops are mainly micro-enterprises in which approximately 15 people work in each workshop in which the owners of the workshop constitute a third of the total workforce, the family employees are mainly made up of the parents and three children, who carry out all the business administration from the purchase of raw materials to the sale of the product.

From the processes used in this type of workshop it could be observed that there are multiple hygienic risks (Cavani, 2003) (Clemente, 1991) such as the use of dangerous substances like toluene, oil paints, large quantities of resin dust, noise, vibrations, handling of loads, etc.

The hygienic risk that motivated this research was the noise generated by a pneumatic polisher, compression equipment, blowing parts, airbrushes and the excessive volume of the music that workers usually listen to during their work, so that this physical agent can put them at risk of suffering an occupational disease and affect their health.

Firstly, a sensory survey was carried out to determine the type of noise produced, resulting in an unstable noise, since the maximum and minimum readings recorded by the sound level meter were higher than the 5 dB recommended by NOM-011-STPS-2011 (Corrales, 2009).

To determine the noise exposure level (NER), the workshop was divided into eight areas, which are also the number of processes used, in order to determine the NSCEAT of each workstation and subsequently determine the NER of the workshop, giving the following results.

Reliability of the measuring instrument

In order to be certain of the determination of the NER, the type 2 integrating sound level meter was sent for calibration to the company Asesoría y Servicios Integrales en Calibración, S.C. (ASIC). (ASIC), which shows the certificate of accreditation of the sound level meter, where the data of the calibration laboratory are presented, such as: name, denomination or company name of the verification unit, approval number granted by the Ministry of Labour and Social Welfare, code and name of the standard verified, result of the verification, name and signature of the authorised representative, place and date of the issuance of the report, validity of the report.

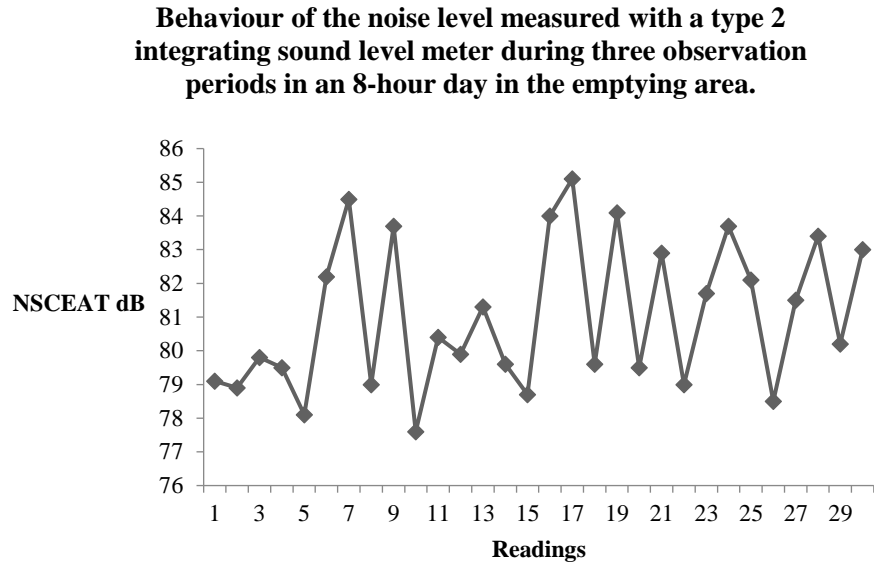
Field calibration, as established in the standard, is carried out before and after obtaining the noise levels, in order to corroborate that there is no de-calibration in the sound level meter and to be able to validate the readings taken.

The calibration was carried out at a level of 114 dB, with a CEL Instruments Ltd® brand calibrator, model CEL-282, series 2/11616221. This resulted in a difference of 0 dB, which validates the measurements taken on that day according to the Mexican standard applied, obtaining the following results as shown below:

Resin casting area

Figure 7.3 NSCEAT measurement with an integrating sound level meter in the resin pouring area



Figure 7.4 Graph of noise behaviour in the casting area**Table 7.1** Recording of 3 observation periods during an 8-hour working day of the noise level with a type 2 integrating sound level meter in the resin casting area

Reading	Noise level dB(A)	Time (s)
First period		
1	79.1	0
2	78.9	30
3	79.8	60
4	79.5	90
5	78.1	120
6	82.2	150
7	84.5	180
8	79.0	210
9	83.7	240
10	77.6	270
Second period		
11	80.4	0
12	79.9	30
13	81.3	60
14	79.6	90
15	78.7	120
16	84.0	150
17	85.1	180
18	79.6	210
19	84.1	240
20	79.5	270
Third period		
21	82.9	0
22	79.0	30
23	81.7	60
24	83.7	90
25	82.1	120
26	78.5	150
27	81.5	180
28	83.4	210
29	80.2	240
30	83.0	270
NSCEAT _i = 81.5 dB(A)		

Development of the equation for the calculation of the NSCEAT for unsteady noise in the casting area.

$$NSCE_{A,Ti} = 10 \log \frac{1}{30} \left[\left(10^{\frac{79.1}{10}}\right) + \left(10^{\frac{78.9}{10}}\right) + \left(10^{\frac{79.8}{10}}\right) + \left(10^{\frac{79.5}{10}}\right) + \left(10^{\frac{78.1}{10}}\right) + \left(10^{\frac{82.2}{10}}\right) + \left(10^{\frac{84.5}{10}}\right) + \left(10^{\frac{79}{10}}\right) + \left(10^{\frac{83.7}{10}}\right) + \left(10^{\frac{77.6}{10}}\right) + \left(10^{\frac{80.4}{10}}\right) + \left(10^{\frac{79.9}{10}}\right) + \left(10^{\frac{81.3}{10}}\right) + \left(10^{\frac{79.6}{10}}\right) + \left(10^{\frac{78.7}{10}}\right) + \left(10^{\frac{84}{10}}\right) + \left(10^{\frac{85.1}{10}}\right) + \left(10^{\frac{79.6}{10}}\right) + \left(10^{\frac{84.16}{10}}\right) + \left(10^{\frac{79.5}{10}}\right) + \left(10^{\frac{82.9}{10}}\right) + \left(10^{\frac{79}{10}}\right) + \left(10^{\frac{81.7}{10}}\right) + \left(10^{\frac{83.7}{10}}\right) + \left(10^{\frac{82.1}{10}}\right) + \left(10^{\frac{78.5}{10}}\right) + \left(10^{\frac{81.5}{10}}\right) + \left(10^{\frac{83.4}{10}}\right) + \left(10^{\frac{80.2}{10}}\right) + \left(10^{\frac{83}{10}}\right) \right] = 81.5 \text{ dB(A)}$$

Moulding area

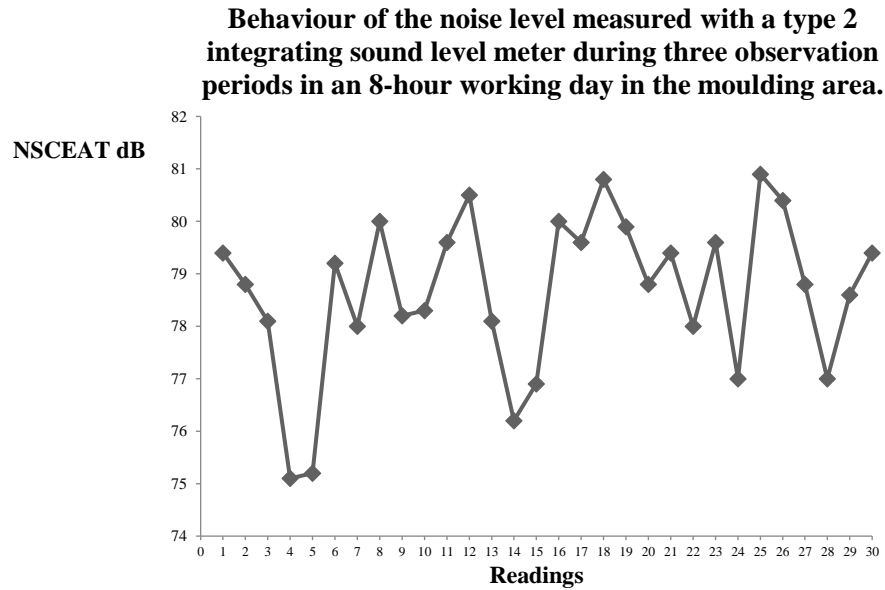
Figure 7.5 NSCEAT measurement with integrating sound level meter type 2, in the moulding area



Table 7.2 Recording of 3 observation periods during an 8-hour working day of the noise level with a type 2 integrating sound level meter in the moulding area

Reading	Noise level dB(A)	Time (s)
First period		
1	79.4	0
2	78.8	30
3	78.1	60
4	75.1	90
5	75.2	120
6	79.2	150
7	78.0	180
8	80.0	210
9	78.2	240
10	78.3	270
Second period		
11	79.6	0
12	80.5	30
13	78.1	60
14	76.2	90
15	76.9	120
16	80.0	150
17	79.6	180
18	80.8	210
19	79.9	240
20	78.8	270
Third period		
21	79.4	0
22	78.0	30
23	79.6	60
24	77.0	90
25	80.9	120
26	80.4	150
27	78.8	180
28	77.0	210
29	78.6	240
30	79.4	270
NSCEATi = 78.8 dB(A)		

Figure 7.6 Noise behaviour graph in the moulding area



Development of the equation for the calculation of the NSCEAT for unsteady noise in the moulding area.

$$\begin{aligned}
 NSCE_{A,T}i = 10 \log \frac{1}{30} & \left[\left(10^{\frac{79.4}{10}}\right) + \left(10^{\frac{78.8}{10}}\right) + \left(10^{\frac{78.1}{10}}\right) + \left(10^{\frac{75.1}{10}}\right) + \left(10^{\frac{75.2}{10}}\right) + \left(10^{\frac{79.2}{10}}\right) + \left(10^{\frac{78}{10}}\right) + \right. \\
 & \left(10^{\frac{80}{10}}\right) + \left(10^{\frac{78.2}{10}}\right) + \left(10^{\frac{78.3}{10}}\right) + \left(10^{\frac{79.6}{10}}\right) + \left(10^{\frac{80.5}{10}}\right) + \left(10^{\frac{78.1}{10}}\right) + \left(10^{\frac{76.2}{10}}\right) + \left(10^{\frac{76.9}{10}}\right) + \left(10^{\frac{80}{10}}\right) + \\
 & \left(10^{\frac{79.6}{10}}\right) + \left(10^{\frac{80.8}{10}}\right) + \left(10^{\frac{79.9}{10}}\right) + \left(10^{\frac{78.8}{10}}\right) + \left(10^{\frac{79.4}{10}}\right) + \left(10^{\frac{78}{10}}\right) + \left(10^{\frac{79.6}{10}}\right) + \left(10^{\frac{77}{10}}\right) + \left(10^{\frac{80.9}{10}}\right) + \\
 & \left. \left(10^{\frac{80.4}{10}}\right) + \left(10^{\frac{78.8}{10}}\right) + \left(10^{\frac{77}{10}}\right) + \left(10^{\frac{78.6}{10}}\right) + \left(10^{\frac{79.4}{10}}\right) \right] = 78.8 \text{ dB(A)}
 \end{aligned}$$

Patching area

Figure 7.7 NSCEAT measurement with type 2 integrating sound level meter, in the patching area



Figure 7.8 Graph of noise behaviour in the patching area

Behaviour of the noise level measured with a type 2 integrating sound level meter during three observation periods in an 8-hour working day in the finishing area.

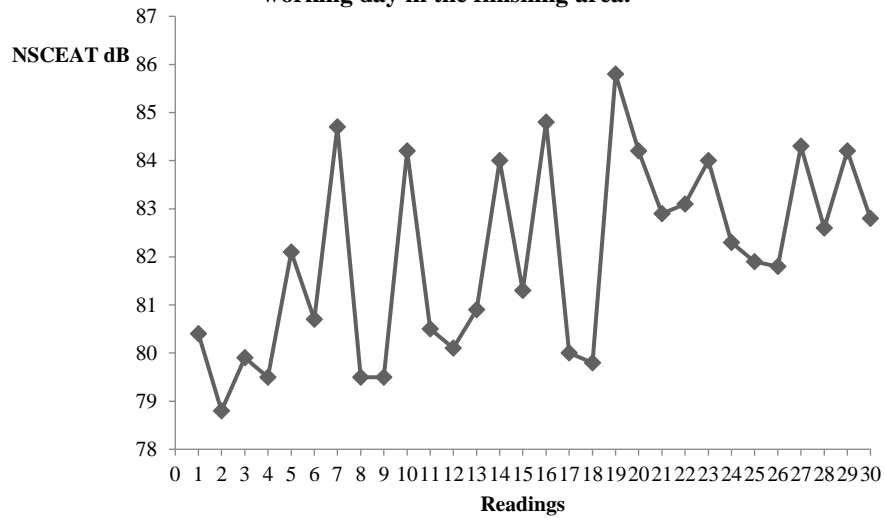


Table 7.3 Recording of the 3 observation periods during an 8 h working day of the noise level with a type 2 integrating sound level meter in the area of the finishing area

Reading	Noise level dB(A)	Time (s)
First period		
1	80.4	0
2	78.8	30
3	79.9	60
4	79.5	90
5	82.1	120
6	80.7	150
7	84.7	180
8	79.5	210
9	79.5	240
10	84.2	270
Second period		
11	80.5	0
12	80.1	30
13	80.9	60
14	84.0	90
15	81.3	120
16	84.8	150
17	80.0	180
18	79.8	210
19	85.8	240
20	84.2	270
Third period		
21	82.9	0
22	83.1	30
23	84.0	60
24	82.3	90
25	81.9	120
26	81.8	150
27	84.3	180
28	82.6	210
29	84.2	240
30	82.8	270
NSCEAT _i = 82.4 dB(A)		

Development of the equation for the calculation of the NSCEAT for unsteady noise in the patching area.

$$NSCE_{A,Ti} = 10 \log \frac{1}{30} \left[\left(10^{\frac{80.4}{10}}\right) + \left(10^{\frac{78.8}{10}}\right) + \left(10^{\frac{79.9}{10}}\right) + \left(10^{\frac{79.5}{10}}\right) + \left(10^{\frac{82.1}{10}}\right) + \left(10^{\frac{80.7}{10}}\right) + \left(10^{\frac{84.7}{10}}\right) + \left(10^{\frac{79.5}{10}}\right) + \left(10^{\frac{79.5}{10}}\right) + \left(10^{\frac{84.2}{10}}\right) + \left(10^{\frac{80.5}{10}}\right) + \left(10^{\frac{80.1}{10}}\right) + \left(10^{\frac{80.9}{10}}\right) + \left(10^{\frac{84}{10}}\right) + \left(10^{\frac{81.3}{10}}\right) + \left(10^{\frac{84.8}{10}}\right) + \left(10^{\frac{80}{10}}\right) + \left(10^{\frac{79.5}{10}}\right) + \left(10^{\frac{85.8}{10}}\right) + \left(10^{\frac{84.2}{10}}\right) + \left(10^{\frac{82.9}{10}}\right) + \left(10^{\frac{83.1}{10}}\right) + \left(10^{\frac{84}{10}}\right) + \left(10^{\frac{82.3}{10}}\right) + \left(10^{\frac{81.9}{10}}\right) + \left(10^{\frac{81.7}{10}}\right) + \left(10^{\frac{84.3}{10}}\right) + \left(10^{\frac{82.6}{10}}\right) + \left(10^{\frac{84.2}{10}}\right) + \left(10^{\frac{82.8}{10}}\right) \right] = 82.4 \text{ dB(A)}$$

Grinding area

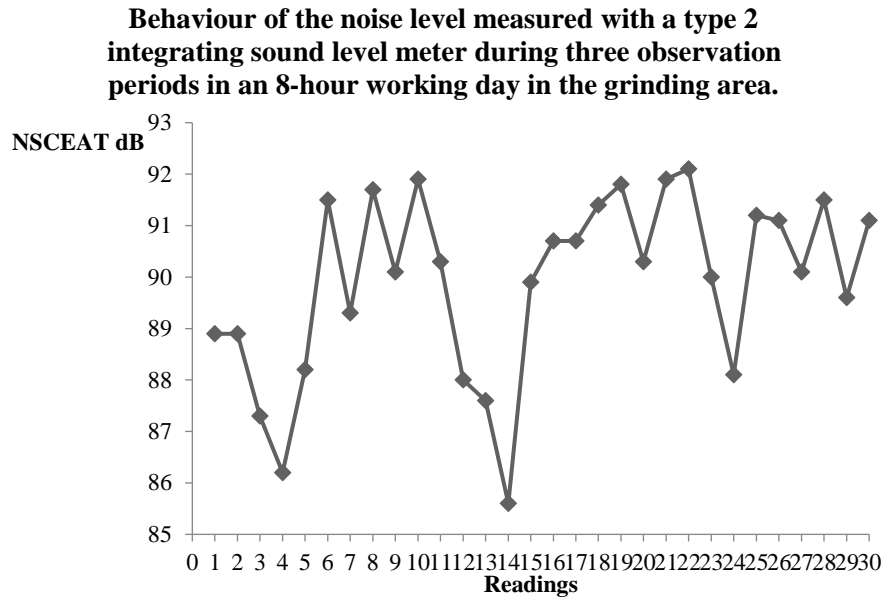
Figure 7.9 NSCEAT measurement with integrating sound level meter type 2, in the grinding area



Table 7.4 Recording of 3 observation periods during an 8-hour working day of the noise level with a type 2 integrating sound level meter in the grinding area

Reading	Noise level (dB(A))	Time (s)
First period		
1	88.9	0
2	88.9	30
3	87.3	60
4	86.2	90
5	88.2	120
6	91.5	150
7	89.3	180
8	91.7	210
9	90.1	240
10	91.9	270
Second period		
11	90.3	0
12	88.0	30
13	87.6	60
14	85.6	90
15	89.9	120
16	90.7	150
17	90.7	180
18	91.4	210
19	91.8	240
20	90.3	270
Third period		
21	91.9	0
22	92.1	30
23	90.0	60
24	88.1	90
25	91.2	120
26	91.1	150
27	90.1	180
28	91.5	210
29	89.6	240
30	91.1	270
NSCEATi = 90.1 dB(A)		

Figure 7.10 Graph of noise behaviour in the grinding area



Development of the equation for the calculation of the NSCEAT for unsteady noise in the grinding area.

$$\begin{aligned}
 NSCE_{A,T}i = 10 \log \frac{1}{30} & \left[\left(10^{\frac{88.9}{10}}\right) + \left(10^{\frac{88.9}{10}}\right) + \left(10^{\frac{87.3}{10}}\right) + \left(10^{\frac{86.2}{10}}\right) + \left(10^{\frac{88.2}{10}}\right) + \left(10^{\frac{91.5}{10}}\right) + \left(10^{\frac{89.3}{10}}\right) + \left(10^{\frac{91.7}{10}}\right) + \left(10^{\frac{90.1}{10}}\right) \right. \\
 & + \left(10^{\frac{91.9}{10}}\right) + \left(10^{\frac{89.3}{10}}\right) + \left(10^{\frac{88}{10}}\right) + \left(10^{\frac{87.6}{10}}\right) + \left(10^{\frac{85.6}{10}}\right) + \left(10^{\frac{89.9}{10}}\right) + \left(10^{\frac{90.7}{10}}\right) + \left(10^{\frac{90.7}{10}}\right) + \left(10^{\frac{91.4}{10}}\right) + \left(10^{\frac{91.8}{10}}\right) \\
 & + \left(10^{\frac{90.3}{10}}\right) + \left(10^{\frac{91.9}{10}}\right) + \left(10^{\frac{92.1}{10}}\right) + \left(10^{\frac{90}{10}}\right) + \left(10^{\frac{88.1}{10}}\right) + \left(10^{\frac{91.2}{10}}\right) + \left(10^{\frac{91.1}{10}}\right) + \left(10^{\frac{90.1}{10}}\right) + \left(10^{\frac{91.5}{10}}\right) + \left(10^{\frac{89.6}{10}}\right) \\
 & \left. + \left(10^{\frac{91.1}{10}}\right) \right] = 90.1dB(A)
 \end{aligned}$$

Decoration area - 1

Figure 7.11 NSCEAT measurement with integrating sound level meter type 2, in the set-1 area



Figure 7.12 Graph of noise behaviour in set area-1

Behaviour of the noise level measured with a type 2 integrating sound level meter during three observation periods in an 8-hour day in the set-1 area.

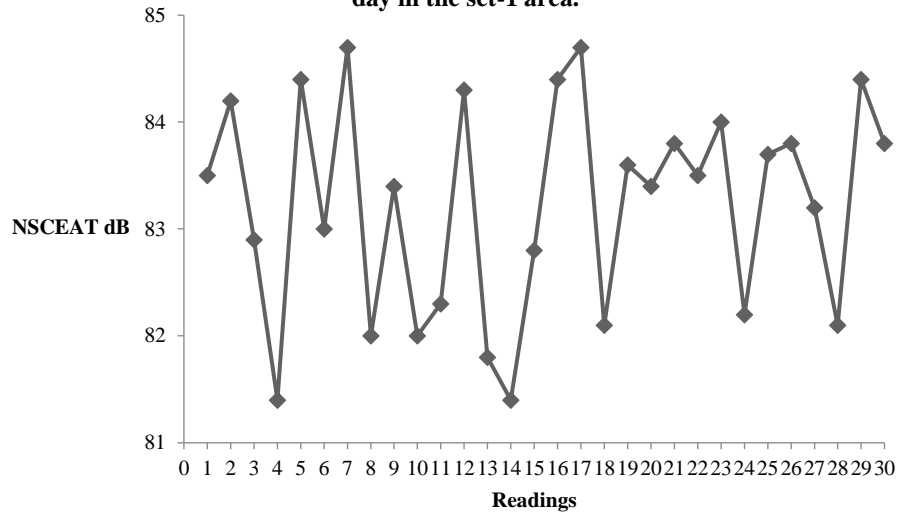


Table 7.5 Recording of the 3 observation periods during an 8 h working day of the noise level with type 2 integrating sound level meter in the set-1 area

Reading	Noise level (dB)	Time (s)
First period		
1	83.5	0
2	84.2	30
3	82.9	60
4	81.4	90
5	84.4	120
6	83.0	150
7	84.7	180
8	82.0	210
9	83.4	240
10	82.0	270
Second period		
11	82.3	0
12	84.3	30
13	81.8	60
14	81.4	90
15	82.8	120
16	84.4	150
17	84.7	180
18	82.1	210
19	83.6	240
20	83.4	270
Third period		
21	83.8	0
22	83.5	30
23	84.0	60
24	82.2	90
25	83.7	120
26	83.8	150
27	83.2	180
28	82.1	210
29	84.4	240
30	83.8	270
NSCEAT _i = 83.3 dB(A)		

Development of the equation for the calculation of the NSCEAT for unsteady noise in the set-1 area.

$$NSCE_{A,Ti} = 10 \log \frac{1}{30} \left[\left(10^{\frac{83.5}{10}}\right) + \left(10^{\frac{84.2}{10}}\right) + \left(10^{\frac{82.9}{10}}\right) + \left(10^{\frac{81.4}{10}}\right) + \left(10^{\frac{84.4}{10}}\right) + \left(10^{\frac{83.0}{10}}\right) + \left(10^{\frac{84.7}{10}}\right) + \left(10^{\frac{82.0}{10}}\right) + \left(10^{\frac{83.4}{10}}\right) + \left(10^{\frac{82.0}{10}}\right) + \left(10^{\frac{82.3}{10}}\right) + \left(10^{\frac{84.3}{10}}\right) + \left(10^{\frac{81.8}{10}}\right) + \left(10^{\frac{81.4}{10}}\right) + \left(10^{\frac{82.8}{10}}\right) + \left(10^{\frac{84.4}{10}}\right) + \left(10^{\frac{84.7}{10}}\right) + \left(10^{\frac{82.1}{10}}\right) + \left(10^{\frac{83.6}{10}}\right) + \left(10^{\frac{83.4}{10}}\right) + \left(10^{\frac{83.8}{10}}\right) + \left(10^{\frac{83.5}{10}}\right) + \left(10^{\frac{84}{10}}\right) + \left(10^{\frac{82.2}{10}}\right) + \left(10^{\frac{83.7}{10}}\right) + \left(10^{\frac{83.8}{10}}\right) + \left(10^{\frac{83.2}{10}}\right) + \left(10^{\frac{82.1}{10}}\right) + \left(10^{\frac{84.4}{10}}\right) + \left(10^{\frac{83.8}{10}}\right) \right] = 83.33 \text{ dB(A)}$$

7.4 Conclusions

Once the methodology for the evaluation of the level of exposure to noise (NER) had been developed and the analysis of the measurements taken in the resin figure workshop of the different workstations in the workshop had been completed, the following conclusions could be drawn:

The analysis of the information collected in the workshop and the evaluation using the method proposed by the NOM-011-STPS-2001, made it possible to obtain information in a simple way on the activities and characteristics of the workstation, in order to evaluate the levels of exposure to noise.

The method followed made it possible to evaluate the workstations in the time allotted for the inspection of the workshop, thus providing valuable information to detect critical areas and guide preventive measures for noise exposure.

Nevertheless, based on a limited sample of workshops, the present study was able to detect some of the most important shortcomings of this craft activity in this area. It was found, for example, the existence of NSCEAT levels that exceed the norm and there is no control over them, which results in significant damage to the health of workers who are often unaware of the situation due to lack of evaluations, examinations and training by the workshop owners.

The analysis of the noise level generated in the workshop dedicated to the elaboration of resin figures concludes that the maximum NSCEAT obtained are in the grinding areas, caused by the use of a manual pneumatic grinding machine that generates a NSCEAT of 90.1 dB(A). In this area only one worker works, the other critical area is the area where the sound equipment or background music is located which generates a NSCEAT of 91.7 dB(A), consequently, this level also affects workers who are close to this equipment such as the decoration area one and two, in addition to the grinding and resurfacing areas where 10 workers work (CANAMA, 2013).

In general the noise exposure level of the workshop (NER) was 86.6 dB(A), which is below the maximum level of 90 dB recommended by the standard for an 8-hour working day, so in general there is no danger of suffering any occupational disease caused by noise, but as the level is above 85 dB the standard recommends that preventive measures be taken to avoid the risk of suffering any disease resulting from exposure to noise.

Therefore, this result obtained in the present study demonstrates that the noise conditions to which the workshop workers are exposed do not represent any risk for the workers.

By virtue of this research, the following recommendations are suggested for the improvement of the working conditions of workers in this type of workshop.

There are areas where the value is greater than 90 dB, establishing that the personnel working in these areas strictly comply with NOM-011-STPS-2001.

Establish a programme every six months for the medical examination of workshop workers, to identify cases of hearing loss in time, as a preventive measure.

In coordination with the owner, establish a programme for the rotation of the most exposed personnel, such as grinding workers, so that exposure time is within safe limits.

Delimit the areas of those areas where noise is generated in order to avoid damaging neighbouring areas that do not have this problem.

Ensure that workers exposed in noisy areas are duly monitored periodically, in order to establish follow-up and control, detecting cases of diminished capacity in a timely manner.

Carry out audiometric examinations to detect diminished capacity in workers in a timely manner in order to establish action plans.

Develop awareness-raising talks, highlighting the effects that prolonged exposure to noise can have on workers, reinforcing the use of hearing protection equipment.

Provide workers with personal protective equipment (PPE), ensuring that it is appropriate for the type and time of exposure to noise.

Build compressor sheds with sound-absorbing walls and ceilings.

Restrict the presence of workers to an adequate distance from noisy equipment.

Evaluate the attenuation of hearing protectors and effectiveness for noise in the specific job.

7.5 References

Alexandry , F. O. (1978). Problema de ruido industrial y sus controles. São Paulo: Fundacentro.

ASIG. (2007). Los accidentes de trabajo. Obtenido de <http://orlandoboada.comunidadcoomeva.com>

Atallah, A. N., Andriolo, R. B., Soares, B. G., & Verbeek, J. (2007). A systematic review of the interventions to promote the wearing of hearing protection. Sao Paulo Med. J.: El Dib RP.

Astete, M. G., & Kitamura, S. (1978). Manual prático de avaliação do barulho industria. São Paulo

Branco, N. A., Ferreira, J. R., & Pereira, M. A. (2007). aparelho respiratório na doença vibroacústica. Retrieved from: <http://www.scielo.oces.mctes>.

Campanhole, H. L., & Campanhole, A. (1993). Consolidação das leis do trabalho e legislação complementar. São Paulo: Atlas,

Cavaní, D. F. (2003). Efectos del Ruido Sobre la Salud. Real Academia de Medicina.

Munch, L., & Ángeles, E. (2005). Métodos y técnicas de investigación. México, D. F.: Trillas.

Clemente, I. M. (1991). Enfermedades profesionales del oído. Medicina y Seguridad del Trabajo

CONAMA. (2013). Comisión Nacional del Medio ambiente), www.conama.cl. Retrieved from: cybertesis.uach.cl/tesis/uach/2004/bmfcit172m/doc/bmfcit172m.pdf: www.conama.cl.

Corrales M, T. H. (2009). Percepción del riesgo sobre protección y pérdida auditiva en trabajadores expuestos a ruido en el trabajo.

Instructions for Scientific, Technological and Innovation Publication

[Title in Times New Roman and Bold Type No. 14 in English and Spanish]

Last Name (IN CAPITAL LETTERS), First Name of 1st Author†*, Last Name (IN CAPITAL LETTERS), First Name of 1st Co-Author, Last Name (IN CAPITAL LETTERS), First Name of 2nd Co-Author and Last Name (IN CAPITAL LETTERS), First Name of 3rd Co-Author.

Author's Institution of Affiliation including dependency (in Times New Roman No.10 and Italics)

International Identification of Science - Technology and Innovation

1st Author ID: (ORC ID - Researcher ID Thomson, arXiv Author ID - PubMed Author ID - Open ID) and CVU 1st Author: (Scholar-PNPC or SNI-CONACYT) (No.10 Times New Roman)

1st Co-author ID: (ORC ID - Researcher ID Thomson, arXiv Author ID - PubMed Author ID - Open ID) and CVU 1st Co-author: (Grantee-PNPC or SNI-CONACYT) (No.10 Times New Roman)

2nd Co-author ID: (ORC ID - Researcher ID Thomson, arXiv Author ID - PubMed Author ID - Open ID) and CVU 2nd Co-author: (Scholar-PNPC or SNI-CONACYT) (No.10 Times New Roman)

3rd Co-author ID: (ORC ID - Researcher ID Thomson, arXiv Author ID - PubMed Author ID - Open ID) and CVU 3rd Co-author: (Grantee-PNPC or SNI-CONACYT) (No.10 Times New Roman)

(Indicate Date of Submission: Month, Day, Year); Accepted (Indicate Date of Acceptance: Exclusive Use by ECORFAN)

Citation: First letter (IN CAPITAL LETTERS) of the Name of the 1st Author. Last Name, First Letter (IN CAPITAL LETTERS) of the 1st Co-author's Name. Last name, first letter (IN CAPITAL LETTERS) of the 2nd Co-author's name. Last Name, First Letter (IN CAPITAL LETTERS) of the Name of the 3rd Co-author. Last name

Institutional Mail [Times New Roman No.10].

First letter (IN CAPITAL LETTERS) of the Name Editors. Surname (eds.) *Title of the Handbook [Times New Roman No.10]*, Selected Topics of the corresponding area ©ECORFAN-Filial, Year.

Instructions for Scientific, Technological and Innovation Publication

Abstract

Text written in Times New Roman No.12, single spaced, in English.

Indicate (3-5) keywords in Times New Roman and Bold No.12.

1 Introduction

Text written in Times New Roman No.12, single spaced.

Explanation of the topic in general and explain why it is important.

What is its added value with respect to other techniques?

Focus clearly on each of its characteristics.

Clearly explain the problem to be solved and the central hypothesis.

Explanation of the sections of the Chapter.

Development of Sections and Sections of the Chapter with subsequent numbering.

[Title in Times New Roman No.12, single space and Bold].

Development of Chapters in Times New Roman No.12, single space.

Inclusion of Graphs, Figures and Tables-Editables

In the content of the Chapter, all graphs, tables and figures must be editable in formats that allow modifying size, type and number of letters, for editing purposes, these must be in high quality, not pixelated and must be noticeable even if the image is reduced to scale.

[Indicating the title in the upper part with Times New Roman No.12 and Bold, indicating the font in the lower part centered with Times New Roman No. 10].

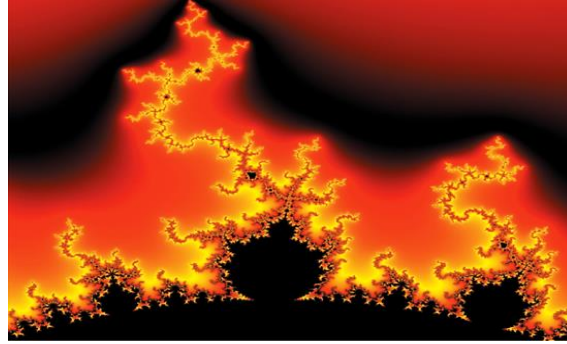
Table 2.1 Title

Variable	Description	Value
P ₁	Partition 1	481.00
P ₂	Partition 2	487.00
P ₃	Partition 3	484.00
P ₄	Partition 4	483.50
P ₅	Partition 5	484.00
P ₆	Partition 6	490.79
P ₇	Partition 7	491.61

Source:

(They should not be images, everything should be editable)

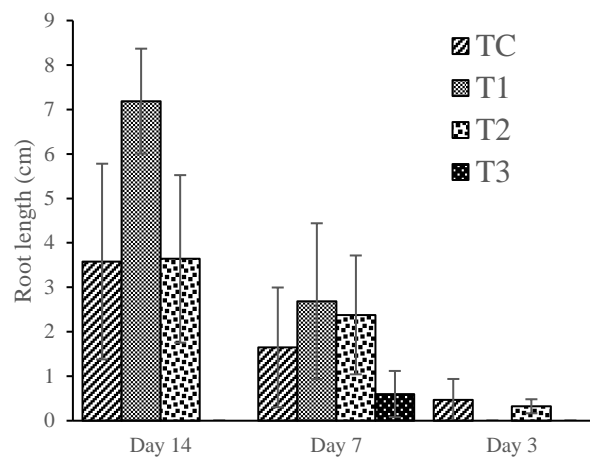
Figure 1.1 Title



Source:

(They should not be images, everything should be editable)

Graphic 1.1 Title



Source:

(They should not be images, everything should be editable)

Each Chapter should be presented separately in **3 Folders**: a) Figures, b) Graphs and c) Tables in .JPG format, indicating the number in Bold and the sequential Title.

For the use of Equations, indicate as follows:

$$\int_{lim^{-1}}^{lim^1} = \int \frac{lim^1}{lim^{-1}} = \left[\frac{1(-1)}{lim} \right]^2 = \frac{(0)^2}{lim} = \sqrt{lim} = 0 = 0 \rightarrow \infty \quad (1)$$

They should be editable and with numbering aligned on the far right.

Methodology to be developed

Give the meaning of the variables in linear wording and it is important to compare the criteria used.

Results

The results should be per section of the Chapter.

Annexes

Tables and appropriate sources.

Instructions for Scientific, Technological and Innovation Publication

Acknowledgements

Indicate if they were financed by any Institution, University or Company.

Conclusions

Clearly explain the results obtained and the possibilities for improvement.

References

Use the APA system. They should not be numbered or bulleted, however, if numbering is necessary, it will be because there is a reference or mention in some part of the Chapter.

Technical Data Sheet

Each Chapter should be presented in a Word document (.docx):

Name of the Handbook

Title of the Chapter

Abstract

Keywords

Sections of the Chapter, e.g:

1. *Introduction*
2. *Description of the method*
3. *Analysis based on demand curve regression*
4. *Results*
5. *Acknowledgement*
6. *Conclusions*
7. *References*

Name of Author(s)

Correspondence E-mail to Author

References

Intellectual Property Requirements for its edition:

- Author's and co-authors' autographic signature in blue colour of the originality form.
- Author's and co-authors' autographic signature in blue colour of the author and co-authors' acceptance form.

Reservation to the Editorial Policy

ECORFAN Handbooks reserves the right to make any editorial changes required to bring the Scientific Work into compliance with the ECORFAN Handbooks Editorial Policy. Once the Scientific Work has been accepted in its final version, ECORFAN Handbooks will send the author the proofs for review. ECORFAN® will only accept the correction of errata and errors or omissions arising from the editing process of the journal, reserving in its entirety the rights of authorship and dissemination of content. Deletions, substitutions or additions that alter the formation of the Scientific Work will not be accepted.

Code of Ethics - Good Practices and Statement of Solution to Editorial Conflicts

Declaration of Originality and unpublished character of the Scientific Work, of Authorship, on the obtaining of data and interpretation of results, Acknowledgements, Conflict of interests, Assignment of rights and distribution.

The Management of ECORFAN-Mexico, S.C. claims to the Authors of the Scientific Work that its content must be original, unpublished and of Scientific, Technological and Innovation content in order to submit it for evaluation.

The Authors signing the Scientific Work must be the same who have contributed to its conception, realization and development, as well as to the obtaining of the data, the interpretation of the results, its writing and revision. The Corresponding Author of the proposed Scientific Work should fill in the following form.

Title of the Scientific Work:

- The submission of a Scientific Paper to ECORFAN Handbooks implies the author's commitment not to submit it simultaneously to the consideration of other serial publications. To do so, he/she must complete the Originality Form for his/her Scientific Paper, unless it is rejected by the Referee Committee, it may be withdrawn.
- None of the data presented in this Scientific Work has been plagiarized or invented. The original data are clearly distinguishable from those already published. And we are aware of the PLAGSCAN test, if a positive plagiarism level is detected, we will not proceed to refereeing.
- The references on which the information contained in the Scientific Work is based are cited, as well as theories and data from other previously published Scientific Works.
- The authors sign the Authorization Form for their Scientific Work to be disseminated by the means that ECORFAN-Mexico, S.C. in its Holding Mexico considers pertinent for the dissemination and diffusion of their Scientific Work, ceding their Scientific Work Rights.
- Consent has been obtained from those who have provided unpublished data obtained through verbal or written communication, and such communication and authorship are properly identified.
- The Author and Co-Authors signing this work have participated in its planning, design and execution, as well as in the interpretation of the results. Likewise, they critically reviewed the work, approved its final version and agree with its publication.
- No signature responsible for the work has been omitted and the criteria for Scientific Authorship have been met.
- The results of this Scientific Work have been interpreted objectively. Any results contrary to the views of the signatories are stated and discussed in the Scientific Work

Copyright and Access

The publication of this Scientific Work implies the assignment of the copyright to ECORFAN-Mexico, S.C. in its Holding Mexico for its ECORFAN Handbooks, which reserves the right to distribute on the Web the published version of the Scientific Work and the availability of the Scientific Work in this format implies for its Authors the compliance with the provisions of the Law of Science and Technology of the United Mexican States, regarding the obligation to allow access to the results of Scientific Research.

Title of the Scientific Work:

Name and surname(s) of Contact Author and Co-authors	Signature
1.	
2.	
3.	
4.	

Principles of Ethics and Editorial Conflict Resolution Statement

Editor's Responsibilities

The Editor undertakes to guarantee the confidentiality of the evaluation process, and may not reveal the identity of the Authors to the Referees, nor may he/she reveal the identity of the Referees at any time.

The Editor assumes the responsibility of duly informing the Author of the stage of the editorial process in which the submitted text is, as well as of the resolutions of the Double Blind Arbitration.

The Editor must evaluate manuscripts and their intellectual content without distinction of race, gender, sexual orientation, religious beliefs, ethnic origin, nationality, or political philosophy of the Authors.

The Editor and its editorial staff of ECORFAN® Holdings will not disclose any information about the submitted Scientific Work to anyone other than the corresponding Author.

The Editor must make fair and impartial decisions and ensure a fair peer review process.

Responsibilities of the Editorial Board

The description of the peer review process is made known by the Editorial Board so that the Authors are aware of the evaluation criteria and will always be ready to justify any controversy in the evaluation process. In case of Plagiarism Detection to the Scientific Work, the Committee notifies the Authors for Violation of the Right of Scientific, Technological and Innovation Authorship.

Responsibilities of the Referee Committee

The Referees undertake to notify any unethical conduct on the part of the Authors and to point out any information that may be a reason to reject the publication of the Scientific Work. In addition, they must undertake to keep confidential the information related to the Scientific Work they evaluate.

Any manuscript received for refereeing must be treated as a confidential document, not to be shown or discussed with other experts, except with the permission of the Editor.

Referees should conduct themselves in an objective manner; any personal criticism of the Author is inappropriate.

Referees should express their views clearly and with valid arguments that contribute to the Scientific, Technological and Innovation achievements of the Author.

Referees should not evaluate manuscripts in which they have conflicts of interest and which have been notified to the Editor before submitting the Scientific Work for evaluation.

Responsibilities of Authors

Authors must guarantee that their Scientific Works are the product of their original work and that the data have been obtained in an ethical manner.

Authors must guarantee that they have not been previously published or that they are not being considered in another serial publication.

Authors must strictly follow the rules for the publication of Scientific Works defined by the Editorial Board.

Authors should consider that plagiarism in all its forms constitutes unethical editorial conduct and is unacceptable; consequently, any manuscript that incurs in plagiarism will be eliminated and will not be considered for publication.

Authors should cite publications that have been influential in the nature of the Scientific Work submitted for refereeing.

Information Services

Indexing - Bases and Repositories

RESEARCH GATE (Germany)

MENDELEY (Bibliographic Reference Manager)

GOOGLE SCHOLAR (Citation Indexes-Google)

REDIB (Ibero-American Network of Innovation and Scientific Knowledge- CSIC)

Editorial Services

Citation Identification and H Index

Originality and Authorization Format Management

Handbooks Testing with PLAGSCAN

Evaluation of Scientific Work

Issuance of Referee Certificate

Scientific Work Editing

Web Layout

Indexing and Repository

Publication of Scientific Work

Scientific Work Certificate

Invoicing for Publishing Services

Editorial Policy and Administration

143 - 50 Itzopan, Ecatepec de Morelos - Mexico. Tel: +52 1 55 6159 2296, +52 1 55 1260 0355, +52 1 55 6034 9181; E-mail: contact@ecorfan.org www.ecorfan.org

ECORFAN®

Editor in Chief

VARGAS-DELGADO, Oscar. PhD

Executive Director

RAMOS-ESCAMILLA, María. PhD

Editorial Director

PERALTA-CASTRO, Enrique. MsC

Web Designer

ESCAMILLA-BOUCHAN, Imelda. PhD

Web Diagrammer

LUNA-SOTO, Vladimir. PhD

Editorial Assistant

TREJO-RAMOS, Iván. BsC

Translator

DÍAZ-OCAMPO, Javier. BsC

Philologist

RAMOS-ARANCIBIA, Alejandra. BsC

Advertising and Sponsorship

(ECORFAN® - Mexico – Bolivia – Spain – Ecuador – Cameroon – Colombia - El Salvador – Guatemala – Nicaragua – Peru – Paraguay - Democratic Republic of The Congo - Taiwan),
sponsorships@ecorfan.org

Site Licenses

03-2010-032610094200-01-For printed material, 03-2010-031613323600-01-For electronic material, 03-2010-032610105200-01-For photographic material, 03-2010-032610115700-14-For Compilation of Data, 04 -2010-031613323600-01-For its Web page, 19502-For Ibero-American and Caribbean Indexing, 20-281 HB9-For Latin American Indexing in the Social Sciences and Humanities, 671-For Indexing in Electronic Scientific Journals in Spain and Latin America, 7045008-For dissemination and publication in the Ministry of Education and Culture-Spain, 25409-For its repository in the University Library-Madrid, 16258-For its indexing in Dialnet, 20589-For Indexing in the Directory in the countries of Iberoamerica and the Caribbean, 15048-For the international registration of Congresses and Colloquia.
financingprograms@ecorfan.org

Management Offices

143 - 50 Itzopan, Ecatepec de Morelos - Mexico.

21 Santa Lucia, CP-5220. Libertadores -Sucre - Bolivia.

38 Matacerquillas, CP-28411. Moralarzal -Madrid-Spain.

18 Marcial Romero, CP-241550. Avenue, Salinas I - Santa Elena-Ecuador.

1047 Avenida La Raza - Santa Ana, Cusco-Peru.

Boulevard de la Liberté, Immeuble Kassap, CP-5963.Akwa- Douala-Cameroon.

Avenida Suroeste, San Sebastian - León-Nicaragua.

31 Kinshasa 6593- Republique Démocratique du Congo.

Avenida San Quentin, R 1-17 Miralvalle - San Salvador-El Salvador.

16 kilometers, U.S. highway, Terra Alta house, D7 Mixco Zone 1-Guatemala.

105 Alberdi Rivarola Capitán, CP-2060. Luque City- Paraguay.

69 Street YongHe District, Zhongxin. Taipei-Taiwan.

43 Street # 30 -90 B. El Triunfo CP.50001. Bogotá-Colombia.

